

DEVELOPMENT OF A MODEL OF WEBS
ENCOUNTERING CONCAVE ROLLERS

By

GREG ALAN KLIEWER

//

Bachelor of Science in Civil Engineering

Oklahoma State University

Stillwater, Oklahoma

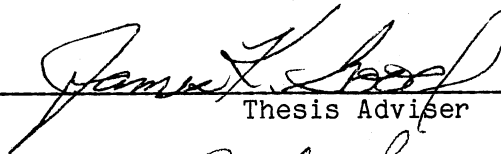
1985

Submitted to the Faculty of the
Graduate College of the
Oklahoma State University
in partial fulfillment of
the requirements for
the Degree of
MASTER OF SCIENCE
December 1988

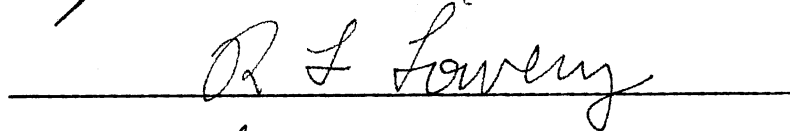
Thesis
1988
K645d
cop. 2

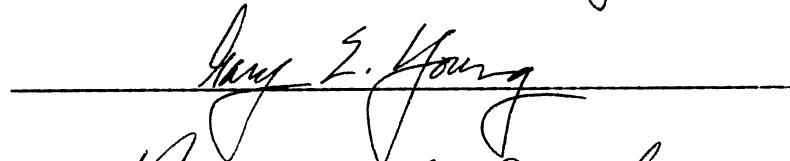
DEVELOPMENT OF A MODEL OF WEBS
ENCOUNTERING CONCAVE ROLLERS

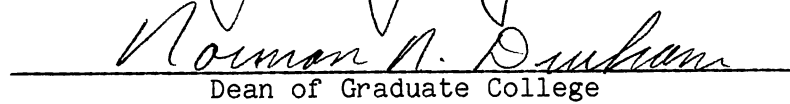
Thesis Approved:



Thesis Adviser







Dean of Graduate College

ACKNOWLEDGEMENTS

I would like to express my gratitude to all the people responsible for helping me during my studies at Oklahoma State University and for assisting me in completing my thesis. Foremost among these is Dr. J. K. Good. Dr. Good gave me the opportunity to work under him in a research assistantship. His instruction, advice, support, and patience proved invaluable throughout my graduate studies. I would also like to thank Dr. R. L. Lowery and Dr. G. E. Young for their participation as committee members. I am also appreciative to Ron Delahoussey for his assistance with the computer codes. Further, I would like to express my thanks to Mrs. Anne Bradley and Ms. Charlene Fries for their excellent work in preparing this manuscript.

My special thanks and love go to my parents, my brother, and all my family for their love, support, and understanding throughout my life, and especially while attending Oklahoma State University. I would also like to thank Stacia for her added support this last year. Finally, I thank God for blessing me with a healthy body and mind.

TABLE OF CONTENTS

Chapter	Page
I. INTRODUCTION.....	1
1.1 Objectives.....	2
1.2 Literature Survey.....	2
1.3 Organization.....	5
II. THEORY DEVELOPMENT FOR BOUNDARY CONDITIONS.....	8
III. ANALYTICAL STUDY.....	16
3.1 Finite Element Model.....	17
3.2 Average Plane Transformation.....	25
3.3 Generation of Boundary Conditions.....	29
3.4 Spreading Analysis.....	37
3.5 Program Summary.....	41
3.6 Parameter Response.....	46
3.7 Parameter Values Studied.....	47
IV. ANALYSIS OF RESULTS.....	49
4.1 Curved Arc Profile Radius of Curvature.....	49
4.2 Angle of Wrap.....	74
4.3 Web Tension.....	78
4.4 Modulus of Elasticity.....	78
4.5 Poisson's Ratio.....	85
4.6 Thickness.....	90
4.7 Coefficient of Friction.....	94
V. CONCLUSIONS.....	103
5.1 Overview.....	103
5.2 Recommendation for Future Study.....	104
BIBLIOGRAPHY	106
APPENDIXES	107
APPENDIX A - MODIFICATION FOR SKEWED BOUNDARY CONDITIONS.....	108
APPENDIX B - CONSTRAINT EQUATIONS FOR SYSTEM OF EQUATIONS.....	110
APPENDIX C - COMPUTER CODE FOR PROGRAM MSHGMR.....	112
APPENDIX D - COMPUTER PROGRAM FOR PROGRAM CONCAVE.....	126

LIST OF TABLES

Table	Page
I. A Partial List of the Computer Input for the Computer Code MSHGNR.....	19
II. List of Parameters Studied.....	46
III. Parameter Values Used for Base Model.....	47
IV. Parameter Values Used In Study.....	48

LIST OF FIGURES

Figure	Page
1. Lateral Web Travel on a Roller.....	4
2. Belt Action on a Concave Roller.....	6
3. Generalized Roller Layout.....	9
4. Graphical Interpretation of Average Strain Criteria.....	12
5. Geometry of Concave Roller.....	14
6. Symmetric Model.....	18
7. Effect of an Enforced Machine Direction Linear Displacement Distribution on the Entry Span.....	21
8. Effect of an Enforced Machine Direction Paraboloid Displacement Distribution on the Entry Span.....	22
9. Planar View of Finite Element Mesh.....	23
10. Planar View of Mesh Used for Study.....	24
11. Graphical Interpretation of Out-of-Plane Displacements.....	26
12. Planes Used for Interior Needs.....	28
13. Planes Used for Edge and Corner Nodes.....	30
14. Search Procedure and Force Calculation Used in MSHGNR.....	33
15. Lateral Displacement "Locks".....	36
16. Friction Forces for Exterior Rows of Nodes.....	39
17. Spreading Analysis.....	42
18. Flowchart of CONCAVE Program.....	44

19.	Edge Displacement on Concave Roller as a Function of the Radius of Curvature.....	50
20.	Edge Displacement for Various Radii of Curvature.....	52
21.	Lateral S_y Distribution at M.D. Distance 16.05 in. for Various Radii of Curvature.....	54
22.	Lateral S_x Distribution at M.D. Distance 16.05 in. for Various Radii of Curvature.....	55
23.	Lateral Strain x Distribution at M.D. Distance 16.05 in. for Various Radii of Curvature.....	56
24.	Net Lateral Spreading for Various Radii of Curvature.....	62
25.	M.D. S_x Distribution at Lateral Distance 3.33 in. for Various Radii of Curvature.....	64
26.	M.D. S_y Distribution at Lateral Distance 3.33 in. for Various Radii of Curvature.....	65
27.	M.D. S_1 Distribution at Lateral Distance 3.33 in. for Various Radii of Curvature.....	66
28.	M.D. S_2 Distribution at Lateral Distance 3.33 in. for Various Radii of Curvature.....	67
29.	Lateral S_1 Distribution at M.D. Distance 16.05 in. for Various Radii of Curvature.....	69
30.	Lateral S_2 Distribution at M.D. Distance 3.33 in. for Various Radii of Curvature.....	70
31.	M.D. Strain x Distribution at Lateral Distance 3.33 in. for Various Radii of Curvature.....	72
32.	Lateral Strain y Distribution at Lateral Distance 16.05 in. for Various Radii of Curvature.....	73
33.	Edge Displacement on Concave Roller as a Function of Wrap Angle.....	75
34.	Lateral S_y Distribution at M.D. Distance 16.05 in. for Various Wrap Angles.....	77
35.	Edge Displacement as a Function of Tension.....	79
36.	Lateral S_y Distribution at M.D. Distance 16.05 in. for Various Tensions.....	80
37.	S_y at M.D. Distance 16.05 in. and Lateral Distance 3.33 in. for Various Tensions.....	81

38.	Edge Displacement on Concave Roller as a Function of the Modulus of Elasticity.....	82
39.	Lateral S_y Distribution at M.D. Distance 16.05 in. for Various Moduli of Elasticity.....	83
40.	S_y at M.D. Distance 16.05 in. and Lateral Distance 3.33 in. for Various Moduli of Elasticity.....	86
41.	Edge Displacement on Concave Roller as a Function of Poisson's Ratio.....	87
42.	Lateral S_y Distribution at M.D. Distance 16.05 in. for Various Poisson's Ratio Values.....	88
43.	M.D. S_y Distribution at Lateral Distance 3.33 in for Various Poisson's Ratio Values.....	89
44.	Net Lateral Spreading for Various Poisson's Ratio Values.....	91
45.	Edge Displacement on Concave Roller as a Function of Web Thickness.....	92
46.	Lateral S_y Distribution at M.D. Distance 16.05 in. for Various Web Thicknesses.....	93
47.	S_y at M.D. Distance 16.05 in. and Lateral Distance 3.33 in. as a Function of Web Thickness.....	95
48.	Edge Displacement on Concave Roller as a Function of the Coefficient of Friction.....	96
49.	Lateral S_y Distribution at M.D. Distance 16.05 in. for Various Coefficients of Friction.....	98
50.	Theoretical Element Incorporating Zero Traction at Outside Web.....	99
51.	Theoretical Element Incorporating $\tau_{xy} = 0$	100

CHAPTER I

INTRODUCTION

A web is defined as any continuous roll of flexible material. Many products experience a web form sometime during processing. Through the years, several devices have been developed to aid in controlling the web material during these processes. One such device is the concave roller. The concave roller is most often used as a spreading device to alleviate wrinkles and ensure a flat sheet run. It therefore becomes necessary to understand the structural impact of the concave roller on the web material.

The steady-state response of a web encountering a concave roller can yield several equilibrium positions. Shelton [1] states that a web will seek normal entry to a roller. However, once on the roller, the web can have several different reactions. They all involve the interaction between spreading friction forces and slippage.

One such case results in the web seeking the maximum spreading until slippage occurs. In this case the concave roller causes the web to hold a fixed lateral position as it travels across the roller. In another case, slippage becomes predominant. The roller initially spreads the web, but the web then slips back down the sides of the roller as the web travels over the roller. Furthermore, continual slippage occurs between the web and roller which can be deleterious to

the web by causing scratching. The condition of normal entry may be violated in this case.

Leport [2] developed a finite element computer model which simulates the spreading of a web on a concave roller. However, no attempt was made to enforce either of the aforementioned responses. This research will be focused upon the first case in which spreading occurs just to the threshold of slip, in which case the web will still attempt to seek normal entry to the concave roller. The effect of various parameters on the system will also be studied.

1.1 Objectives

The objectives of this study are:

1. To develop and enforce new boundary conditions associated with the first spreading response and to incorporate these into the model developed by Leport.
2. To add additional parameters to the existing model.
3. To study both the validity and the response of the model by analyzing variations in the parameters.

1.2 Literature Survey

There is a lack of significant background material on the analysis of concave rollers. Leport [2] acknowledges this and uses belt theory to describe the spreading action of a concave roller. The initial theory he cites was developed by Swift [3].

Swift addresses the principles behind a belt reacting to coned pulleys and relates this to other pulley geometries. He also develops a general theory of pulley camber. Referring to power transmission,

he develops the concept of an idle arc in which tension is invariant and no relative slipping between belt and pulley occurs. This results in the strain of each longitudinal fiber of the belt conforming to the underlying pulley. This is an important consideration in the upcoming boundary condition development, whereby a strain profile corresponding to a concave roller will be enforced.

Swift also mentions that when a belt enters a pulley at some angle θ from perpendicular, a helical track will result over the pulley in this idle arc region. The lateral rate of travel of the belt across the roll can be found from

$$V_L = V \cdot \tan\theta \quad (1.1)$$

where

V_L = lateral velocity of belt across roll;

V = belt speed; and

θ = helix angle.

This relationship is expressed graphically in Figure 1. Swift continues by mathematically developing a camber associated with the stress distribution related to the pulley profile. This camber acts on the belt as it enters the pulley. Swift expands by developing the cambers associated with various drives and geometries.

Pfeiffer [4] also describes the lateral behavior on a roll. He states that, given some lateral displacement on the roll with an associated helix angle, a web strip will travel laterally driving the helix angle to zero. In other words, the web will seek normal entry to the roll.

This response is aided by "planar action." This action, as described by an unpublished information pamphlet [5], is characterized

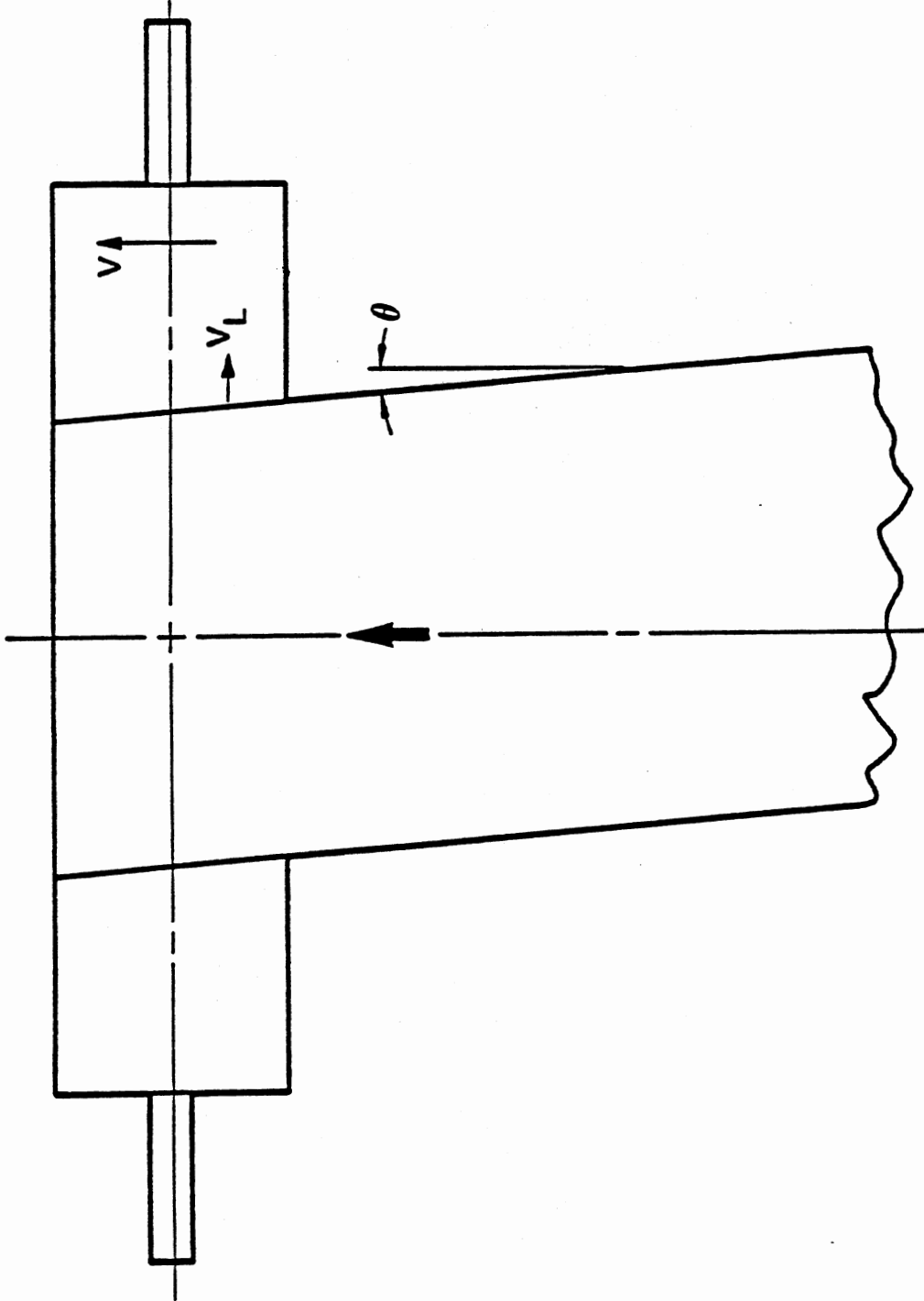


Figure 1. Lateral Web Travel on a Roller

by each point being carried over the surface of the roll in planes perpendicular to the axis of rotation of the roll. In other words, the lateral location that a point first contacts a roll remains unchanged around the roll. The pamphlet also mentions concave rollers but only to address them from an undesirable centering standpoint. The action of a belt on a concave roller is shown in Figure 2.

Shelton [6] applies these and other principles to develop corollaries for web transport. He advances these corollaries by providing various examples of application. Among these is one addressing a web encountering spreaders, particularly mentioning a concave roller. He states that the edges of the web will contact the concave roller tangent to planes perpendicular to the axis of rotation. He concludes that, if friction is sufficient, web edges will remain in planes of lateral locations as the web is carried over the roller. This is the particular case this research addresses.

Daly [7] considers the traction between webs and rolls. He, however, includes the interaction between the porosity of the material and the air entrainment over the roll. This research includes the effect of air entrainment only through the input coefficient of friction.

1.3 Organization

Since this study is an extension of the work done by Leport [2], all of the underlying theory will not be covered again. Instead, the theory behind the generation of new boundary conditions is of primary interest and covered in Chapter II. Chapter III describes the application of this theory to the model. Some of the finer points of the

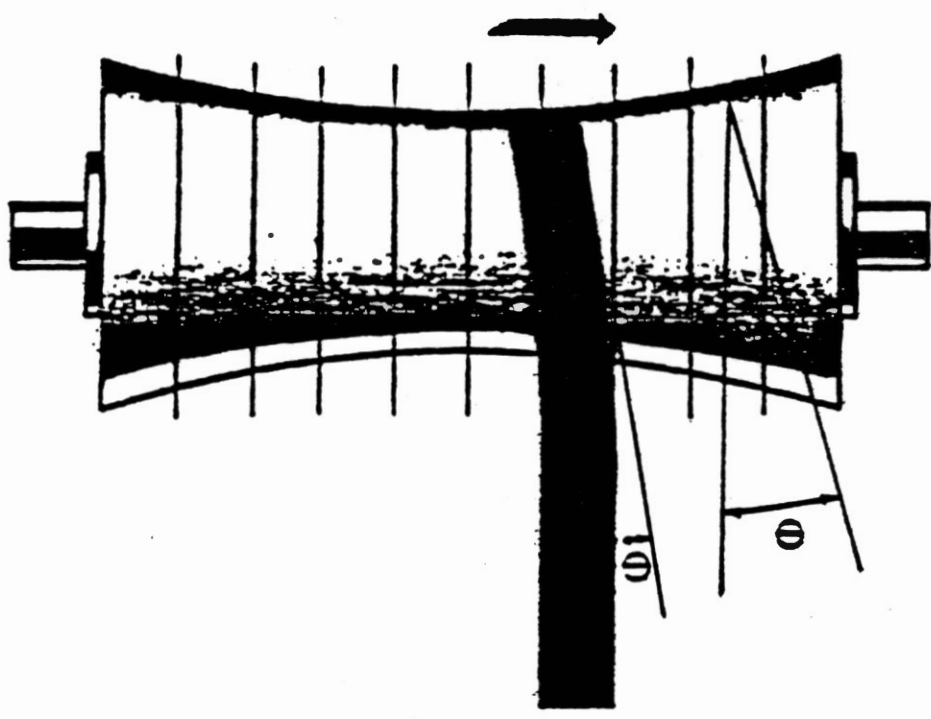


Figure 2. Belt Action on a Concave Roller

model are repeated for clarity. Chapter IV provides a discussion of the results. Numerous plots are provided to both clarify and validate the results of the study. Chapter V contains a general summary of the results and conclusions based on these results. A recommendation for future study is also provided.

CHAPTER II

THEORY DEVELOPMENT FOR BOUNDARY CONDITIONS

To develop the theory behind the interaction of web material and concave rollers, a generalized roller layout must be assumed. Figure 3 shows this generalized model. The model begins with a web span preceding a cylindrical roller labeled A and proceeds over the roller into another span bounded by a concave roller labeled B. The web then wraps around the concave roller and exits into a web span bounded by a cylindrical roller labeled C.

For steady-state conditions, the net amount of material passing through each span must be equal. The net amount of material passing through the spans is a function of both the strain present in the web span and the velocity of the web span. This net amount of material can be found by subtracting the amount of strain in the span from the total amount of material passing through the span. This relationship can be expressed in equation form as

$$(1 - \epsilon_A) \cdot V_A = (1 - \epsilon_B) \cdot V_B \quad (2.1)$$

where

ϵ_A = strain in web immediately prior to roller A;

V_A = velocity of web immediately prior to roller A;

ϵ_B = strain in web immediately prior to roller B; and

V_B = velocity of web immediately prior to roller B.

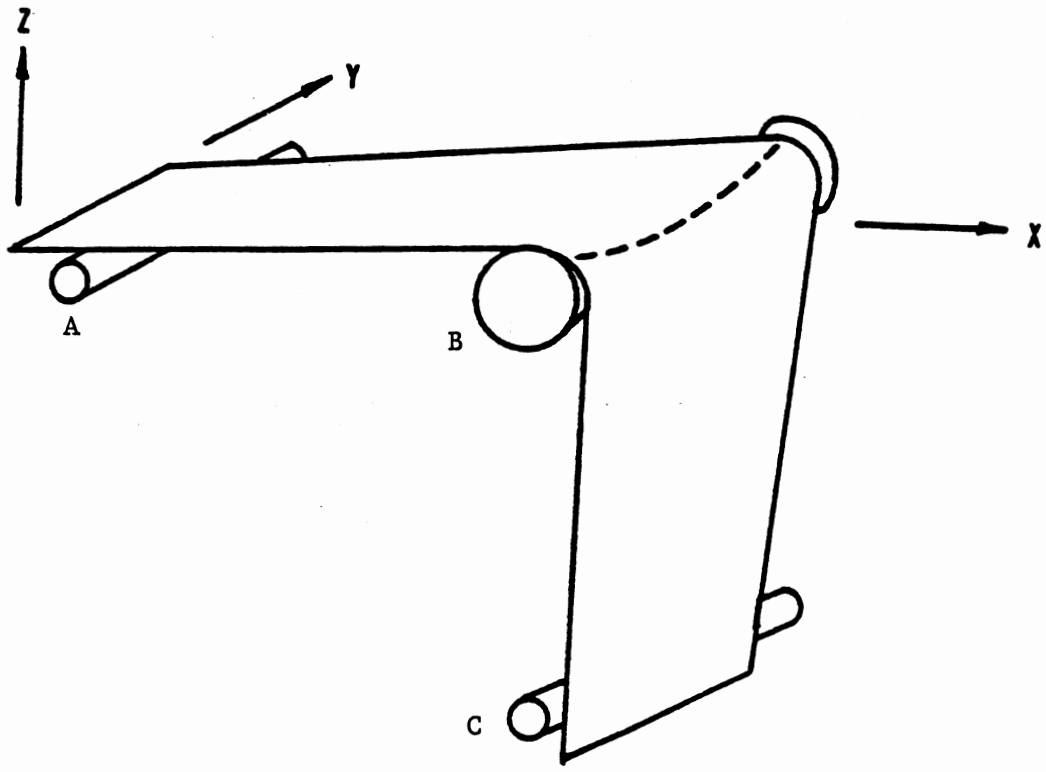


Figure 3. Generalized Roller Layout

Since the velocity of the web span immediately prior to a roller is a function of the radius and the angular velocity of that roller, Equation (2.1) can be rewritten as

$$(1 - \epsilon_A) \cdot r_A \cdot \omega_A = (1 - \epsilon_B) \cdot r_B \cdot \omega_B \quad (2.2)$$

or

$$\frac{(1 - \epsilon_A)}{(1 - \epsilon_B)} = \frac{r_B \cdot \omega_B}{r_A \cdot \omega_A} \quad (2.3)$$

where

r_A = radius of roller A;

r_B = radius of roller B;

ω_A = angular velocity of roller A; and

ω_B = angular velocity of roller B.

Equation (2.3) is Shelton's [8] continuity equation for web spans between rollers.

Several of the variables in Equation (2.3) are either known or can be directly calculated due to the physical and operating constraints of the system. The radii of both rollers are directly known. Since roller A is cylindrical, r_A is constant. Roller B is a concave roller and the radius is a function of the lateral location on that roller. Since the nominal web line velocity of the system can be measured and r_A is constant, ω_A can be found from the relationship

$$V_A = r_A \cdot \omega_A \quad (2.4)$$

The strain immediately prior to roller A can also be calculated. If the tension in the web is known, the stress in an axially loaded member can be found from

$$S_x = \frac{T}{A} \quad (2.5)$$

where

S_x = x-direction stress;

T = total tension in the line; and

A = cross-sectional area of the web.

The area is also known and expressed as

$$A = t \cdot ww \quad (2.6)$$

where t is the thickness of the web, and ww is the width of the web.

From Hooke's Law,

$$\epsilon = \frac{S_x}{E} \quad (2.7)$$

where E is the modulus of elasticity. Substituting Equations (2.5) and (2.6) into (2.7) yields

$$\epsilon = \frac{T}{t \cdot ww \cdot E} \quad (2.8)$$

Equation (2.8) can now be used to find the strain immediately prior to roller A.

Since Equation (2.3) contains two unknowns, ϵ_B and ω_B , another equation is needed to obtain a unique solution. This second equation can be found by assuming a constant line tension exists from one span to the next. If the line tension between spans is constant, the average machine direction strain must also be constant between spans. Enforcing these average strains will yield the second equation. Figure 4 shows a graphical interpretation of the strains.

Since roller A has a constant radius, the average strain immediately prior to it is constant throughout the width of the web. This yields

$$\epsilon_{A \text{ avg}} = \frac{1}{WW} \int_0^{WW} \epsilon_A \, dy = \epsilon_A \quad (2.9)$$

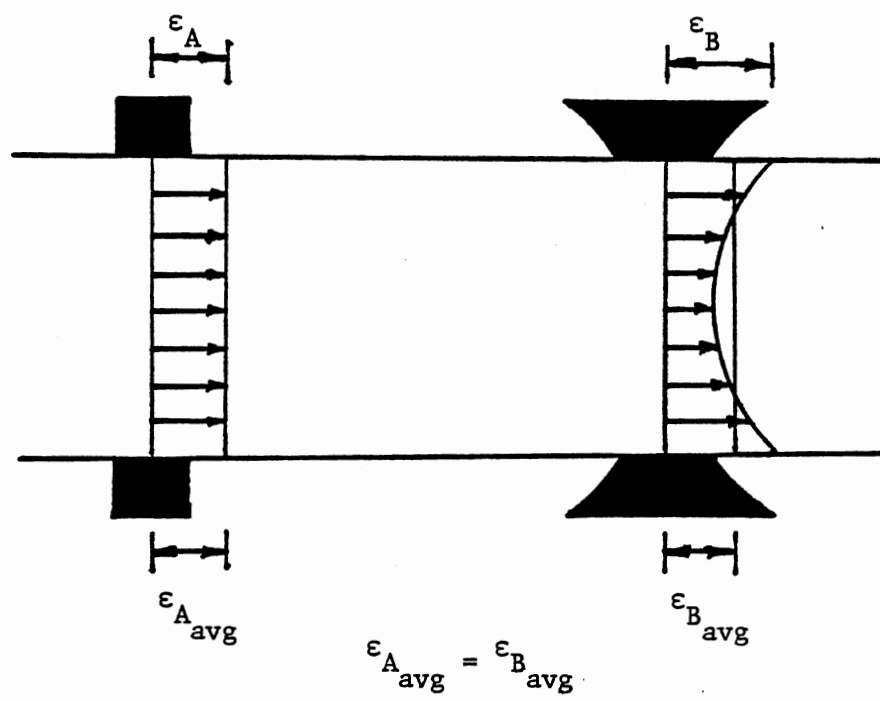


Figure 4. Graphical Interpretation of Average Strain Criteria

The strain immediately prior to the concave roller can be found from Equation (2.3). Solving for ϵ_B yields

$$\epsilon_B = 1 - \frac{(1 - \epsilon_A) \cdot r_A \cdot \omega_A}{r_B \cdot \omega_B} \quad (2.10)$$

However, the radius of a concave roller is a function of the lateral location on the roller, as shown in Figure 5. From Figure 5, r_B can be found. In equation form,

$$r_B = \text{Capr} + \text{Rzero} - \sqrt{\text{Capr}^2 - y^2} \quad (2.11)$$

where the variables are the same as indicated in Figure 5. Substituting Equation (2.11) into Equation (2.10) yields

$$\epsilon_B = 1 - \frac{(1 - \epsilon_A) \cdot r_A \cdot \omega_A}{(\text{Capr} + \text{Rzero} - \sqrt{\text{Capr}^2 - y^2}) \cdot \omega_B} \quad (2.12)$$

For the average strain,

$$\epsilon_{B_{\text{avg}}} = \frac{1}{\text{WW}} \int_0^{\text{WW}} \left[1 - \frac{(1 - \epsilon_A) \cdot r_A \cdot \omega_A}{(\text{Capr} + \text{Rzero} - \sqrt{\text{Capr}^2 - y^2}) \cdot \omega_B} \right] dy \quad (2.13)$$

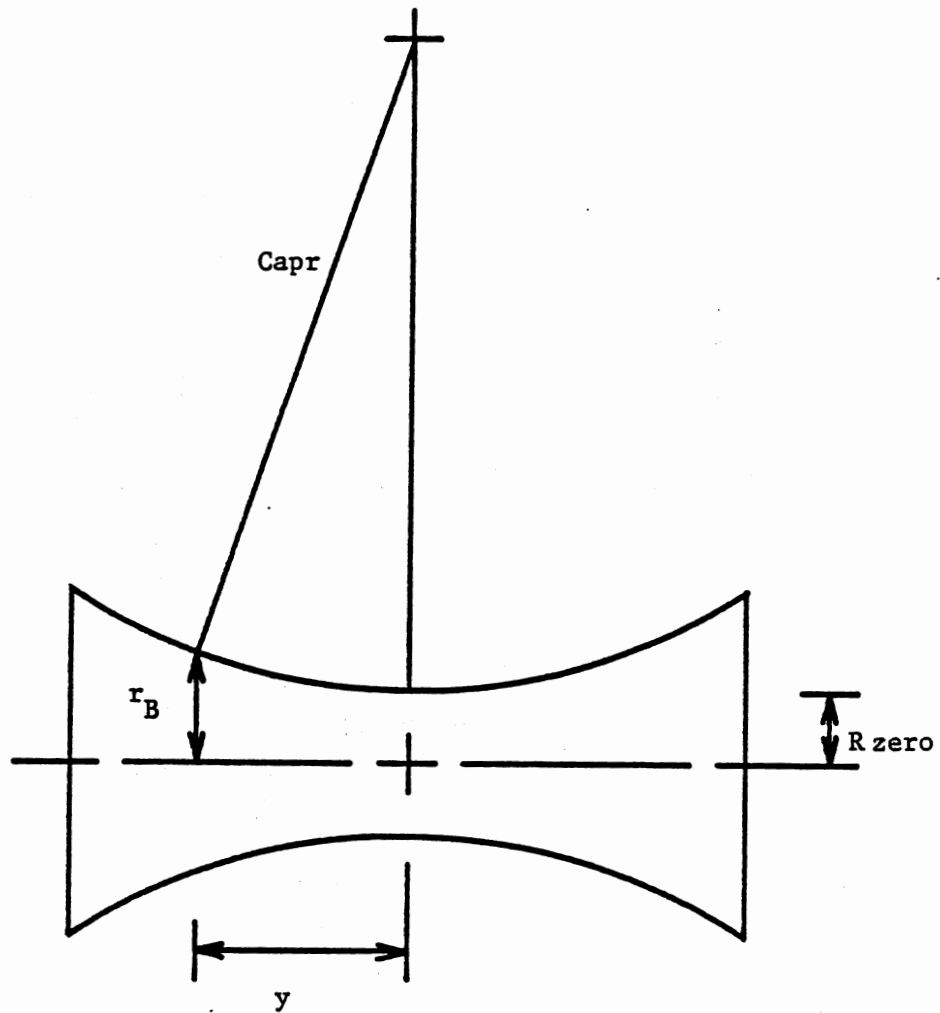
The second equation can now be found. As mentioned, the second equation arises from equating the average strains of the web regions immediately prior to the two rollers, or

$$\epsilon_{A_{\text{avg}}} = \epsilon_{B_{\text{avg}}} \quad (2.14)$$

Substituting in the appropriate values yields

$$\epsilon_A = \frac{1}{\text{WW}} \int_0^{\text{WW}} \left[1 - \frac{(1 - \epsilon_A) \cdot r_A \cdot \omega_A}{(\text{Capr} + \text{Rzero} - \sqrt{\text{Capr}^2 - y^2}) \cdot \omega_B} \right] dy \quad (2.15)$$

This equation cannot be directly solved for ω_B because the radius of the concave roller is a function of the lateral location. A search



where $Capr$ = Circular arc profile radius
of curvature

$Rzero$ = Roller base radius

y = Lateral location from
Centerline

r_B = Radius of Concave Roller at
Lateral Location y

Figure 5., Geometry of Concave Roller

for ω_B must therefore be performed until the one that satisfies the equation is found. In other words, a trial value of ω_B is chosen, the argument is integrated and averaged, and the answer is then compared to ϵ_A . If the difference is not within a specified tolerance, a new ω_B is chosen and the procedure is repeated.

CHAPTER III

ANALYTICAL STUDY

The purpose of this study is to develop new boundary conditions which better represent the response of a web on a concave roller. The existing programs are also modified to incorporate additional parameters to make them more flexible and realistic. Variations in the parameters are also studied to gain insight to the impact of these parameters on the steady-state response of webs encountering concave rollers, as well as aid in checking the validity of the model.

This report assumes the reader has adequate background in the theory and formulation of the finite element method. For review, the reader may consult Segerlind [9] or Leport [2] for a comprehensive explanation of the fundamentals. This finite element program utilizes two-dimensional elasticity for plane stress conditions. Plane stress is required because webs are typically very thin with respect to their overall width and length. Simplex triangles are used throughout the model. This type of element is acceptable for axially loaded conditions where bending has no significant contribution.

The following assumptions were made to reduce the problem size or to represent physical boundary conditions which the concave roll enforces upon the web. Both lateral symmetry and machine direction symmetry are assumed and incorporated. Laterally, an axis of symmetry occurs in the middle of the web extending the full machine direction

distance. This prompts the coordinate system to originate at the middle of the cylindrical roller. The x-axis is typically associated with the machine direction. The y-axis is extended laterally across the web. The modeling technique incorporates a machine direction symmetry about the concave roller. The model therefore ends halfway around the roller. The symmetric model is shown in Figure 6. To enforce the lateral symmetry, the nodes along the x-axis are constrained to resist any lateral movement, yet allowed to displace in the machine direction.

3.1 Finite Element Model

The computer code MSHGNR develops the finite element mesh for the model. Although the model is continuous, the code acknowledges two distinct spans. The first span is the entry span which begins at the cylindrical roller and proceeds to contact the concave roller. The second span deals with that portion of the web in contact with the concave roller.

The user is required to input variables which sufficiently define the system. MSHGNR uses some of these variables to generate global coordinates and the associated element connectivities. A list of these variables is shown in Table I. Other parameters are also required by MSHGNR. These additional values deal with the material properties of the web (e.g., thickness, modulus of elasticity, Poisson's ratio) and the operating constraints of the system (e.g., tension, wrap angle around concave roller). Appendix C contains a complete list and description of the user definable input in the comments of the code MSHGNR.

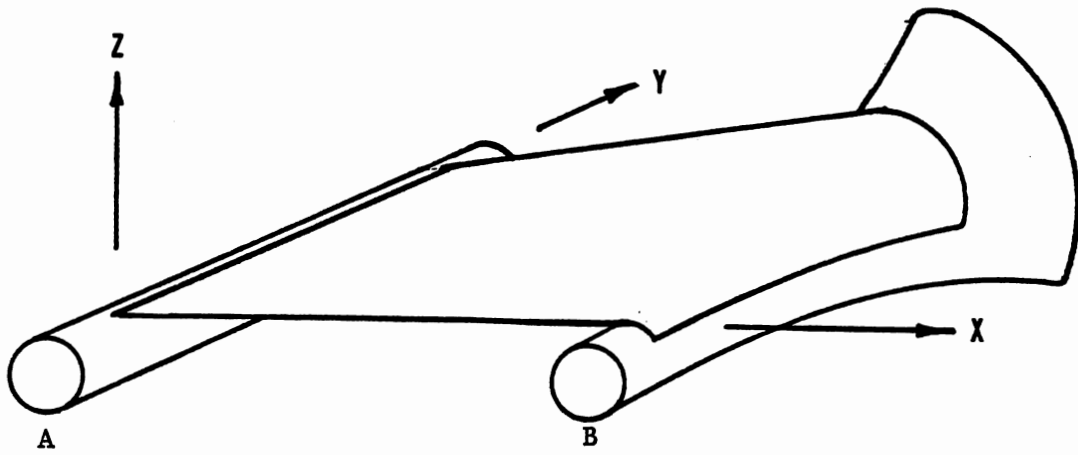


Figure 6. Symmetric Model

TABLE I
A PARTIAL LIST OF THE REQUIRED INPUT FOR
THE COMPUTER CODE MSHGNR

Variable Name	Variable Description
WW	Width of the web
ALBR	Length of the web before the concave roller (entry span length)
RZERO	Roller base radius (applies to both the cylindrical and concave rollers)
CAPR	Circular arc profile radius of curvature
NXB	Number of element intervals in the x-direction
NAR	Number of element intervals over the concave roller
NY	Number of element intervals in the y-direction

The entry span just prior to the concave roller is a region of sharp transition due to the abrupt changes induced in the web by the concave roller. MSHGNR automatically increases the element density in the region just prior to the concave roller for a distance of 25 percent of the entry span length. This approximate distance of 25 percent is based upon computer runs using the two-dimensional finite element code STRESS [10]. A completely planar mesh using only the entry span was used in the analyses. Linear and parabolic displacements were input at one end of the span. The results of the analyses showed that the input displacement distributions caused a cross machine direction variation in machine direction stresses from the applied displacement

end of the span to a point which was about 25 percent of the span length downstream. At this location, the lateral distribution of the machine direction stresses became approximately uniform and continued this uniform lateral distribution throughout the remaining length of the web. In other words, the major effect of the linear and parabolic input distributions had been lost in the aforementioned distance away from that end of the web. Figures 7 and 8 show this transition for linear and parabolic displacements, respectively.

A more accurate modeling of this transition region was incorporated into MSHGNR. For example, if the entry span is 16 inches long and 16 machine direction element intervals have been specified, MSHGNR places 8 machine direction element intervals in the first 12 inches of the entry span and 8 intervals in the remaining 4 inches. If an odd number of element intervals is specified, the smaller number of intervals is placed in the increased element density region. A planar view of the general mesh is shown in Figure 9. The variables shown are the same as those defined in Table I.

A single finite element mesh was used throughout the analysis. The entry span length was 16 inches long and the symmetric width of the web was 4 inches. Fifteen element intervals were used in the machine direction and ten intervals were used laterally. Five machine direction element intervals were specified around the concave roller. A roller base radius of 1.125 inches was also used. Figure 10 shows the mesh used for the analysis. This figure does not show the increase in the machine direction lengths of the elements laterally across the concave roller. The increase in length is due to the

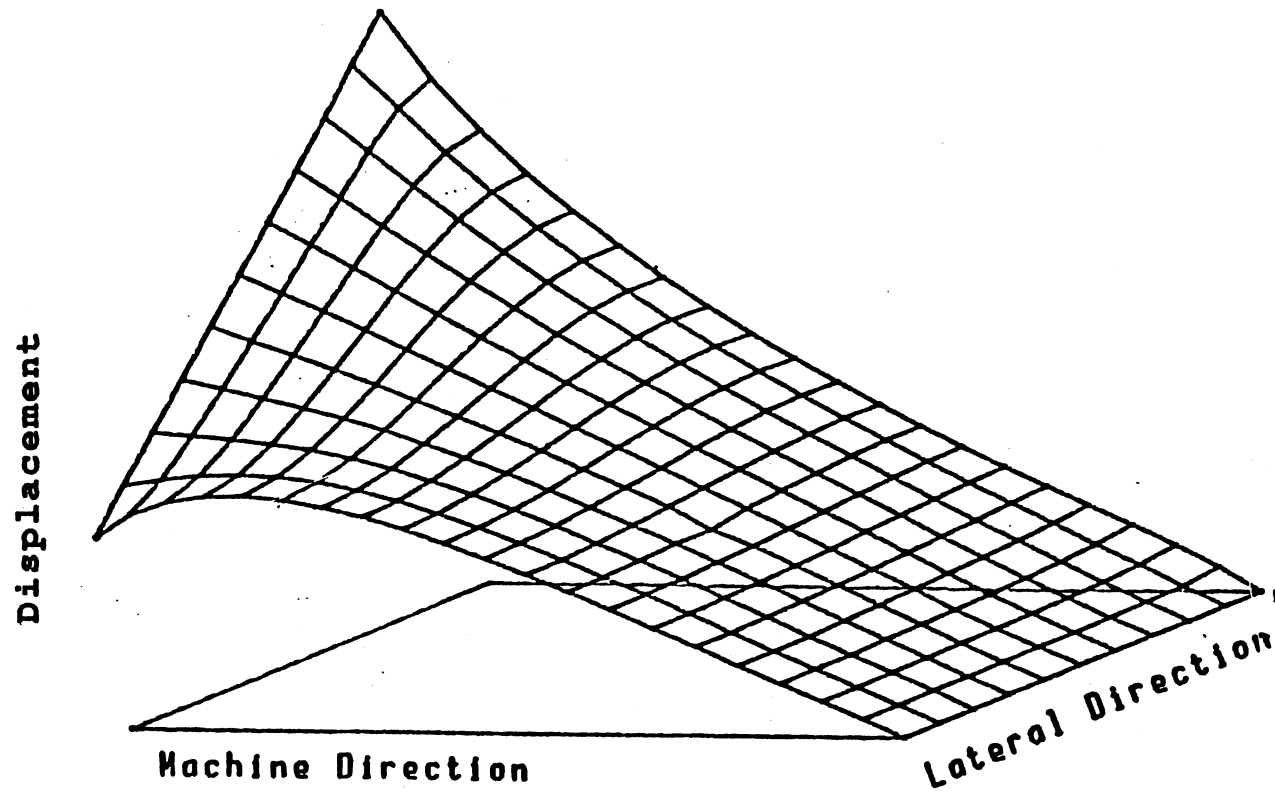


Figure 7. Effect of an Enforced Machine Direction Linear Displacement Distribution on the Entry Span

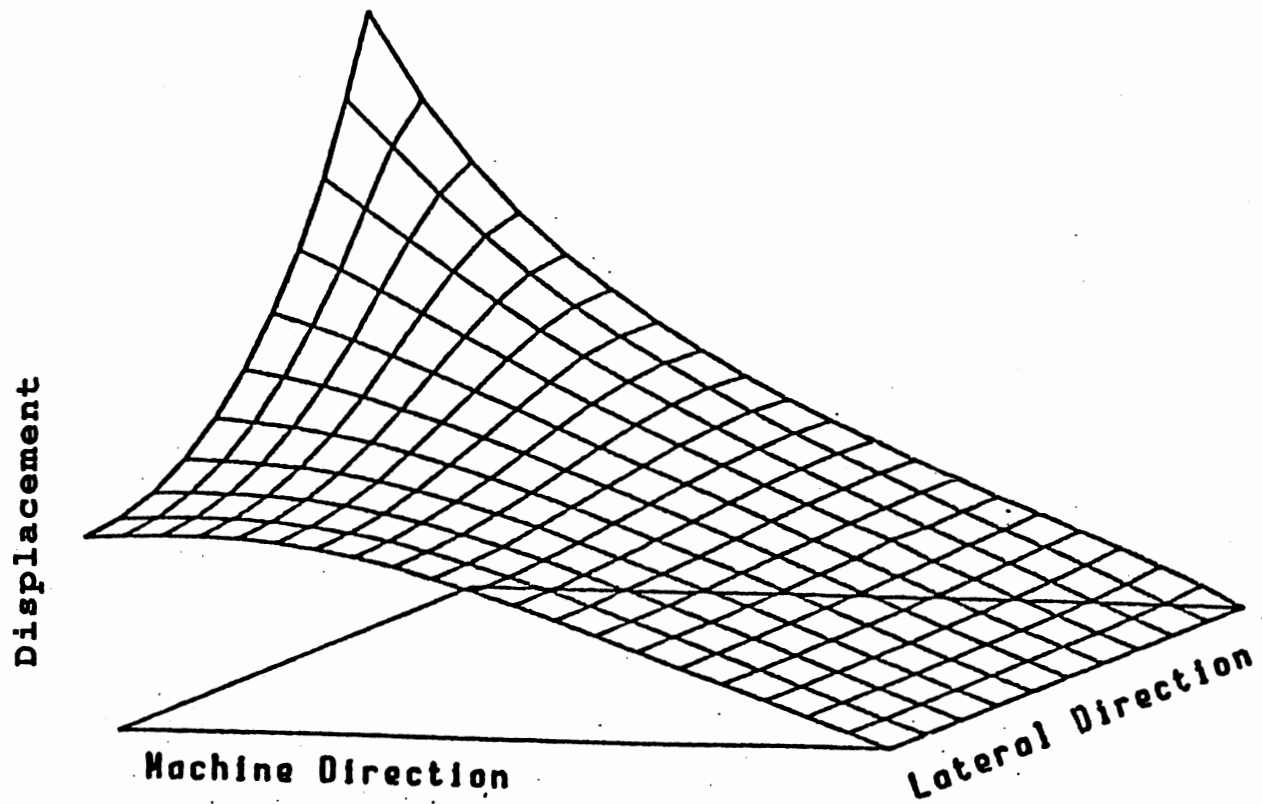


Figure 8. Effect of an Enforced Machine Direction Parabolic Displacement Distribution on the Entry Span

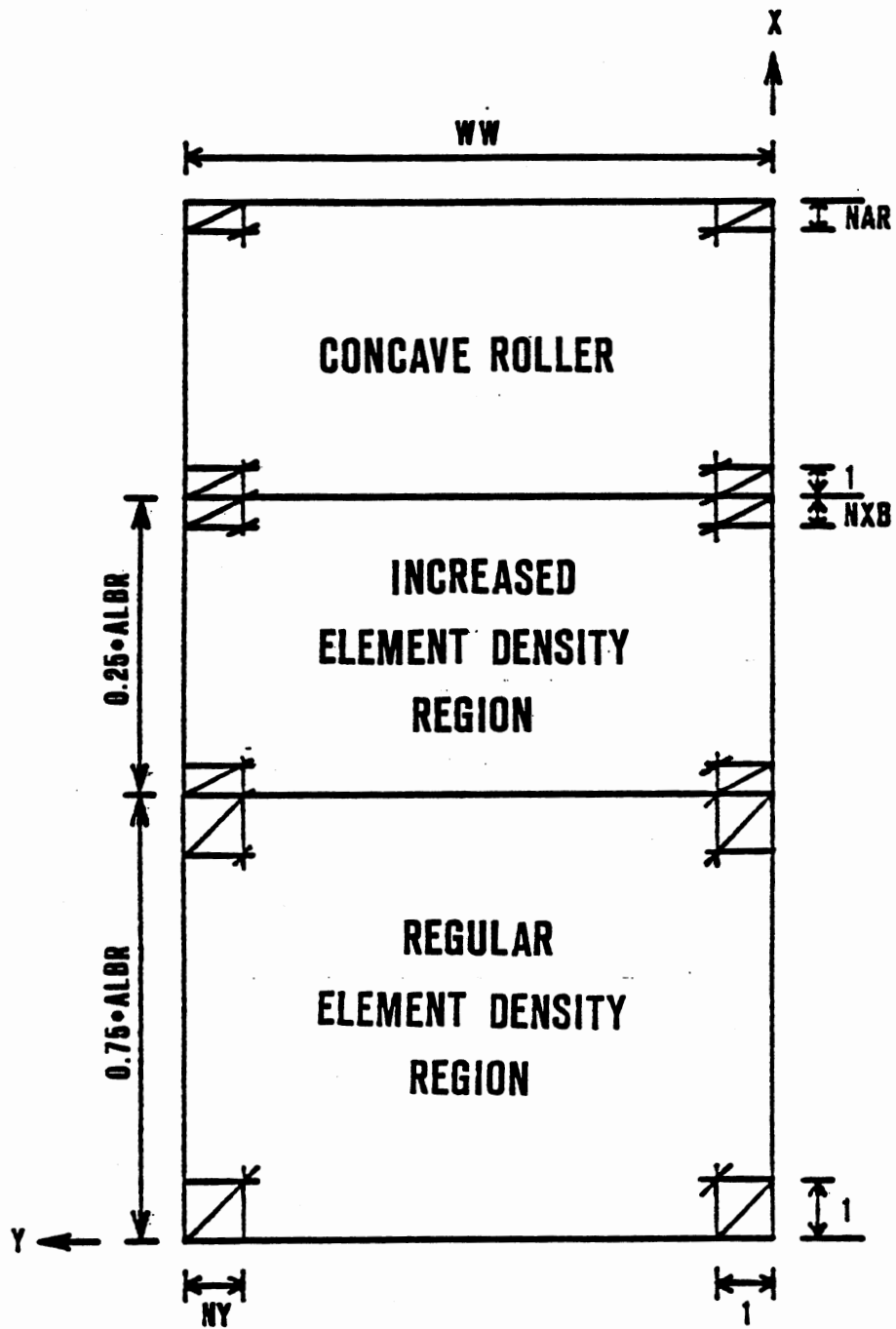


Figure 9. Planar View of Finite Element Mesh

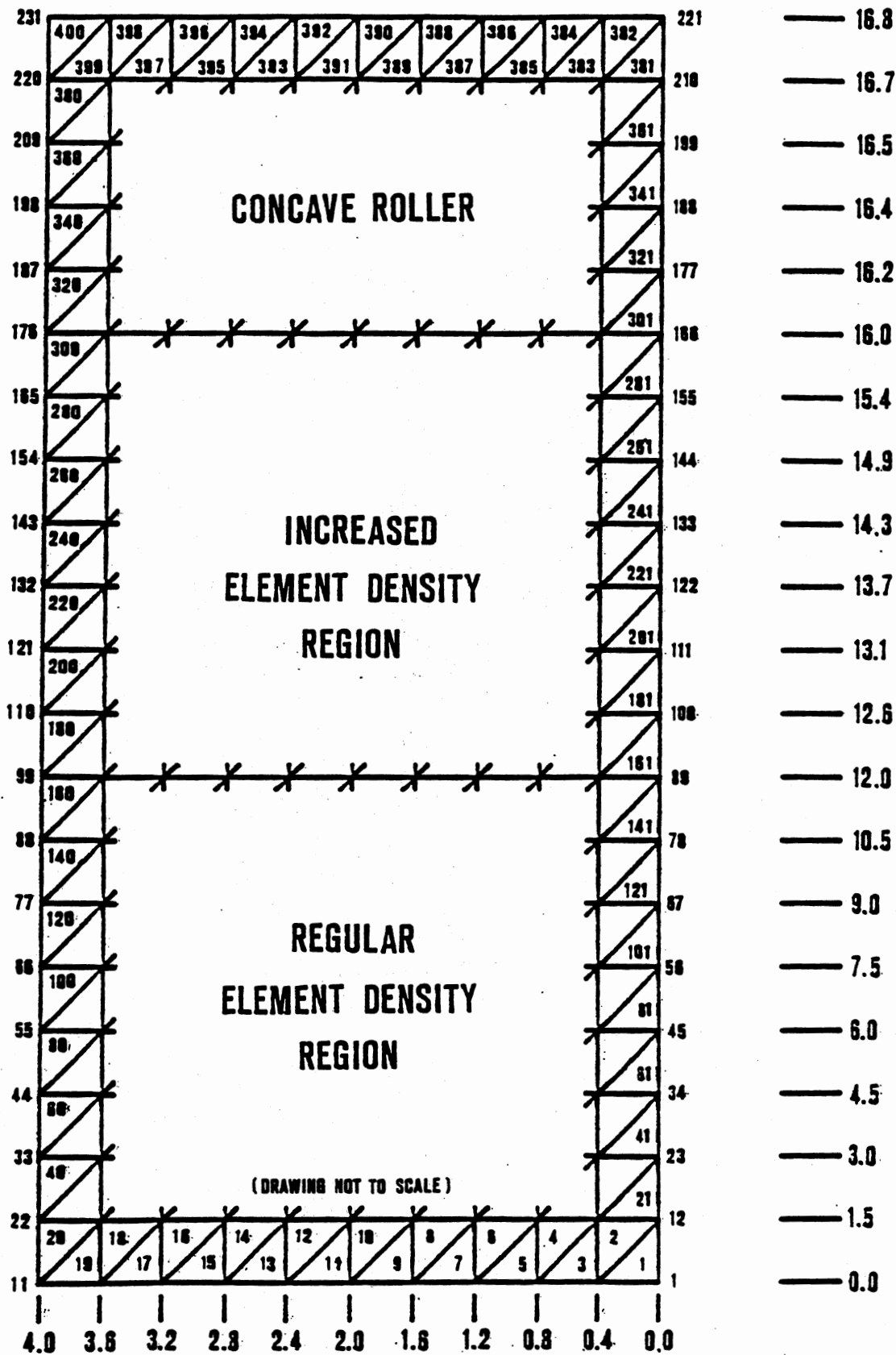


Figure 10. Planar View of Mesh Used for Study

changing radius of the concave roller. The machine direction distances shown correspond to the centerline of the web.

3.2 Average Plane Transformation

The presence of the concave roller and the resulting web wrap around it cause out-of-plane (z) coordinate locations. As mentioned in theory, the outer radii of a concave roller are larger than the inner radii. By referring again to Figure 6, it is seen that the entry span must move out of the x - y plane contact with the cylindrical roller to the out-of-plane contact with the concave roller. A linear transition is assumed for the entry span between the in-plane contact with the cylindrical roller to the out-of-plane contact with the concave roller. More out-of-plane locations occur in the web span that wraps around the concave roller. These out-of-plane coordinates cause a problem with the two-dimensional analysis. A node displacement in one element causes out-of-plane displacements for the adjoining elements. Figure 11 shows a graphical representation of this problem. To address this problem, the code develops a new coordinate system for the nodes based on adjacent planes surrounding the node.

As previously mentioned, the MSHGNR program generates global coordinates and element connectivities based on user input. These values are then written to an output file to be read by the main program, CONCAVE. CONCAVE reads in the coordinates associated with each element. A coordinate transformation matrix $[T]$ is computed (see Segerlind [9] or Leport [2]) to transform the coordinates to a local system associated with each particular element. Once transformed, an elemental stiffness matrix is developed using the procedure described

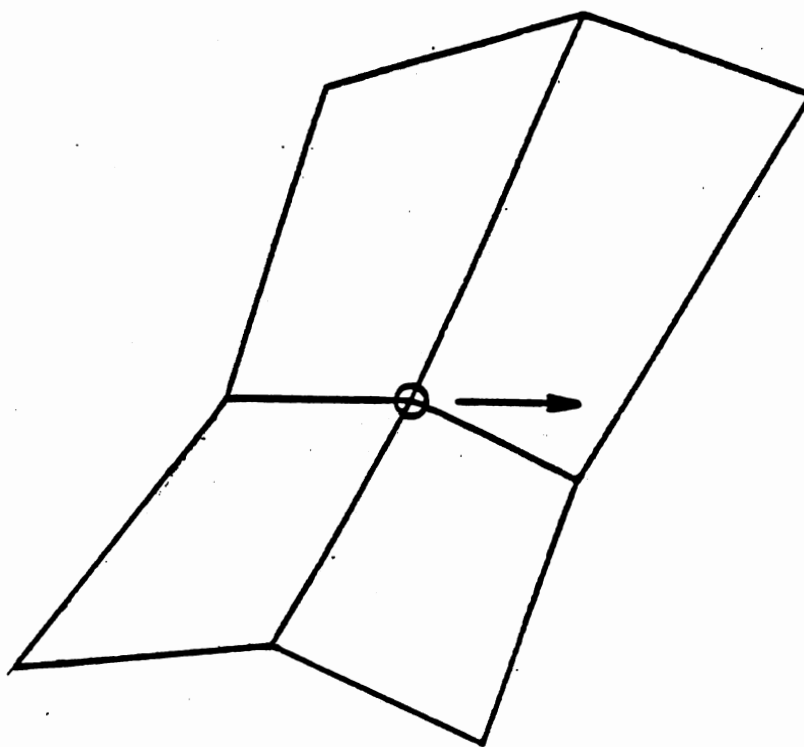


Figure 11. Graphical Interpretation of Out-of-Plane Displacements

in Segerlind [9]. The elemental stiffness matrix, denoted by $[K^{(e)}]$, is then expanded to three dimensions by inserting rows and columns of zeros in the third, sixth, and ninth degree-of-freedom locations. $[K^{(e)}]$ is then converted back to the global coordinate system by the relationship

$$[K_G^{(e)}] = [T]^T \cdot [K^{(e)}] \cdot [T] \quad (3.1)$$

A global stiffness matrix for the system is assembled by placing the entries from the global elemental matrix into the corresponding degree-of-freedom locations for the global matrix.

All of the procedures to this point have involved standard assembly techniques and transformations. The problem of out-of-plane displacements still has not been addressed. This is done by transforming the global stiffness matrix to a new local system based on nodes instead of elements. This new coordinate system is based on averaging the planes surrounding each node. The coordinate system is then able to better represent nodal displacements because the nodes displace only in the plane associated with it. Consequently, the z degree-of-freedom of every node throughout the model must be constrained against displacement.

This procedure is accomplished in the CONCAVE subroutine called SKEWED. For interior nodes, the program finds the four closest nodes to develop planes as shown in Figure 12. The planes are then averaged and a coordinate transformation matrix, denoted by $[T']$, is developed based on directional cosines. The degree-of-freedoms in the global stiffness matrix associated with this node are then modified. This modification is accomplished by pre-multiplying the appropriate rows

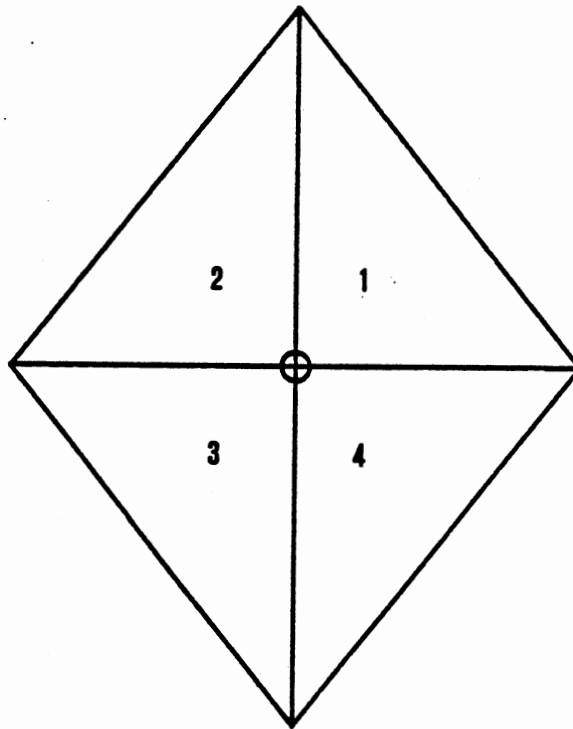


Figure 12. Planes Used for
Interior Needs

of the global stiffness matrix by the new transformation matrix $[T']$ and then post-multiplying the appropriate columns by the transpose of $[T']$. Appendix A describes this procedure in detail. This procedure is repeated for all the nodes with a slight modification for edge and corner nodes. Edge nodes only average two planes and corner nodes use only one plane as shown in Figure 13.

3.3 Generation of Boundary Conditions

A variety of boundary conditions is required to develop an accurate model. Some of these conditions are obtained by a preliminary partial run through the computer program. Others are applied by appending the stiffness matrix with additional compatibility equations.

A preliminary run through the entry span of the model is required to generate displacements to enforce in the final run. These values are needed to compensate for the abrupt changes occurring between the entry span and the span on the concave roller. Since, for a concave roller, the exterior radii are larger than the interior radii, the exterior web fibers experience more strain than the interior fibers. However, as described in the theory section, the average strain of the system must remain constant. The constant strain immediately prior to the cylindrical roller must therefore be redistributed for the web portion immediately prior to the concave roller such that the average strains are equal. The program must be able to do this to accurately represent the steady-state response of the system. The preliminary run is used to find this redistribution so it can be applied to the final run in the form of displacements.

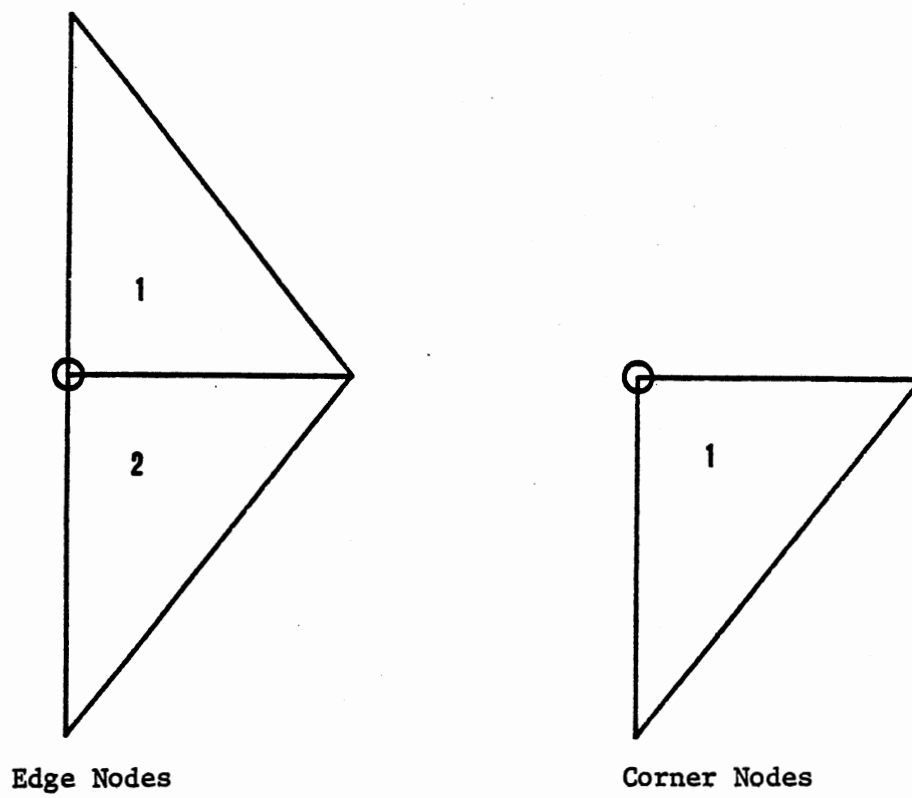


Figure 13. Planes Used for Edge and Corner Nodes

The theory section presented the equations required to find $\epsilon_{A_{avg}}$ and $\epsilon_{B_{avg}}$, the average strains immediately prior to the cylindrical and concave rollers, respectively. The average ϵ_A can be found from Equation (2.8) via Equation (2.9), or

$$\epsilon_{A_{avg}} = \frac{T}{t \cdot WW \cdot E} \quad (2.8)$$

where the variables are the same as previously defined. Likewise, Equation (2.13) shows the average strain immediately prior to the concave roller B as

$$\epsilon_{B_{avg}} = \frac{1}{WW} \int_0^{WW} \left[1 - \frac{(1 - \epsilon_A) \cdot r_A \cdot \omega_A}{(Capr + Rzero - \sqrt{Capr^2 - y^2}) \cdot \omega_B} \right] dy \quad (2.13)$$

Since the average ϵ_B cannot be directly found, MSHGNR performs an incremental search to find the ω_B necessary to satisfy Equation (2.14).

Once ω_B is found, the resulting strains immediately prior to the concave roller are found at the desired lateral locations from Equation (2.12), or

$$\epsilon_B = 1 - \frac{(1 - \epsilon_A) \cdot r_A \cdot \omega_A}{(Capr + Rzero - \sqrt{Capr^2 - y^2}) \cdot \omega_B} \quad (2.12)$$

With the strains now known, differential forces can be found to apply to the preliminary entry span run. The output machine direction displacements at the entry span nodes in contact with the concave roller can then be used to provide adjustments for the final run. MSHGNR calculates the required forces by the following procedure:

1. $\epsilon_B - \epsilon_A$ is calculated for each lateral node location Y.
2. Forces are then found for each node by

$$F_i = (\epsilon_{B_i} - \epsilon_A) \cdot E \cdot A_i \quad (3.2)$$

E = modulus of elasticity;

A = contribution area for each node location; and

i = index ranging from 1 to the number of lateral node locations.

A flowchart for the search procedure and force calculation used in MSHGNR is shown in Figure 14. The calculated forces are written to an output file to be read by the program CONCAVE.

The preliminary execution of CONCAVE involves only the entry span of the web. The same stiffness matrix formulation and transformation procedure previously described are used but only for the elements and nodes associated with the entry span. The forces are applied in the machine direction at the end of the web in contact with the concave roller. The cylindrical roller end of the entry span is constrained against machine direction displacements yet allowed to displace laterally. Once the system of equations is solved, the resulting machine direction displacements at the end of the entry span portion of the web are the desired adjustments for the concave roller.

MSHGNR is also used to calculate other displacements for the nodes wrapping around the concave roller. Enforced machine direction displacements are required around the roller to enforce the no slip-page requirement of the web response this model addresses. These displacements induce the proper machine direction stresses which in turn induce the required normal forces necessary to generate the lateral stresses. In other words, the machine direction stress contribution to the normal force is initially constant around the concave roller for each lateral location. This ensures that a relaxation of the normal forces does not occur around the roller, which would result in a decrease of the lateral spreading traction around the roller. If

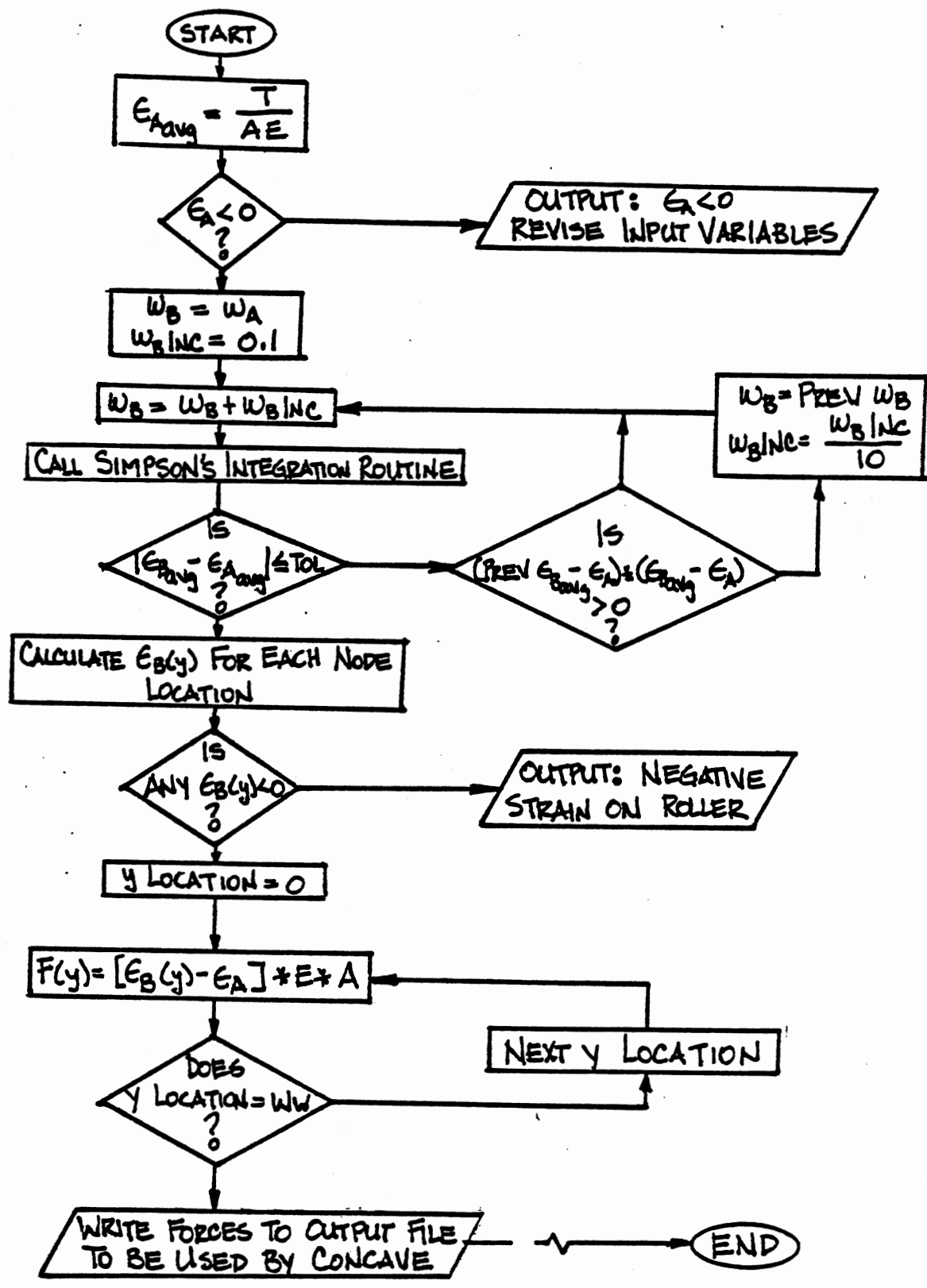


Figure 14. Search Procedure and Force Calculation Used in MSHGNR

this decrease were allowed, it would result in the web "slipping" back to lesser lateral displacements. MSHGNR provides these desired machine direction displacements for the nodes around the roller. By using half of the wrap angle, the number of elements around the roller, and the strain at the desired lateral location, the machine direction displacements for each node on the roller can be calculated from the relationship

$$u_i = \left(\frac{\theta_n}{360}\right) \cdot 2 \cdot \pi \cdot r_{B_i} \cdot \epsilon_{B_i} \quad (3.3)$$

For this equation, i represents the nodes on the roller and u_i the desired displacements; r_{B_i} and ϵ_{B_i} represent the radius and associated strain for the desired node i ; θ_n represents the cumulative angle associated with the corresponding row of nodes around the roller in degrees. θ_n is found by dividing half the wrap angle (taking advantage of symmetry) by the number of elements around the roller. For example, if the wrap angle is 90° and five element intervals are specified around the roller, the angle increment would be 45° divided by 5, or 9° . The corresponding θ_n values would then be 0° , 9° , 18° , 27° , 36° , and 45° . Obviously, the first row of nodes would have no displacement associated with it. MSHGNR writes these values to an output file to be read by CONCAVE. CONCAVE then adds these displacements to the adjustments found from the preliminary run. The final displacements are enforced in the machine direction around the concave roller.

Another set of applied boundary conditions deals with the lateral displacements of the web on the concave roller. As mentioned in the introduction, the case this program models requires uniform lateral

spreading around the concave roller. In other words, each node within a column must have the same lateral displacement. The term column is used here to denote all the nodes around the concave roller which have the same lateral location. The required lateral displacement "locks" can be achieved by appending the stiffness matrix with additional constraint equations. The equations stem from the relationship that the subtraction of the lateral degree-of-freedom of any node in a column from the lateral degree-of-freedom of the first node in that column must equal zero. Figure 15 shows a graphical representation of this requirement. Letting v_i represent the lateral displacement of the node associated with lateral location i , the equations may be written as

$$\begin{aligned}
 v_1 - v_2 &= 0 \\
 v_1 - v_3 &= 0 \\
 &'' \\
 v_1 - v_i &= 0 \\
 &'' \\
 v_1 - v_n &= 0
 \end{aligned}
 \tag{3.4}$$

where n is the number of nodes around the concave roller.

These equations can be added to the stiffness matrix by simply placing 1's and -1's in the appropriate degree-of-freedom locations and 0's in all other locations. This must be done for both the rows and columns to maintain matrix symmetry. Since the general stiffness equation has the form

$$\{F\} = [K] \cdot \{X\}
 \tag{3.5}$$

the force vector $\{F\}$ and displacement vector $\{X\}$ must also be appended to maintain consistency. The force vector is appended with the displacements of the constraint equations, in this case zeros. When the system of equations is solved, the displacement vector will be

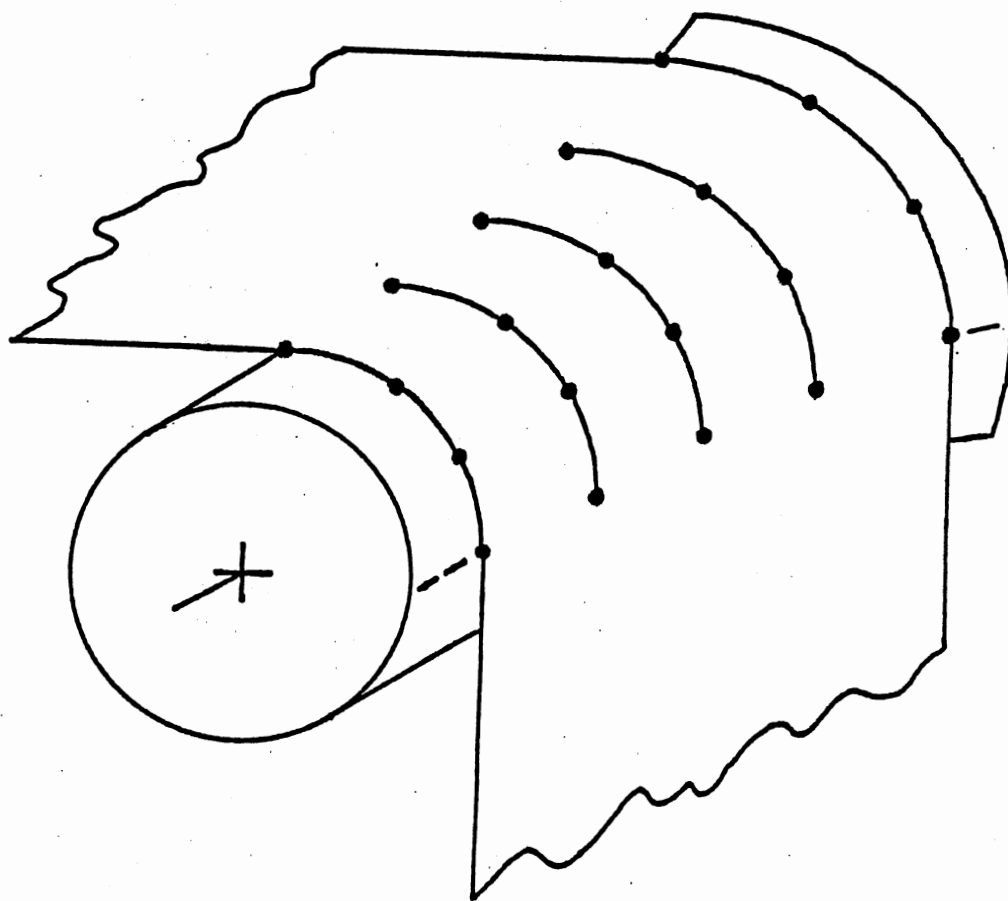


Figure 15. Lateral Displacement "Locks"

appended with the forces required to enforce the constraint equations. The modifications are shown again in Appendix B.

The final set of boundary conditions deals with the operating tension of the system. The tension is input to the upstream web span at the upstream cylindrical roller in the form of displacements. To find the required displacements, Equation (2.9) is again used to find the strain for the cylindrical roller A. This uniform strain is then multiplied by the entry span length to obtain the proper displacements. These displacements are applied in the negative of the machine direction to the beginning of the model. MSHGNR is used to find these displacements. The operating tension is input to the elements on the concave roller via the displacement boundary conditions associated with Equation (3.3). Recall that the average value of ϵ_A is the uniform strain associated with the operating tension.

3.4 Spreading Analysis

The spreading of the web due to the concave roller is a non-linear response. Any computer analysis of the spreading behavior cannot be directly solved and must therefore be approached from an iteration standpoint. Two stiffness matrices are used throughout the analysis. Both are in the local coordinate system of average planes as previously described. The first matrix, labeled GSM, is the full unmodified matrix. The term unmodified indicates that the z degree-of-freedom and all symmetric considerations as well as all known displacements have not yet been enforced. The modified matrix is labeled GTSM.

The spreading analysis begins by solving the modified stiffness matrix GTSM for the displacements. The nodes in contact with the concave roller are of primary concern. The forces and corresponding displacements of these nodes are iterated upon in the spreading analysis.

A problem exists with the entry and exit of the web to and from the concave roller. The first and last rows of nodes generate some negative normal forces. These resulting negative normal forces are best understood in physical terms. The internal rows of nodes have other rows of nodes on both sides in contact with the roller, thereby keeping them fully confined to the roller. The two exterior rows of nodes on the roller have only one adjacent row of nodes in contact with the roller. This results in the web trying to "lift-off" the roller at these exterior rows and thus the negative normal forces.

To address this problem, only the interior rows of nodes are used to calculate the friction forces. The friction forces for the nodes on the exterior rows are supplied by using half of the friction force of the corresponding lateral node on the adjacent row in contact with the roller. Only half of the friction forces are applied at the last row of nodes because machine direction symmetry is enforced. Likewise, half of the friction forces are applied to the first row of nodes because only half the area associated with this row of nodes is in contact with the roller. Figure 16 is supplied to better explain this assumption. This figure represents the portion of the web in contact with the concave roller. If this web span were unwrapped from the roller and laid on a flat surface, it would appear as shown. The exterior nodes simply have half of the spreading force associated with their adjacent interior counterparts.

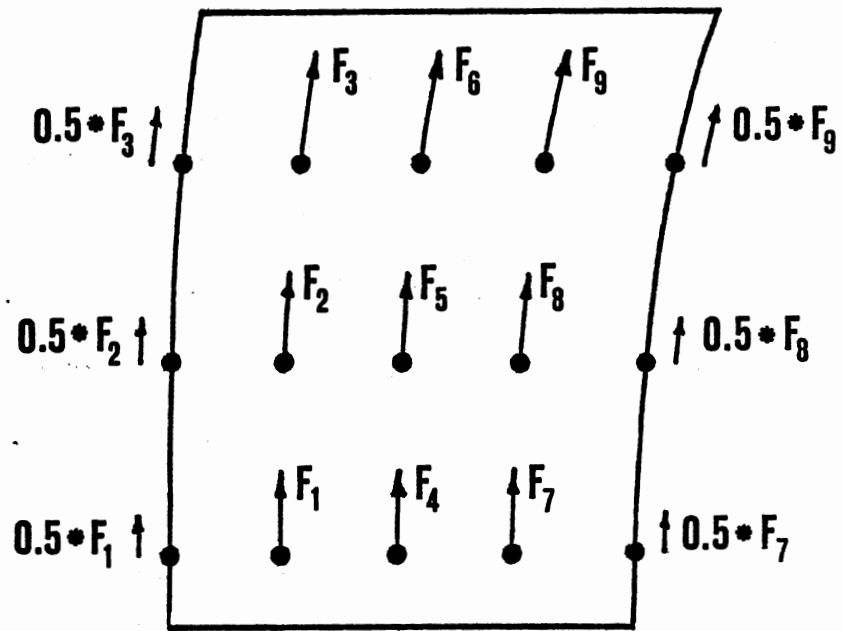


Figure 16. Friction Forces for Exterior Rows of Nodes

Once the initial system of equations has been solved, the degrees-of-freedom associated with the spreading nodes are multiplied by the unmodified GSM matrix. This multiplication yields local normal forces for each node. The friction forces are then found from the classic relationship:

$$F_f = \mu \cdot N \quad (3.6)$$

where

F_f = friction force;

μ = coefficient of friction; and

N = normal force.

These friction forces are shifted to the y degrees-of-freedom and then applied as a force vector. The forces for the nodes on the exterior rows are applied as described above. The new system is solved and new displacements are generated. Local forces are again found and converted to friction forces. The new friction forces are compared to the old friction forces. This comparison applies only to the rows of nodes interior to the concave roller. If any nodal friction force is not within a specified tolerance envelope, the procedure is repeated until all nodes meet the convergence criteria.

To aid convergence, the new friction forces are weighted and then added to the old spreading forces. This is the force that is then re-applied. The weighting equation is

$$(F_s)_{i,n} = (F_s)_{i,n-1} + \frac{1}{n} [(F_f)_{i,n} - (F_s)_{i,n-1}] \quad (3.7)$$

where F_s = spreading force;

F_f = friction force;

i = node number; and

n = iteration number.

A flowchart for the iteration process is shown in Figure 17.

The number of iterations required for convergence increases with changes in various parameters. Lowering the radius of curvature, for example, results in a higher number of iterations required for convergence. The user must be aware of this iteration number. It is the last entry in the output file OUT.DAT. An iteration number of 101 indicates the model did not fully converge and the resulting data must therefore be used with caution or the input variables must be modified.

3.5 Program Summary

This study utilizes two programs, MSHGNR and CONCAVE, both previously mentioned. Both are file oriented programs which require input files to receive the necessary information. Accordingly, the results are written to output files.

As mentioned, the program MSHGNR develops the finite element mesh and boundary conditions required by the main program CONCAVE. MSHGNR uses the user definable variables found in the file INPUT.DAT to develop the global coordinates and element connectivities of the mesh. The information as well as an echo of the original input is written to the output file MESH.DAT. MSHGNR is also used to solve the compatibility requirement

$$\epsilon_{A_{avg}} = \epsilon_{B_{avg}} \quad (2.14)$$

employing the subroutine SMPINT, a Simpson's integration routine. This analysis was outlined in Figure 14. Once the equation is satisfied, adjustments in the form of forces are written to the file FORCE.DAT to be used in the preliminary run of CONCAVE. The final

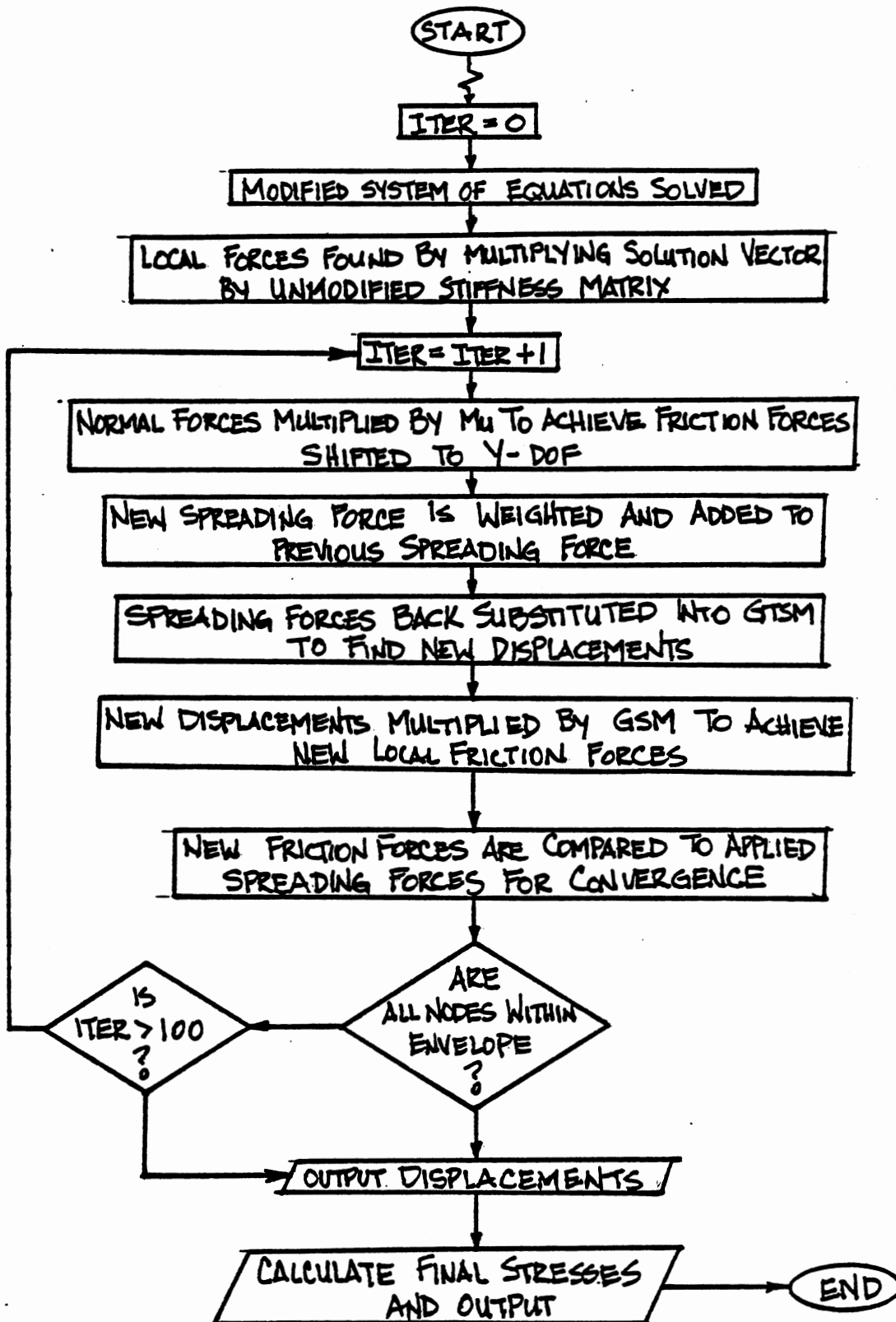


Figure 17. Spreading Analysis

data generated by MSHGNR involve the constraints of the system. Since the preliminary and final runs of CONCAVE incorporate slightly different constraints, two output files are used. They are CONSTR.DAT and BCNSTR.DAT, both required by CONCAVE. The main analysis sections of CONCAVE have already been discussed. Figure 18 shows a generalized flowchart for the program. Following is a description of the sub-routines used by CONCAVE:

- INPUT - Reads in data files generated by MSHGNR.
- Performs some diagnostic checks of data.
- ELSTMX - Calculates local elemental stiffness matrix $[K^{(e)}]$.
- LAMDA - Generates directional cosine matrix $[\lambda]$ used to develop transformation matrix $[T]$.
- Also used to generate $[\lambda']$ used by SKEWED for an average plane transformation $[T']$.
- TRNSMX - Evaluates transformation matrices $[T]$ and $[T]^T$.
- TRNSFM - Performs transformation of local elemental stiffness matrix $[K^{(e)}]$ to global $[K_G^{(e)}]$.
- ASSEMB - Uses direct stiffness assembly procedure to assemble global stiffness matrix $[K_G]$.
- SKEWED - Performs transformation of global stiffness matrix to average plane system.
- MODIFY - Reads enforced nodal displacements and nodal forces applied to web.
- Modifies system of equations.
- SANDS - Calculates stress and strain vectors and principal stresses.
- FACTOR - Transforms system of equations to upper triangular form.
- SUBST - Back-substitutes into equations to find solution vector.
- FRICTN - Calculates friction force for each node.
- APFORS - Applies force to force vector.

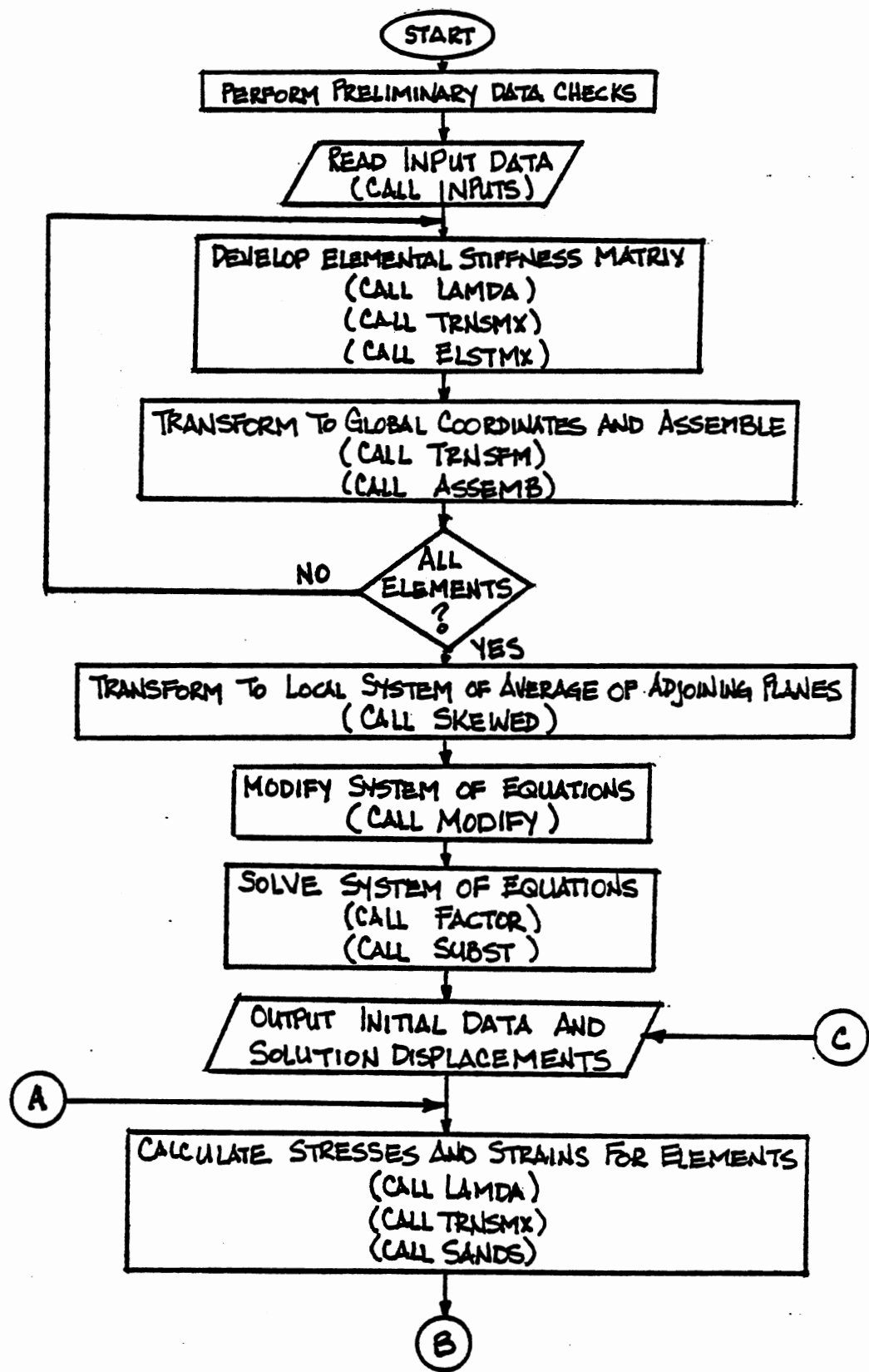


Figure 18. Flowchart of CONCAVE Program

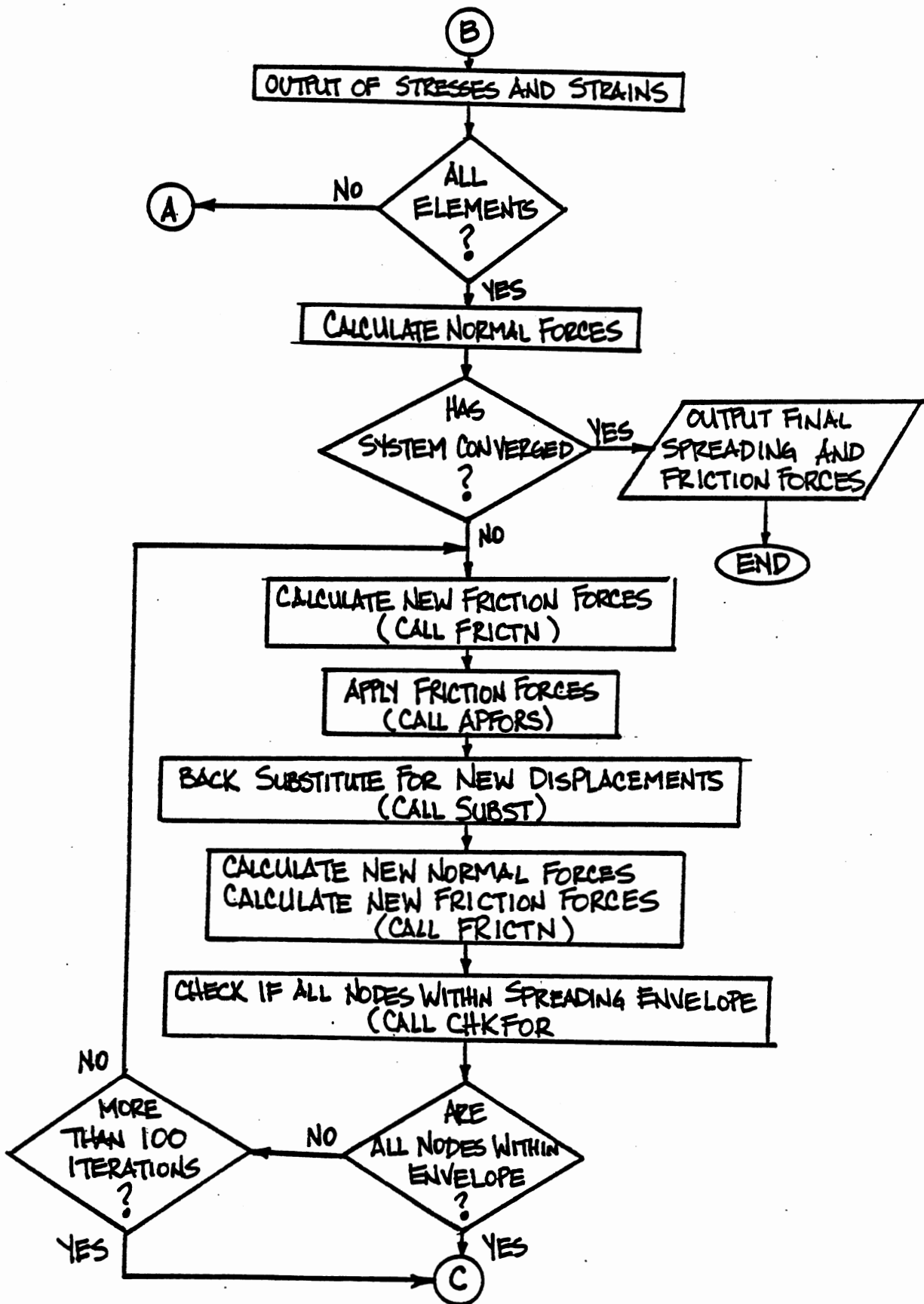


Figure 18. (continued)

- CHKFOR - Calculates ratio of spreading force to friction force for interior nodes on roller.
- Checks if ratio is within limits

3.6 Parameter Response

The last portion of the analytical study deals with the parameters of the model. Ranges of several of the user definable parameters were studied to aid in checking the validity of the model as well as gain insight to the effect of the parameters on the response of the system. Table II shows a list of the parameters studied and their associated descriptions.

TABLE II
LIST OF PARAMETERS STUDIED

Parameters	Description
CAPR	Circular arc profile radius of curvature
EM	Modulus of Elasticity
TH	Thickness
PR	Poisson's Ratio
AMU	Coefficient of Friction
WRAP	Wrap angle around concave roller
FORCE	Nodal tensile force

A range of values for each of the parameters was input and the resulting response of the system was then analyzed. To effectively analyze the response, a base model was developed. The base model values are shown in Table III.

TABLE III
PARAMETER VALUES USED FOR BASE MODEL

Parameter	Value
CAPR	1250 in.
EM	220,000 psi.
TH	0.002 in.
PR	0.3
AMU	0.3
WRAP	90°
FORCE	6.25 lbs/inch

3.7 Parameter Values Studied

The parameter study involved seven parameters: four represented the operating constraints of the system and three represented material properties of the web. Each parameter included a range of values that corresponded to actual practice.

Table IV shows the various parameter values for the radius of curvature; 175 inches was the lowest radius of curvature possible

given the other base parameters. Values lower than 175 inches produced negative strain on the concave roller. When this case exists, the program stops execution. For the analysis to continue, the user must either increase the radius of curvature and/or increase the operating tension. The web has no compressive stiffness and therefore a negative strain indicates wrinkling.

TABLE IV
PARAMETER VALUES USED IN STUDY

Capr (in.)	Wrap (deg.)	Force (lb/in.)	EM (psi.)	PR	TH (in.)	AMU (Mu)
175	30	1.0	50,000	0.0	0.0002	0.001
300 ^a	60	2.0	150,000	0.1	0.0010	0.010
750	90 ^b	3.0	220,000 ^b	0.2	0.0020 ^b	0.050
1250 ^b	120	4.0	350,000	0.3 ^b	0.0030	0.100
3500	150	6.25 ^b	500,000	0.4	0.0100	0.300 ^b
	180					

^a300 was added later to help clarify results.

^bindicates parameter values used for base model

CHAPTER IV

ANALYSIS OF RESULTS

Once the boundary conditions were enforced into the model, the effect of the various parameters on the model was studied. The parameters studied and their associated values can again be viewed by referring to Table IV. Plots which represented the response of the system were generated for each parameter. A wide range of plots were generated for variations in the radius of curvature to better understand the trends of the system and to check the validity of the model. Once the general responses of the system were described, the plots for the remaining parameters were isolated to only the particular trends they involved. For example, plots of the entry span were not generated for many of the parameters since for most cases the response of this portion of the web will be the same and will simply be a function of the spreading on the roll.

4.1 Curved Arc Profile Radius of Curvature

One of the primary concerns of this parameter was the spreading ability of the various radii of curvature as shown in Figure 19. The edge displacement of the web is plotted as a function of the various radii of curvature. This edge displacement, as shown on this and other plots, is relative to a relaxed web state. A radius of curvature of 300 inches was added to this and a few of the other plots to

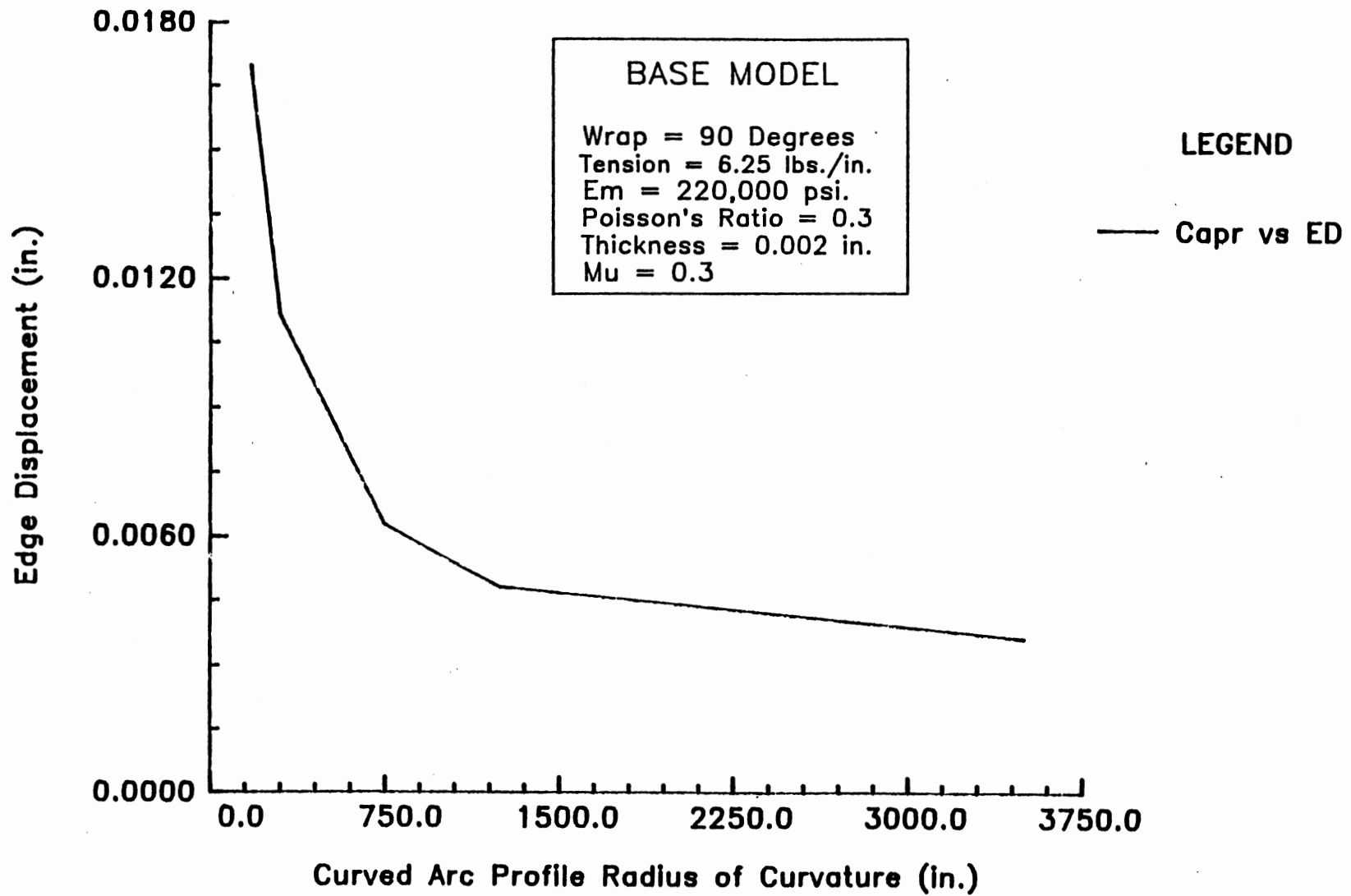


Figure 19. Edge Displacement on Concave Roller as a Function of the Radius of Curvature

better represent the nonlinear behavior of the lower radii of curvature. Given the base model values of the other parameters, a radius of 175 inches was the lowest value possible because lower values produced negative strain on the concave roller.

The plot shows that lower radii of curvature produce much more spreading of the web. This result was expected because lower radii produce larger normal forces, thus larger spreading forces. Theoretically, the curve should approach zero as the radius approaches infinity. An infinite radius of curvature would represent a cylindrical roller, which has no spreading capability.

Figure 20 shows the edge displacements down the length of the web. Since the web is not laterally constrained at the beginning of the model, the web seeks the Poisson contraction of the material. The smaller radii of curvature begin spreading the web sooner than the larger radii. The majority of the transition, however, occurs in the span approximately 25 percent of the entry span length upstream of the concave roller. Again it can be seen that the smaller radii produce more spreading in the web.

This plot also indicates that the web entry into the concave roller is not perfectly normal. Although this was an initial assumption used in the generation of the theory, it was not enforceable in a finite element model using Simplex elements (i.e., rotations are undefined). However, this is a local inconsistency related only to the one or two rows of nodes immediately preceding the concave roller. The localized effect of this inconsistency will be verified by the following plots. This minor inconsistency does not significantly influence the other results because the spreading of the web is

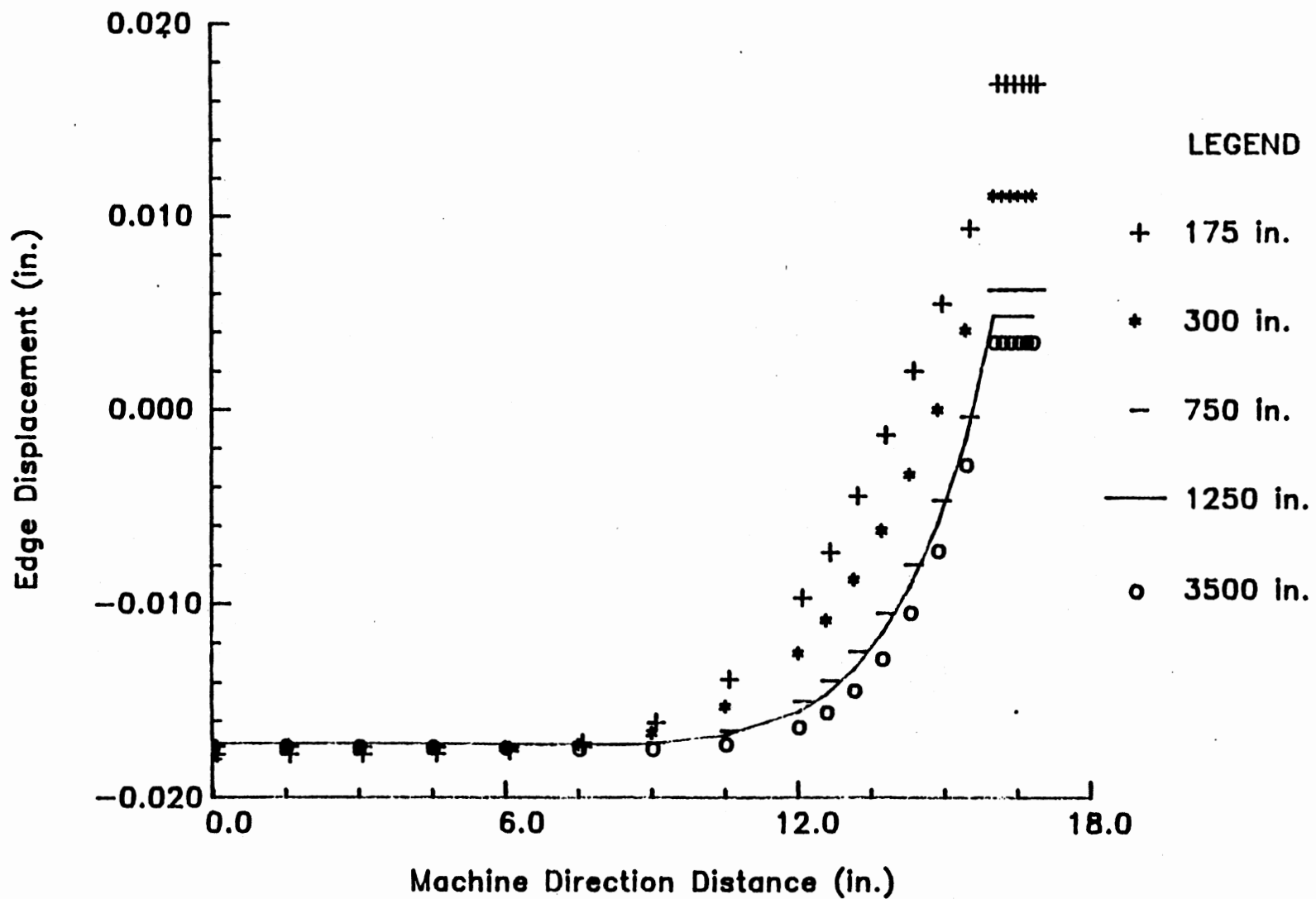


Figure 20. Edge Displacement for Various Radii of Curvature

controlled by only friction forces at the interior row of nodes on the roller. Since the stresses are computed separately upon each iteration, an accumulation error buildup does not occur.

The trends shown in Figures 21 and 22 can be explained physically via the continuity expression of Equation (2.3). Refer to Figure 23 which shows the machine direction strain distributions across the first row of elements on the roll for various radii of curvature. These distributions result from satisfying the average strain criteria expressed by Equation (2.14). The normal forces which are available to provide spreading tractions are highly dependent on the machine direction stresses which stem from these machine direction strains, via Equation (2.7). However, the lateral location on the concave roller also contributes to the normal force. Recall that the radius of a concave roller increases laterally across the roll, with the largest increases on the outside edge. This translates to the lateral location contribution to the normal force also increasing laterally across the roll, again with the largest increases on the outside edge. To clarify, a small displacement applied to a node near the centerline of the web results in a minor additional contribution of the lateral location to the normal force. However, the same displacement applied to a node near the outside edge of the web results in a much more significant contribution to the normal force. Therefore, although the normal force is highly dependent on the machine direction stress throughout the lateral span of the web, it is even more dependent in the laterally interior region of the roll than in the exterior region. This relationship is necessary to understand the S_y and S_x stress plots presented in Figures 21 and 22, respectively.

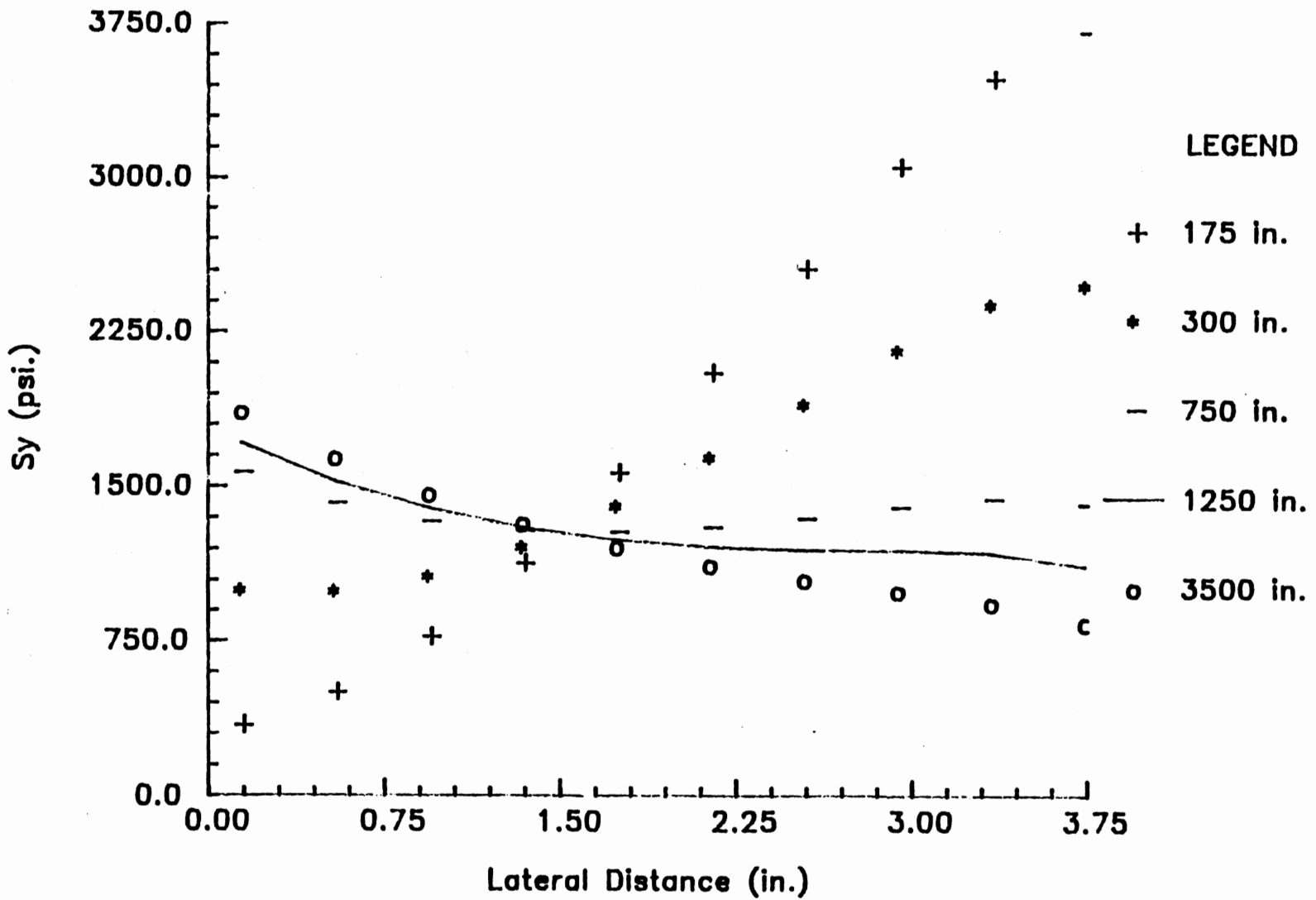


Figure 21. Lateral S_y Distribution at M.D. Distance 16.05 in. for Various Radii of Curvature

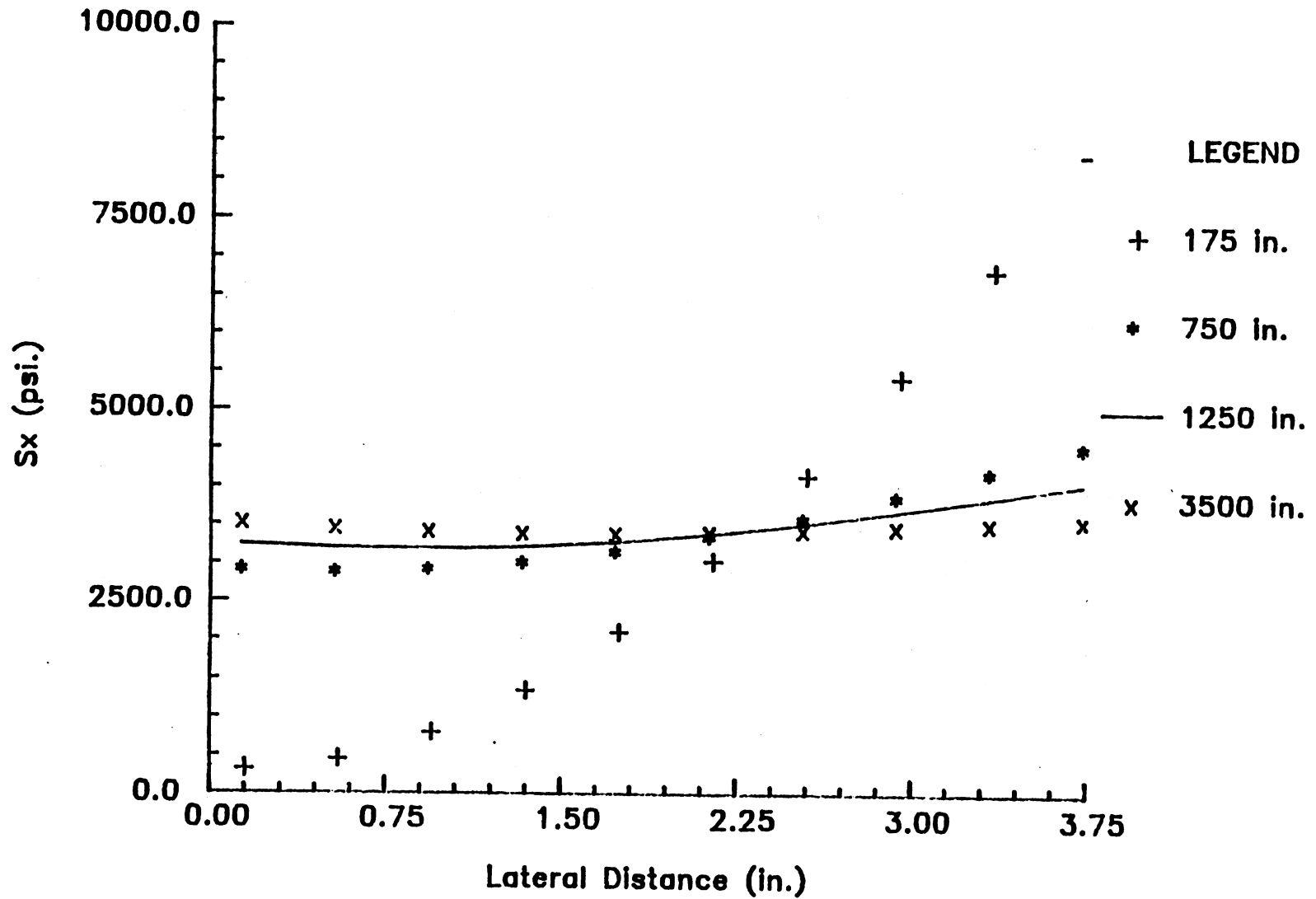


Figure 22. Lateral S_x Distribution at M.D. Distance 16.05 in. for Various Radii of Curvature

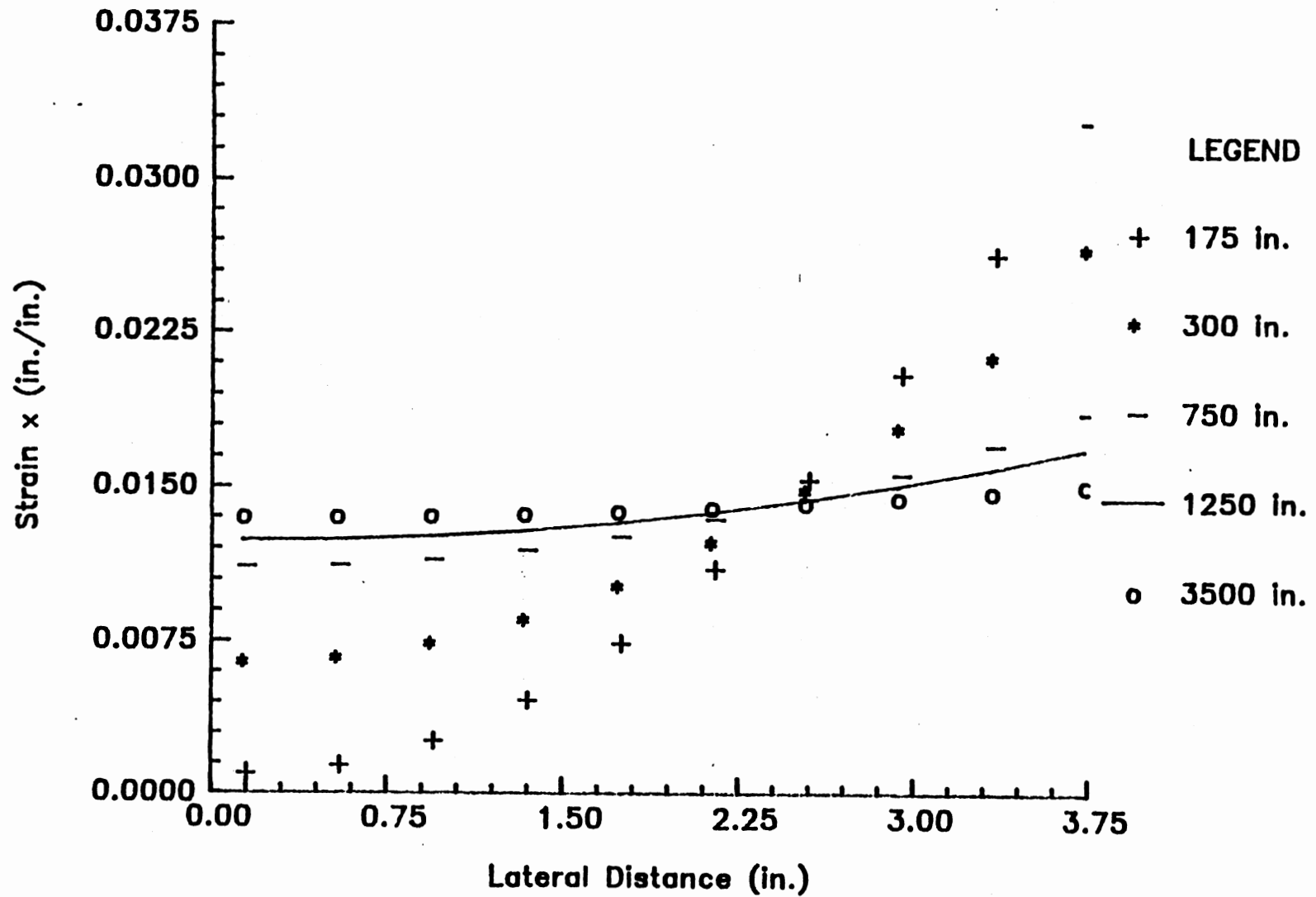


Figure 23. Lateral Strain x Distribution at M.D. Distance 16.05 in. for Various Radii of Curvature

It is also necessary to again review the spreading technique applied by the program. Recall that spreading forces are applied to the nodes in that portion of the web in contact with the concave roller on an individual basis. Each node is spread on the basis of the available friction capability, derived from the available normal force. Again recall that both the initial machine direction stress and the lateral location on the roll both contribute to the normal force. The term "initial machine direction stress" refers only to the resulting stress distribution obtained from satisfying the average strain criteria, and is not to be confused with the machine direction stress of the system, a product of both the initial machine direction stress and the machine direction stress component resulting from the spreading of the web. This relationship will be discussed later.

Beginning with the contracted state of the web resulting from the Poisson effect, frictional forces are applied as spreading forces to achieve new lateral displacements, or a spreading of the web. These new lateral displacements are used in conjunction with the initial machine direction stresses to find new normal forces resulting in new friction forces. The new friction forces are then weighted and applied, resulting in the web being spread further upon each iteration. The spreading is finally stopped when each interior node on the web on the concave roller has achieved a state of impending lateral slip. In other words, the new spreading forces are checked against the previous spreading forces for convergence. Since the spreading forces are derived from the normal forces, it follows that new normal forces must be of sufficient magnitude over the previous normal force for nodal spreading to continue.

Figures 21 and 22 can now be more fully explained. The initial machine direction stress distribution is simply the machine direction strain distribution, shown in Figure 23, multiplied by the modulus of elasticity, a constant for the analysis of the radius of curvature parameter. The initial machine direction stress distribution will therefore be the same as the machine direction strain distribution shown in Figure 23, with only the y-axis values changing. With the understanding that the trends are equivalent, the machine direction strain distribution will be frequently referred to as the initial machine direction stress distribution. Since all values in this distribution are positive, they all provide positive normal forces resulting in spreading. Considering only the interior portion of the roll, larger changes are shown for smaller radii of curvature relative to larger radii of curvature. Since the normal force, especially in this interior region, is highly dependent on the initial machine direction stress, an increase in this stress between successive nodes will result in more spreading of the latter node, thereby increasing the lateral stress. This is easily seen by comparing the increasing trends of the smaller radii of curvature shown in Figure 23 to the increasing trends of the lateral stress as shown in Figure 21. Likewise, each increase in the lateral direction stress, S_y , results in an increase in the machine direction stress via

$$S_x = E \cdot \epsilon_x + \nu \cdot S_y \quad (4.1)$$

The variables for this equation have all been previously defined. The machine direction strain, ϵ_x , is presented graphically in Figure 23. Equation (4.1) is a two-dimensional elasticity equation representing the interaction between directional stresses of the system. The

increasing trends of machine direction stresses for the smaller radii of curvature resulting from Equation (4.1) are shown in Figure 22.

Although slightly increasing, larger radii of curvature supply a much more uniform initial machine direction stress distribution for the interior portion of the roll. These uniform trends are again the same trends shown in Figure 23. With the initial machine direction stresses virtually the same for each consecutive node in the interior region of the roll, each node has the same initial spreading ability. Due to the nature of the larger radii of curvature, the nodes do not receive much additional contribution to the normal force from the lateral location of the web on the roll. Therefore, the impending lateral slip is achieved sooner for each successive node due to the increasing radius of the concave roller. A decrease in the spreading should therefore occur for each successive lateral location in the interior portion of the roll for larger radii of curvature. This trend can be seen by again referring to Figure 21. This decreasing trend is also reflected in the machine direction stresses as shown in Figure 22 again via Equation (4.1). The slight increases in the initial machine direction stresses depicted in Figure 23 are almost entirely removed due to the decreasing contribution of the lateral spreading stresses in this interior portion of the roll.

The previous analogies also hold for the laterally exterior portion of the roll with the exception that each change in the normal force contribution is significant enough to provide additional spreading for a longer time in terms of the impending lateral slip criteria. In other words, the lateral locations of the exterior portion of the roll provide additional spreading abilities relative to the interior

portion of the roll. With this in mind, again refer to Figure 23 for initial machine direction stress trends of the various radii of curvature. All distributions show a lateral increase in the outer portion of the roll, with the smaller radii increasing more dramatically. These dramatic increases for smaller radii of curvature coupled with the increasing contributions of the lateral locations provide the trends shown in Figure 21. Spreading stresses for small radii of curvature increase sharply laterally across the roll. These sharp increases again combined with machine direction strain increases via Equation (4.1) result in the increases shown in Figure 22 for machine direction stresses for smaller radii of curvature.

Figure 23 indicates that larger radii of curvature experience less dramatic increases in the machine direction stress distribution. Although increasing, these larger radii represent a more uniform spreading ability for this outer region of the web relative to smaller radii. Recall the lateral slip criteria. With no substantial increase in the machine direction stresses laterally across the web, each new lateral location satisfies this criteria sooner in a lateral displacement sense. The result is the uniform spreading trends demonstrated in Figure 21 for the larger radii of curvature. Particularly note the 3500-inch radius of curvature in which the spreading stress continues to decrease laterally across the roll due to the insufficient increases in the initial machine direction stress.

Figure 22 shows machine direction stresses of larger radii of curvature increasing gradually in the outer portion of the roll. However, slopes of the increase are smaller than the slope of the machine direction stress distribution because each lateral location

receives less of an impact from the spreading stress again via Equation (4.1).

It is important to note that all spreading stresses shown in Figure 21 should theoretically converge to zero at the outside edge of the web, since the edge has no ability to support stresses. The stresses shown represent the values at the interior of the corresponding elements. For the edge convergence to be modeled accurately, many additional elements would be required. The width of these elements would need to decrease laterally until the outermost element had an infinitesimally small width. It is not feasible, nor physically possible, to incorporate such decreasing elements and the user must therefore remain aware of this exterior convergence.

The trends of Figure 21 for the various radii of curvature can be used to explain Figure 24. Figure 24 represents the net lateral spreading of each lateral node location, derived from subtracting the Poisson contraction of each lateral node location from the spreading experienced by the corresponding nodal location on the concave roller. Realize that each subsequent lateral node for a particular radius of curvature has an increased Poisson contraction associated with it as per Figure 23. A more complete discussion of the Poisson effect will be provided later. The spreading tractions shown in Figure 21 represent the ability of the web to spread beyond this Poisson effect. Figure 24 shows that, although the exterior nodes for the larger radii represent less spreading ability relative to their interior nodes, the overall net spreading is higher. This is because each outer node also experiences the contraction of all of the interior nodes, giving each outer node increased contractions beyond

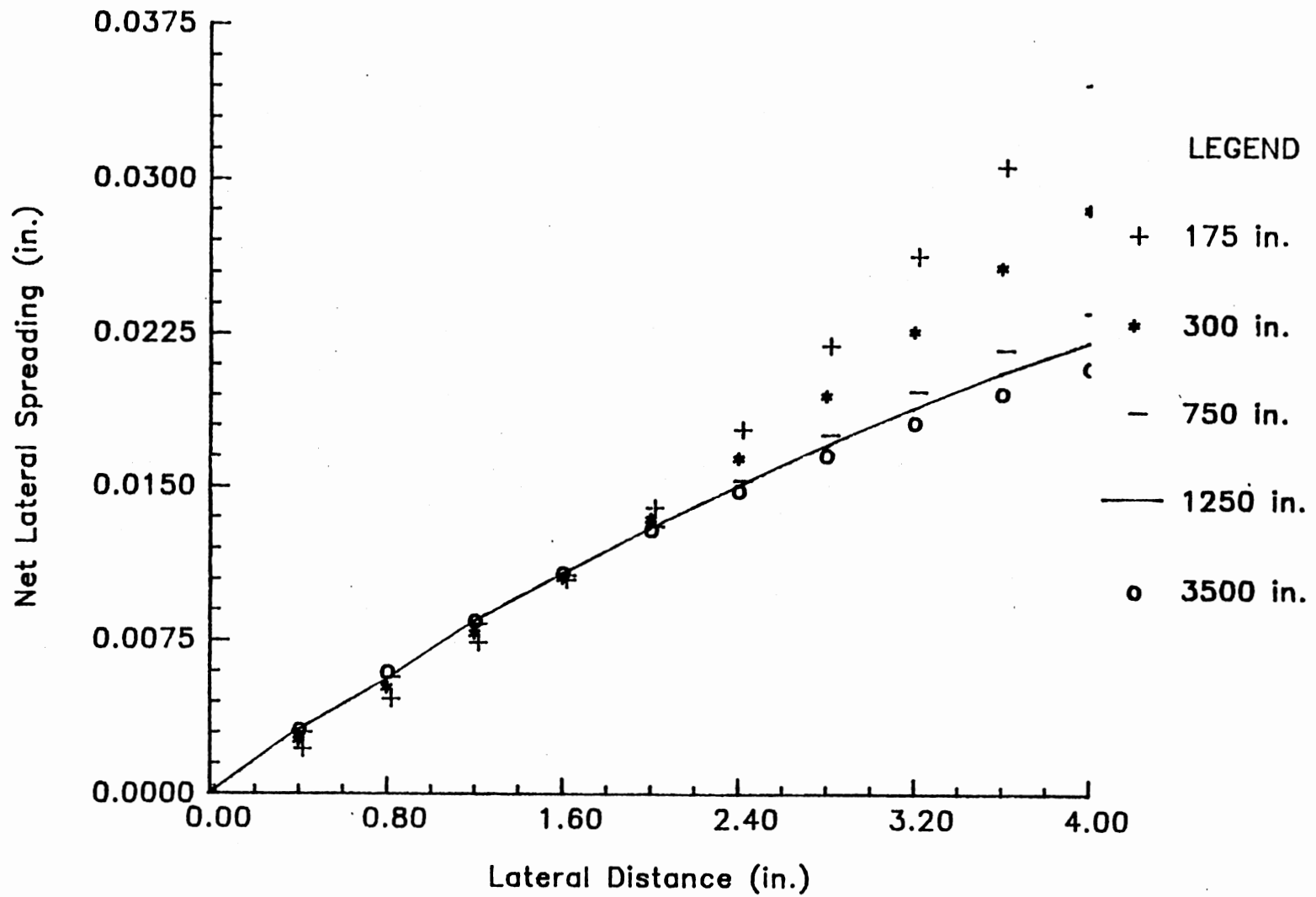


Figure 24. Net Lateral Spreading for Various Radii of Curvature

their individual Poisson contraction. As the interior nodes spread, they also move out the outer nodes. This results in the cumulative spreading curves shown in Figure 24, whereby the outer nodes also experience the spreading associated with the interior nodes. The smaller radii shown in Figure 21 indicate continually increasing spreading stresses. This results in the larger net increases per consecutive node as shown in Figure 24.

The machine direction stress, S_x , and the lateral stress, S_y , distributions at a lateral location of 3.33 inches are shown throughout the length of the web in Figures 25 and 26, respectively. Figure 25 is very similar to the edge displacement plot shown in Figure 20. Stresses are constant in the beginning portion of the web and rapidly increase as the concave roller is approached. Stresses on the roller are constant, as enforced by the constraints of the model. Again the localized inconsistency of the row of nodes immediately preceding the concave roller is seen.

Lateral stresses (shown in Figure 26) are nearly zero in the beginning portion of the model. However, they begin to increase close to the concave roller. Again, there is a drop between stresses on the roller and those immediately prior to the roller. The stresses are constant on the roller itself. This was one of the main concerns of the model. Constant lateral stresses were desired to adequately model the spreading condition which assumes a constant lateral spreading for each column of nodes and machine direction force symmetry.

Primary and secondary stress distributions, S_1 and S_2 , throughout the machine direction distance are plotted in Figures 27 and 28, respectively. Both plots show the same trends as discussed for the

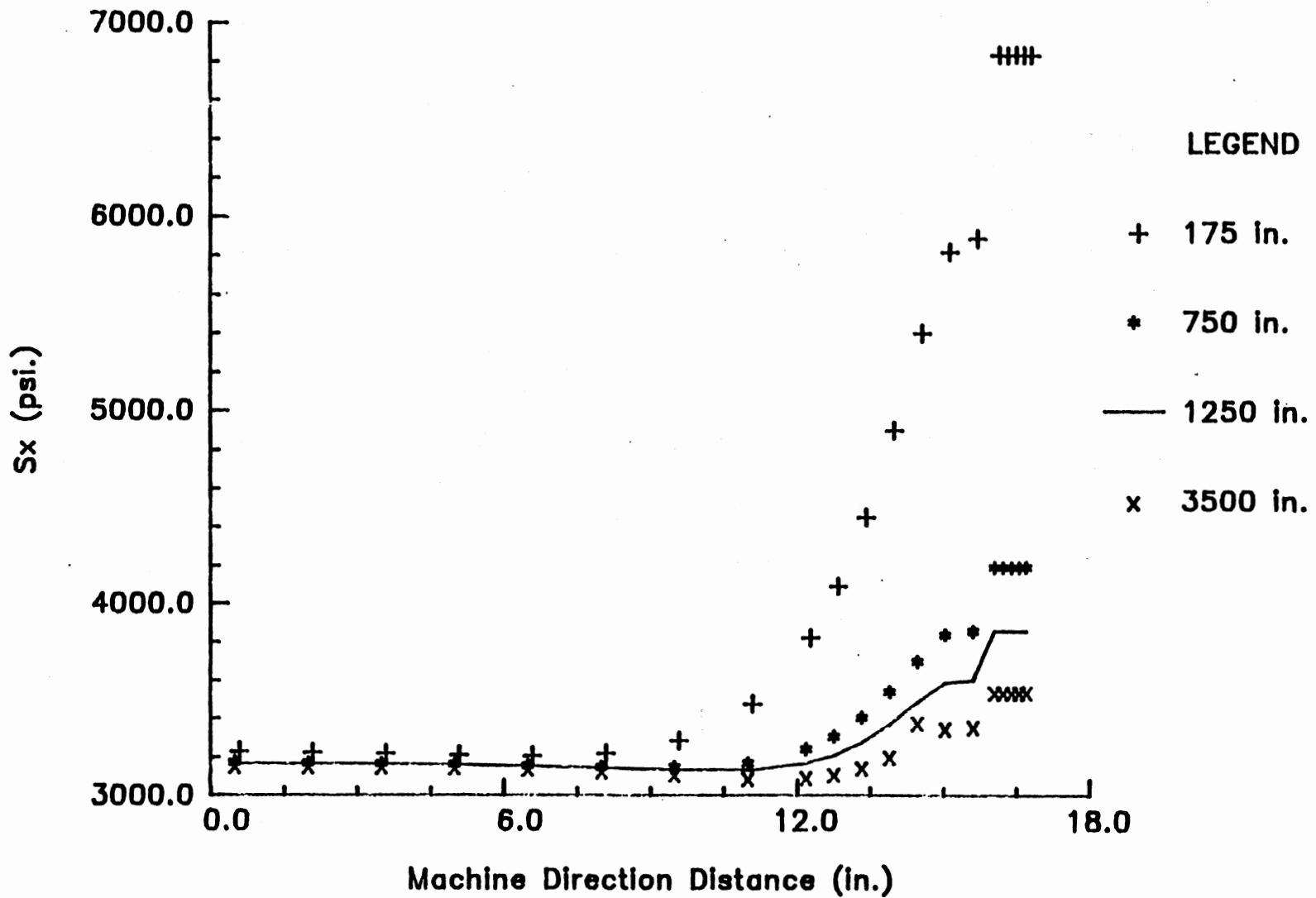


Figure 25. M.D. Sx Distribution at Lateral Distance 3.33 in. for Various Radii of Curvature

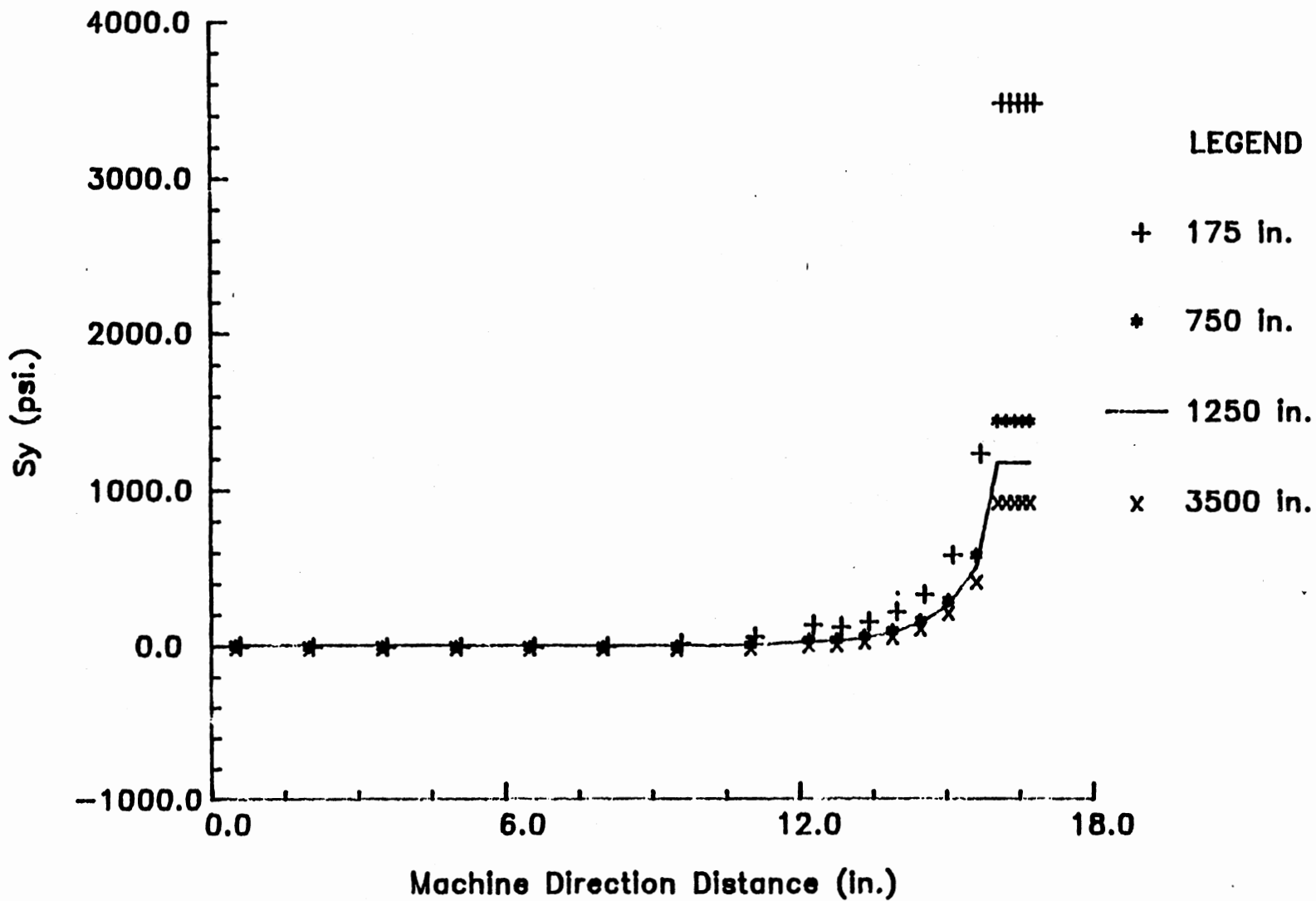


Figure 26. M.D. Sy Distribution at Lateral Distance 3.33 in. for Various Radii of Curvature

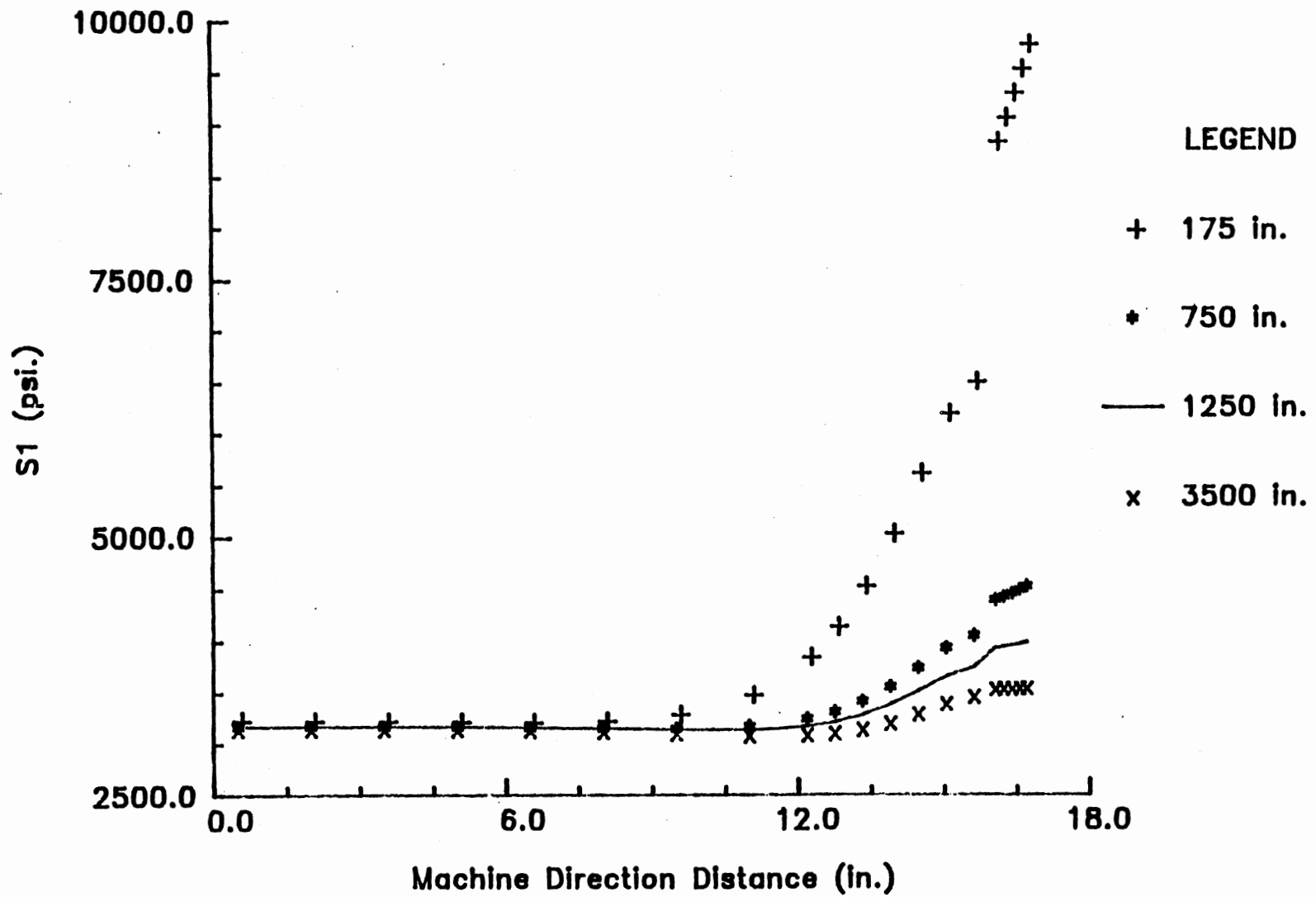


Figure 27. M.D. S1 Distribution at Lateral Distance 3.33 in. for Various Radii of Curvature

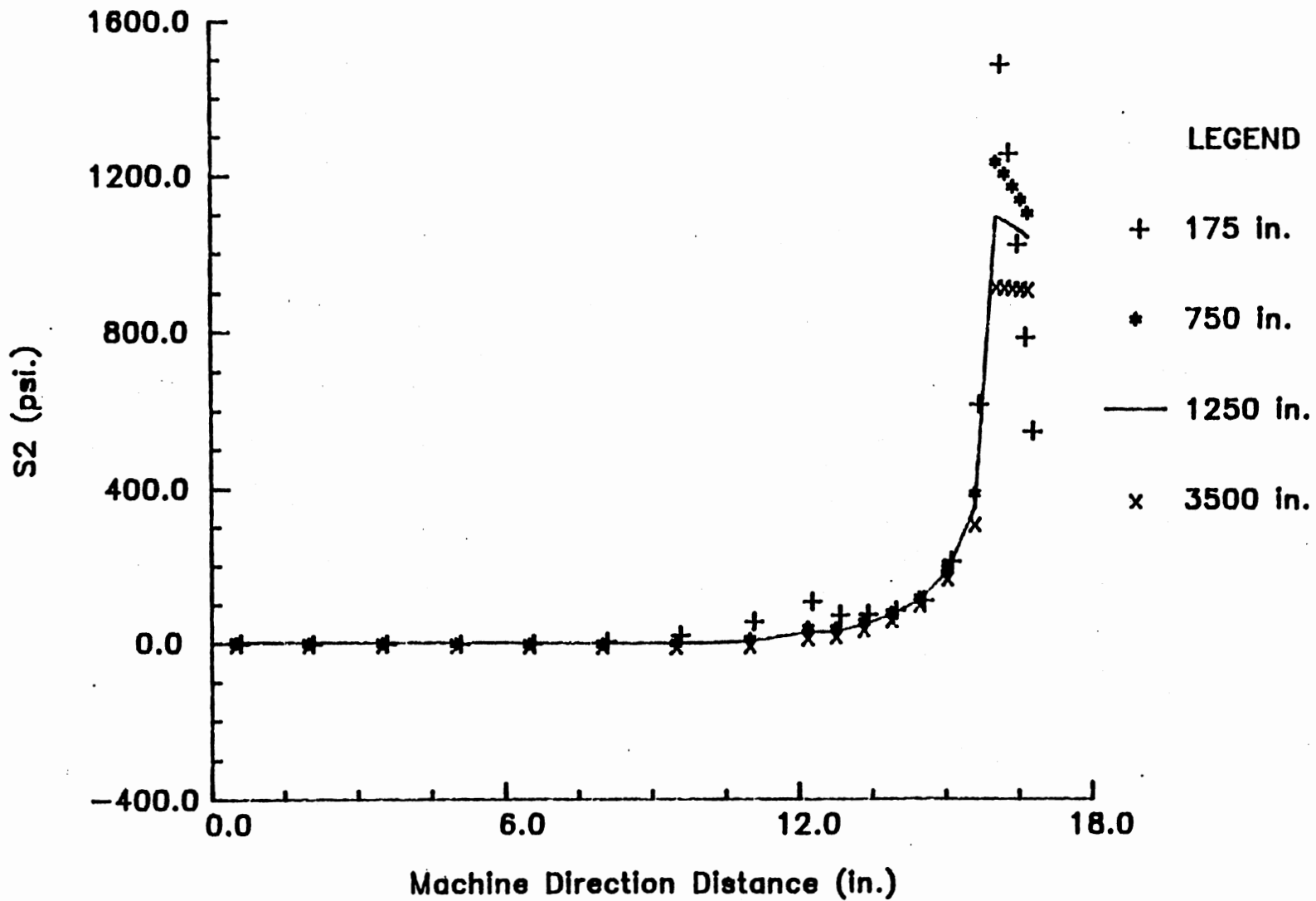


Figure 28. M.D. S2 Distribution at Lateral Distance 3.33 in. for Various Radii of Curvature

machine direction variations of S_x and S_y . However, these plots are not constant on the roller and have slightly different values in the region prior to the roller. This variation is understood by again considering enforced machine direction displacements on the concave roller. These displacements increase as the outside of the web is approached. Elements in this region experience different enforced displacements for nodes associated with it. Nodes at one lateral location have a different enforced displacement than nodes interior and exterior to it. This creates shear in the elements. This shear is a cumulative value as the elements proceed around the concave roller. Cumulative shear values have a positive impact on the principle stress S_1 and a negative impact on the secondary stress S_2 as seen by Equations (4.2) and (4.3):

$$S_1 = \frac{S_x + S_y}{2} + \sqrt{\left(\frac{S_x - S_y}{2}\right)^2 + \tau_{xy}^2} \quad (4.2)$$

$$S_2 = \frac{S_x + S_y}{2} - \sqrt{\left(\frac{S_x - S_y}{2}\right)^2 + \tau_{xy}^2} \quad (4.3)$$

Shear values therefore become additive to S_x and negative to S_y . This results in S_1 showing an increase on the roller and S_2 showing a decrease on the roller. Shear contributions also account for slight changes in the span just prior to the concave roller due to the contraction and expansion (spreading) experienced by the web.

Figures 29 and 30 show the S_1 and S_2 distribution laterally across the web. Both follow the analysis presented for the lateral behavior of S_x and S_y with only slight variations. Again, S_1 and S_2 consider the shear present in the elements. This results in slightly higher values for S_1 than expressed for S_x , but the overall trend is

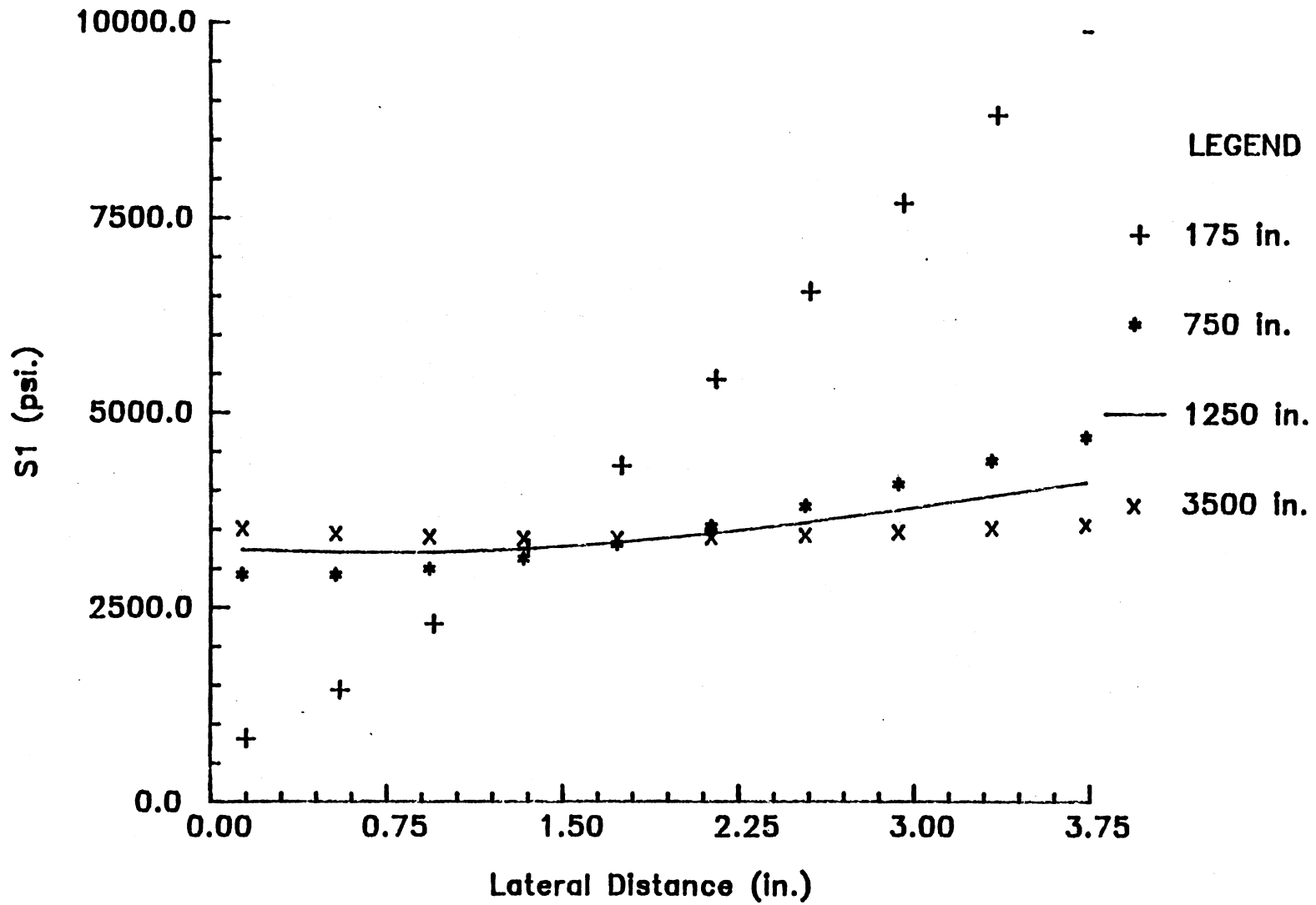


Figure 29. Lateral S1 Distribution at M.D. Distance 16.05 in. for Various Radii of Curvature

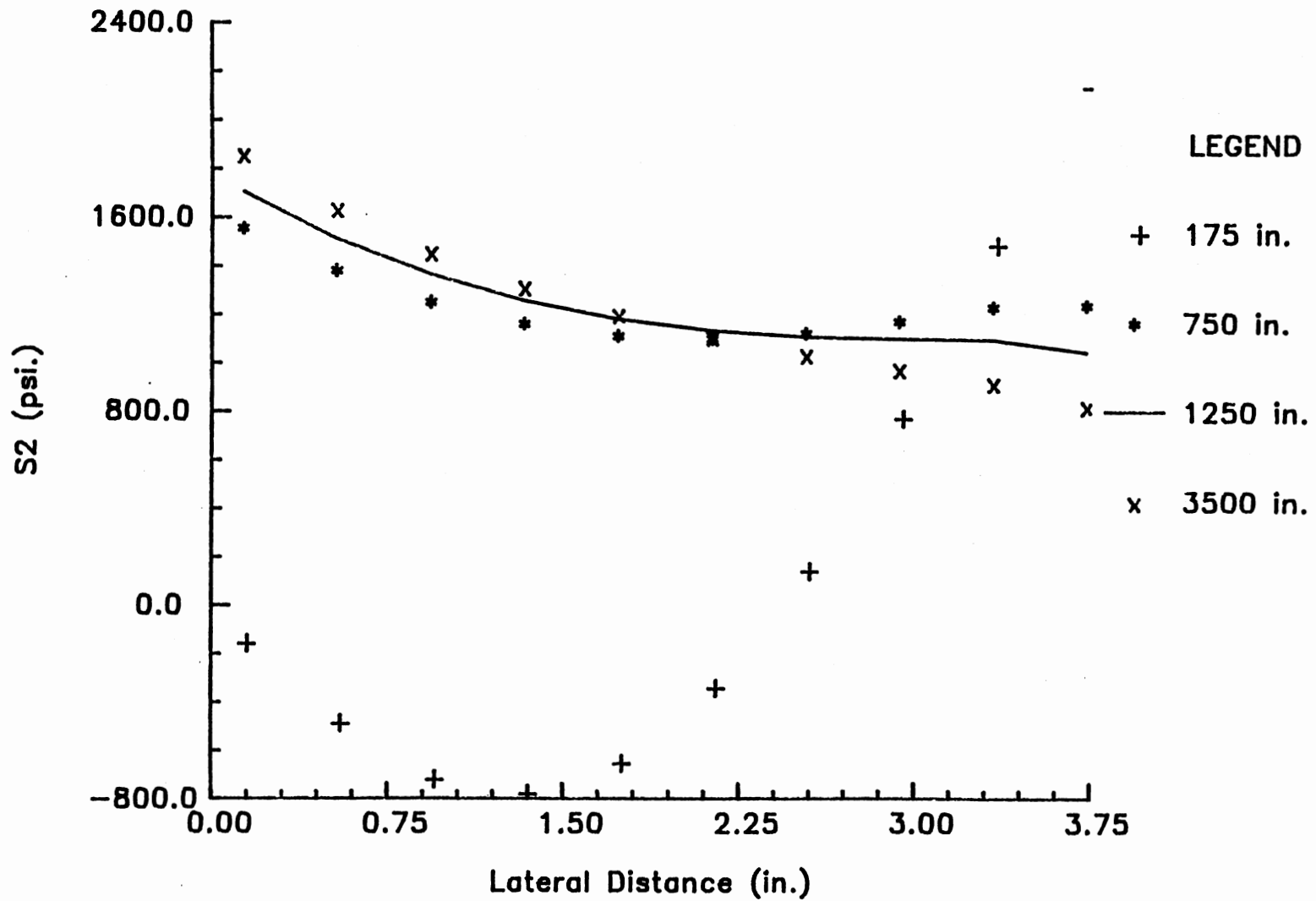


Figure 30. Lateral S2 Distribution at M.D. Distance 3.33 in. for Various Radii of Curvature

the same. Likewise, S_2 shows lower values than S_y . The shear contribution outweighs the lateral spreading contribution for the 175-inch radius of curvature, thereby creating negative S_2 values. This is because the trend for S_y is different as previously discussed. The values start out much lower than the other values and increase more rapidly to produce the overall spreading effect. The shear contribution is greater for the smaller radii of curvature and therefore the 175-inch case is greatly influenced by the shear at the interior portion of the web. However, spreading tractions again become dominant as the edge of the web is approached.

The final data analyzed was the machine direction ϵ_x distribution and the lateral ϵ_y distribution, shown in Figures 31 and 32, respectively. Figure 31 again shows the discontinuity involved with the row of nodes immediately prior to the concave roller. However, aside from this one row of nodes, the plot shows a reasonable continuous ϵ_x distribution throughout the length of the web. Slightly higher values of the larger radii prior to the roller can be explained by the relationship

$$\epsilon_x = \frac{1}{E} (S_x - \nu S_y) \quad (4.4)$$

This equation shows ϵ_x results from the difference of the machine direction S_x and the Poisson contribution of S_y . Refer to Figures 25 and 26 for the machine direction S_x and S_y distributions. Note particularly from Figure 25 that the S_x resulting from the roller has a further influence upstream into the entry span than the S_y influence from the roller, shown in Figure 26. The higher ϵ_x value prior to the roller for the larger radii of curvature represents the prolonged influence of S_x upstream into the entry span via Equation (4.4). This

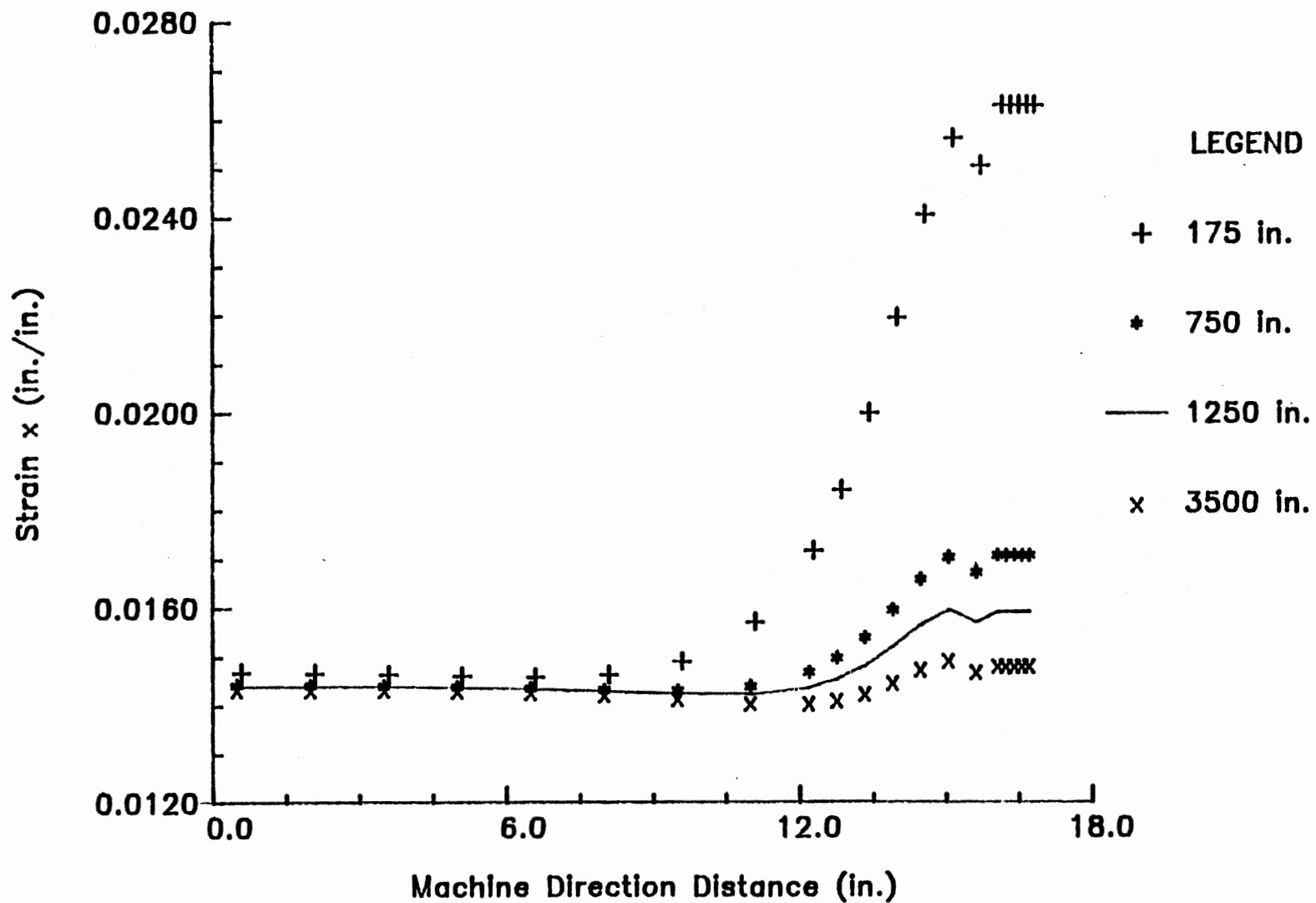


Figure 31. M.D. Strain \times Distribution at Lateral Distance 3.33 in. for Various Radii of Curvature

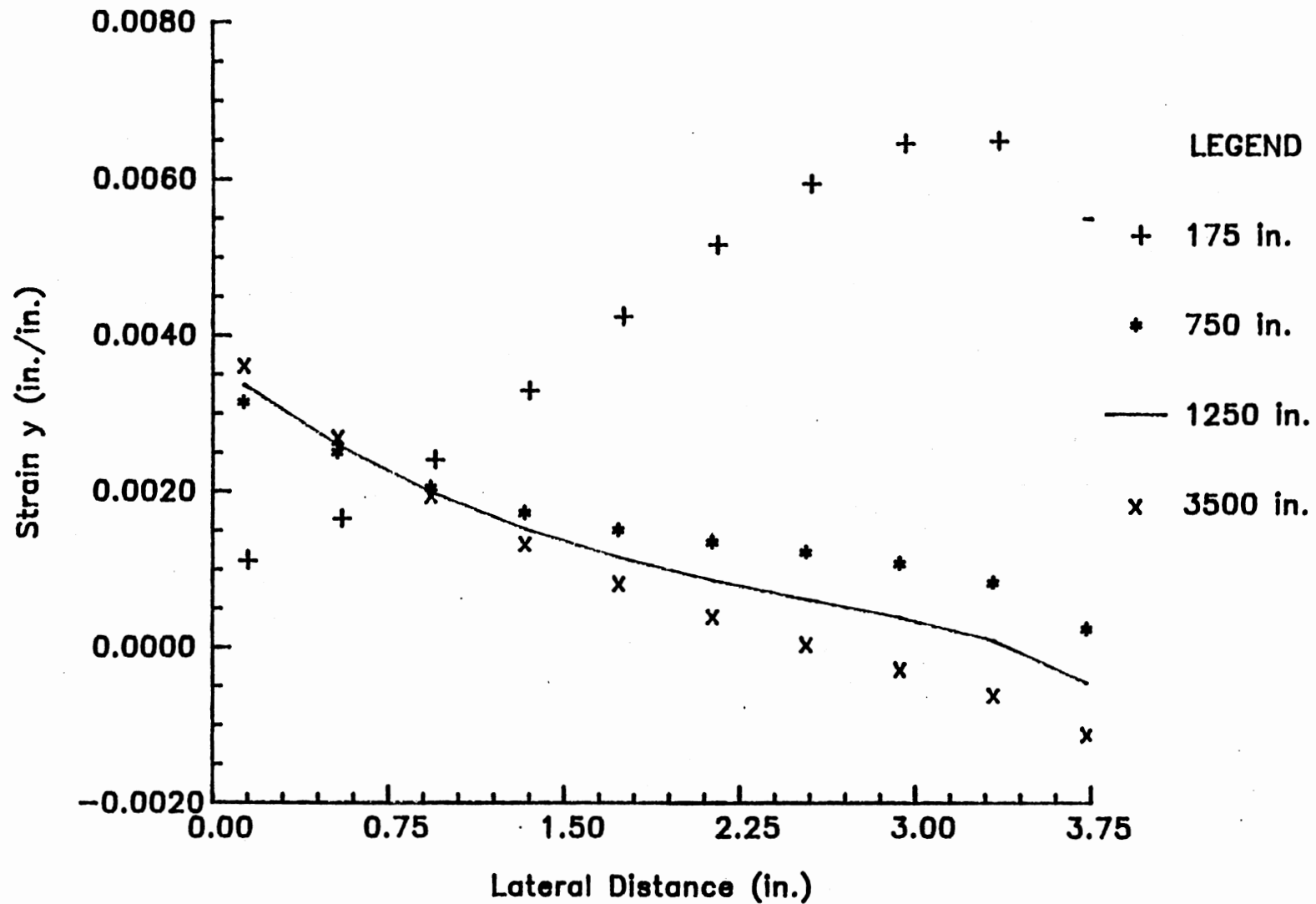


Figure 32. Lateral Strain y Distribution at Lateral Distance 16.05 in. for Various Radii of Curvature

trend is not as pronounced for the 175-inch radius due to the increased S_y influence into the entry span.

Figure 32 shows the ϵ_y distribution across the roller. Recall that machine direction strains are enforced across the roller by machine direction displacements, with the largest values in the outer region of the web. These machine direction strains are related to lateral strains by Poisson's ratio. In general terms, Poisson's ratio represents the relationship between the transverse contraction of a specimen resulting from a longitudinal elongation, and can be expressed as

$$\epsilon_y = - \nu \epsilon_x \quad (4.5)$$

where ν represents Poisson's ratio. The largest lateral contractions will therefore correspond to the largest enforced machine direction displacements or, the outer regions of the web. Recall the increased spreading ability of the smaller radii of curvature as shown in Figure 21. This increased ability creates positive strains in excess of the Poisson contraction induced by the machine direction displacements. The larger radii do not have this increased spreading ability. Therefore, as machine direction strains increase laterally across the web, spreading stresses provide a lesser ability to overcome the increasing contractions, thus resulting in the decreasing trends of the larger radii as shown in Figure 32.

4.2 Angle of Wrap

The next parameter studied was the angle of wrap around the concave roller. Figure 33 shows the edge displacement of the web on the

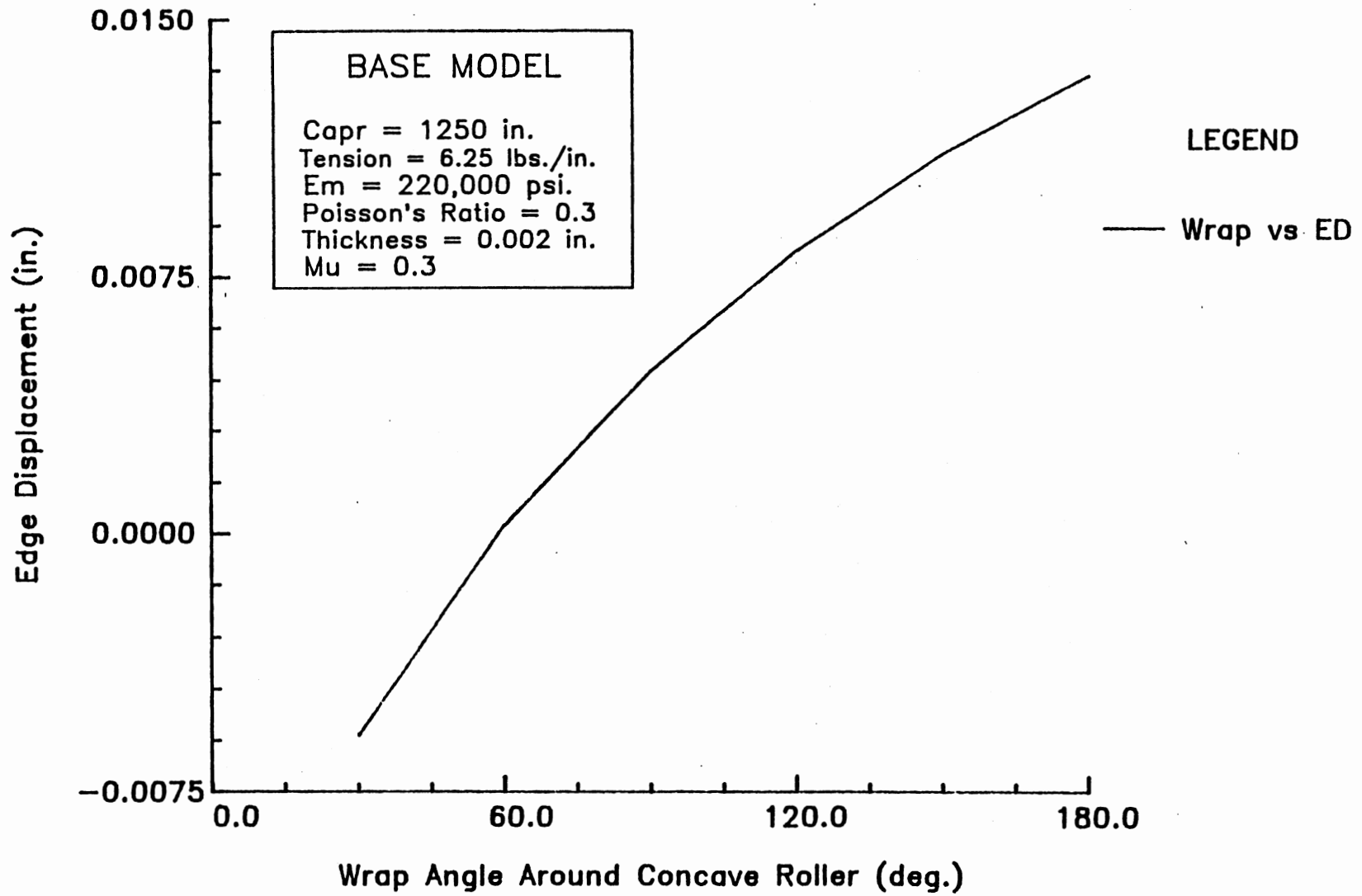


Figure 33. Edge Displacement on Concave Roller as a Function of the Wrap Angle

concave roller as a function of the wrap angle. The plot indicates that larger wrap angles produce more spreading in the web. This result was expected because larger wrap angles translate to more web material in contact with the roll, thus generating higher normal forces. These higher normal forces represent an increased spreading ability. For the given base model parameters, a wrap angle of approximately 60 degrees was required to return the web to its original undeformed lateral width. Angles less than 60 degrees were unable to generate enough spreading force to produce positive displacements in the web.

Figure 34 shows the lateral S_y distribution across the web at the machine direction location corresponding to the first row of elements on the roll. Smaller wrap angles produce lower spreading stresses. Refer to Figure 23 for the initial machine direction distribution of the base parameter radius of curvature of 1250 inches. The initial machine direction stress is virtually uniform in the interior portion of the web. Therefore, any changes in any values which affect the normal force--in this case the amount of area in contact with the roll--will have a more significant effect on spreading of the web. This impact is represented in Figure 34 by indicating the larger wrap angles produce more spreading ability of the nodes in the interior region of the roll. The convergence of the lateral stresses at the edge of the web result from the equilibrium requirements of the model. These equilibrium requirements will be shown in detail under section 4.7 for the coefficient of friction. For now it is sufficient to note they do converge.

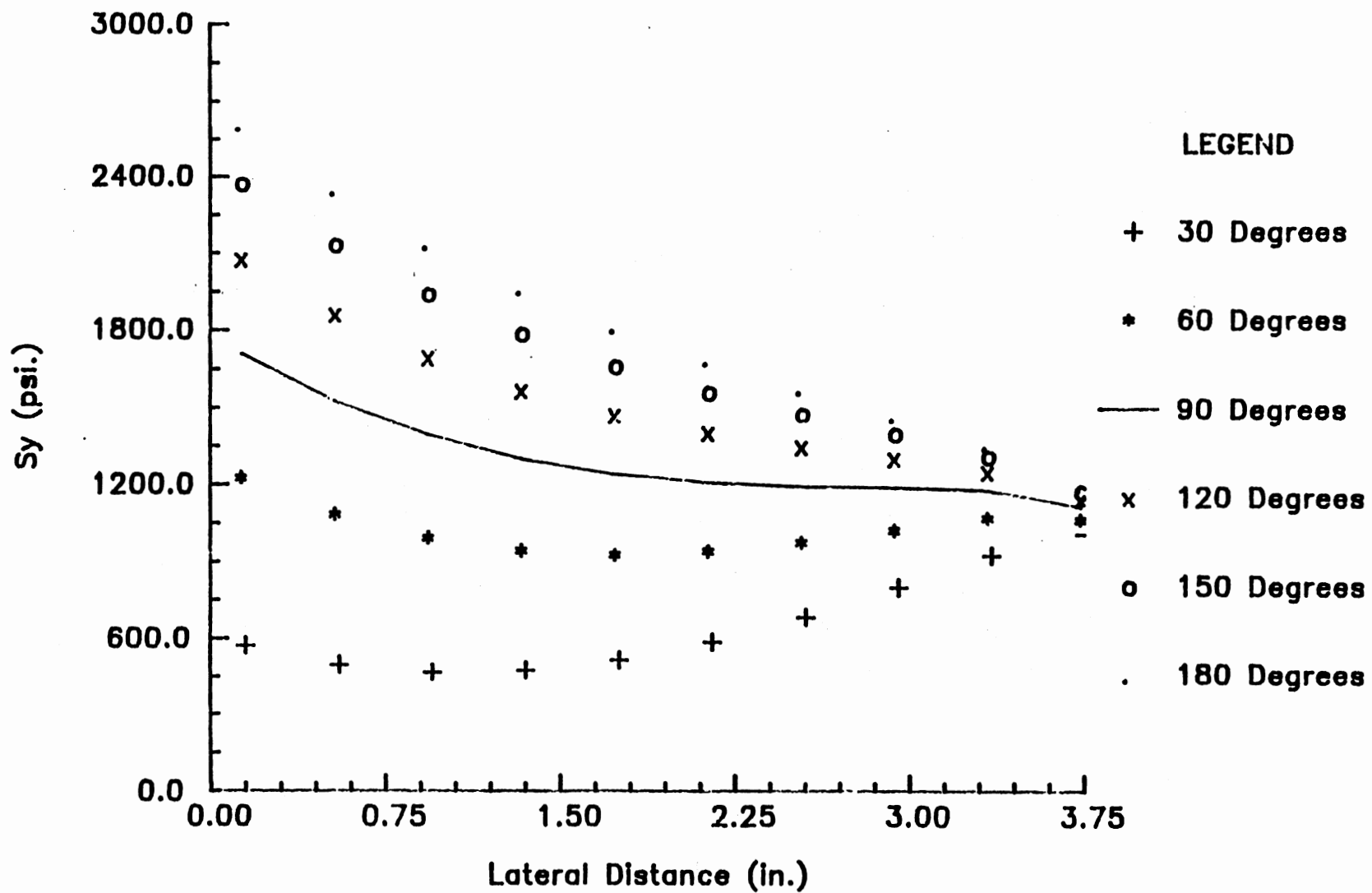


Figure 34. Lateral Sy Distribution at M.D. Distance 16.05 in. for Various Wrap Angles

4.3 Web Tension

Effects of changes in the input tension to the model are shown in Figure 35. The plot shows the edge displacement on the roll as a function of the tension of the system. A linear trend is shown with the higher tensions producing increased edge displacements. Recall that the input distribution is the same for all forces since the radius of curvature is a constant, namely 1250 inches. Only the magnitude of each distribution changes. This results in higher normal forces generated for the higher tensions. The elastic properties of the web are also a constant for this parameter. Thus, the edge displacements become linearly proportional to the forces as shown in the plot.

Trends shown in Figure 36 again represent this relationship. The higher tensions produce higher lateral stresses. The relation between the stresses of the various curves is again linear, as shown in Figure 37. Discussion of the convergence at the edge of the web will again be delayed until Section 4.7.

4.4 Modulus of Elasticity

Changes in the modulus of elasticity produce a nonlinear effect on spreading of the web on the concave roll, as shown in Figure 38. The modulus of elasticity is a measurement of material stiffness. It is therefore expected that larger moduli would indicate a stiffer material and thus a lower spreading response on the concave roller. This corresponds to the trends shown in Figure 38.

Effects of the various moduli of elasticity on the S_y distribution laterally across the roll are shown in Figure 39. To address

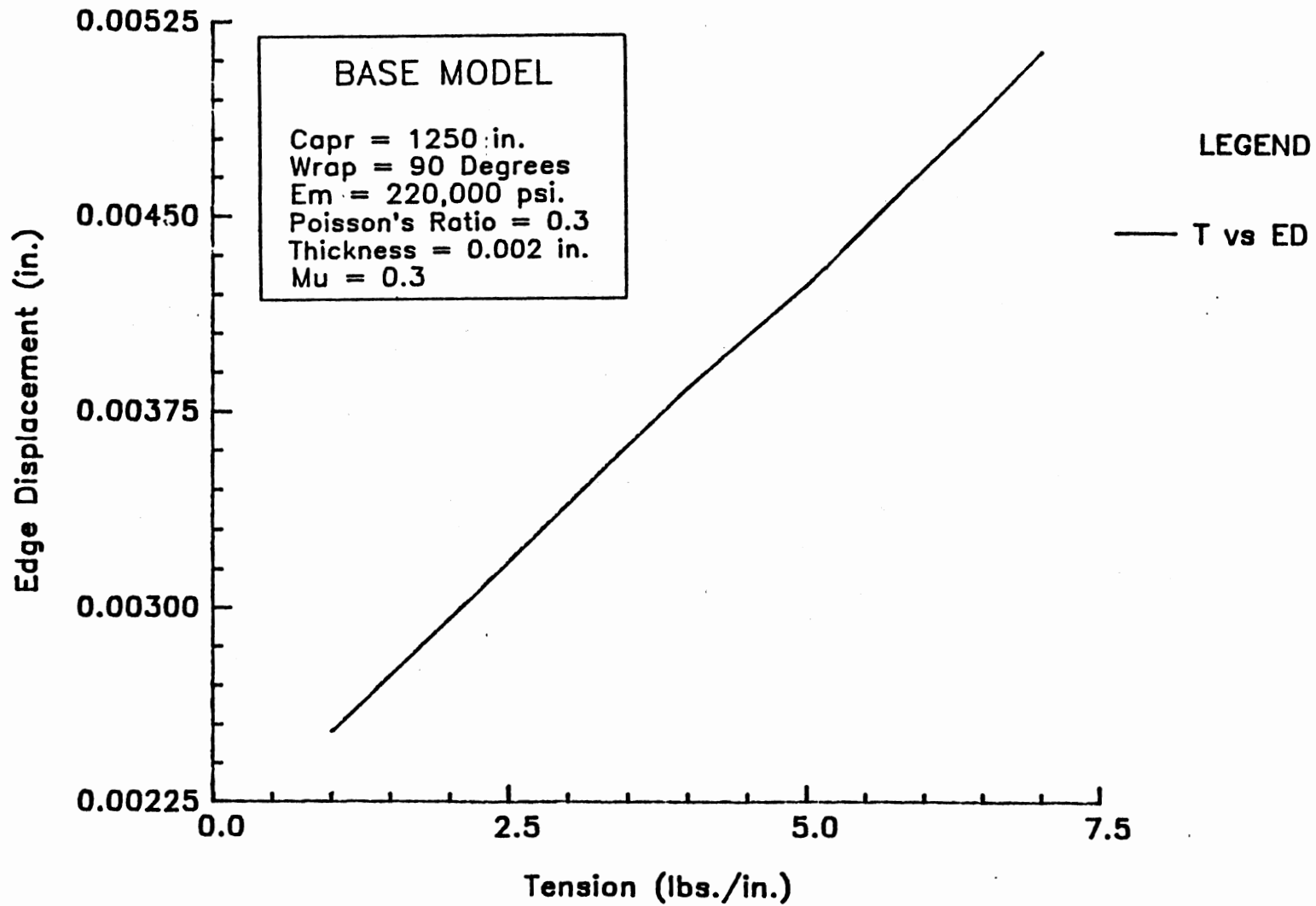


Figure 35. Edge Displacement as a Function of Tension

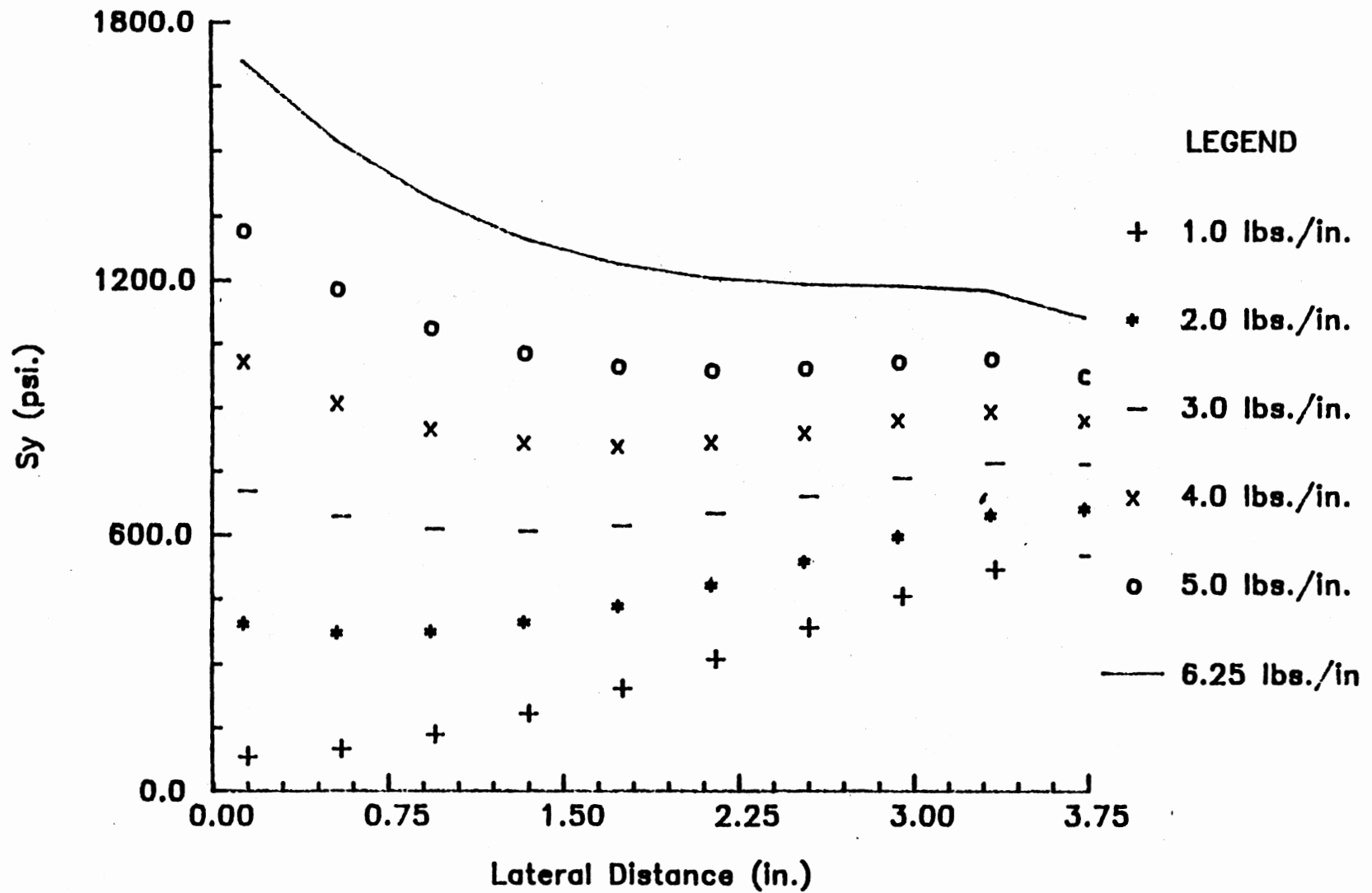


Figure 36. Lateral S_y Distribution at M.D. Distance 16.05 in. for Various Tensions

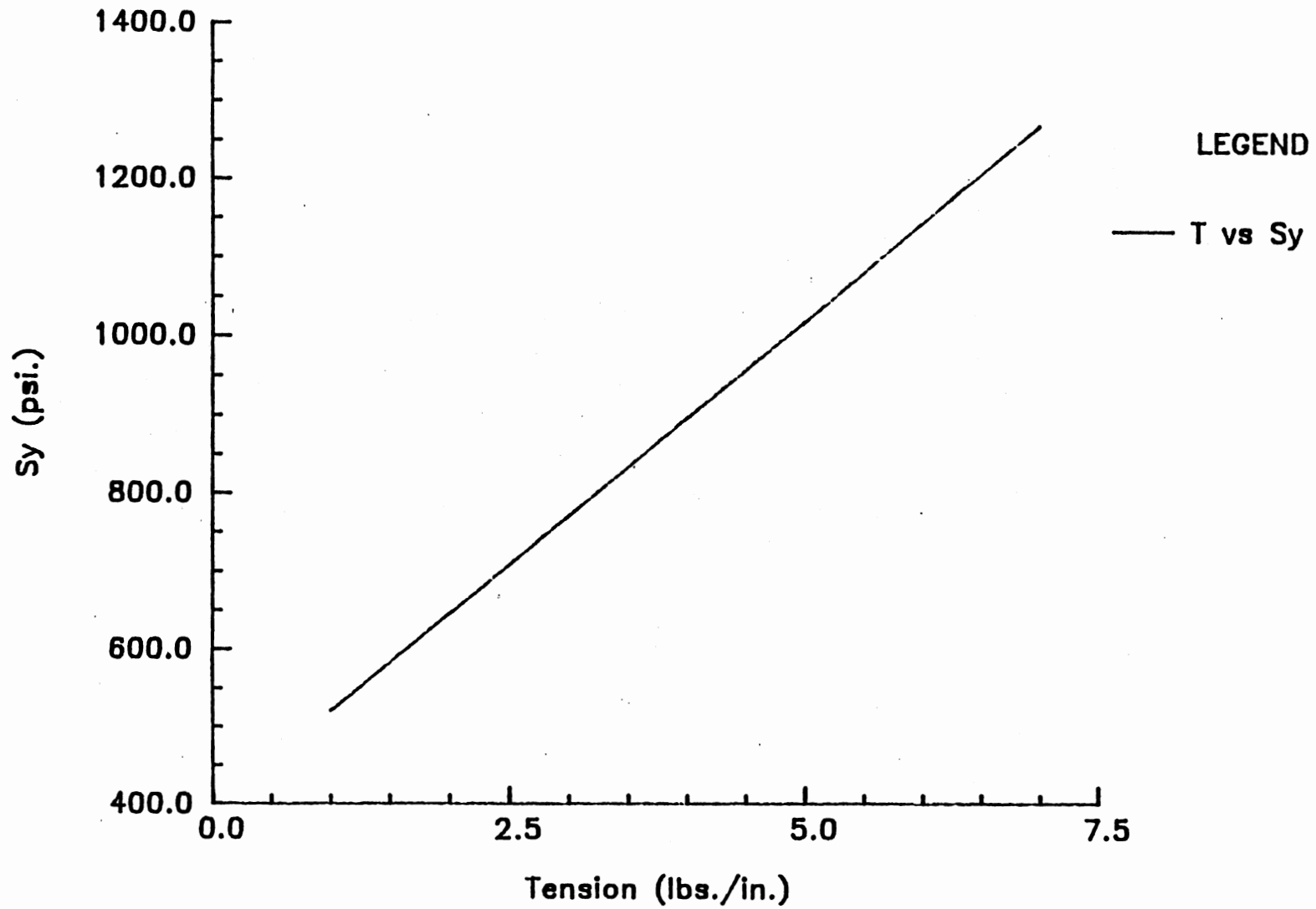


Figure 37. Sy at M.D. Distance 16.05 in. and Lateral Distance 3.33 in. for Various Tensions

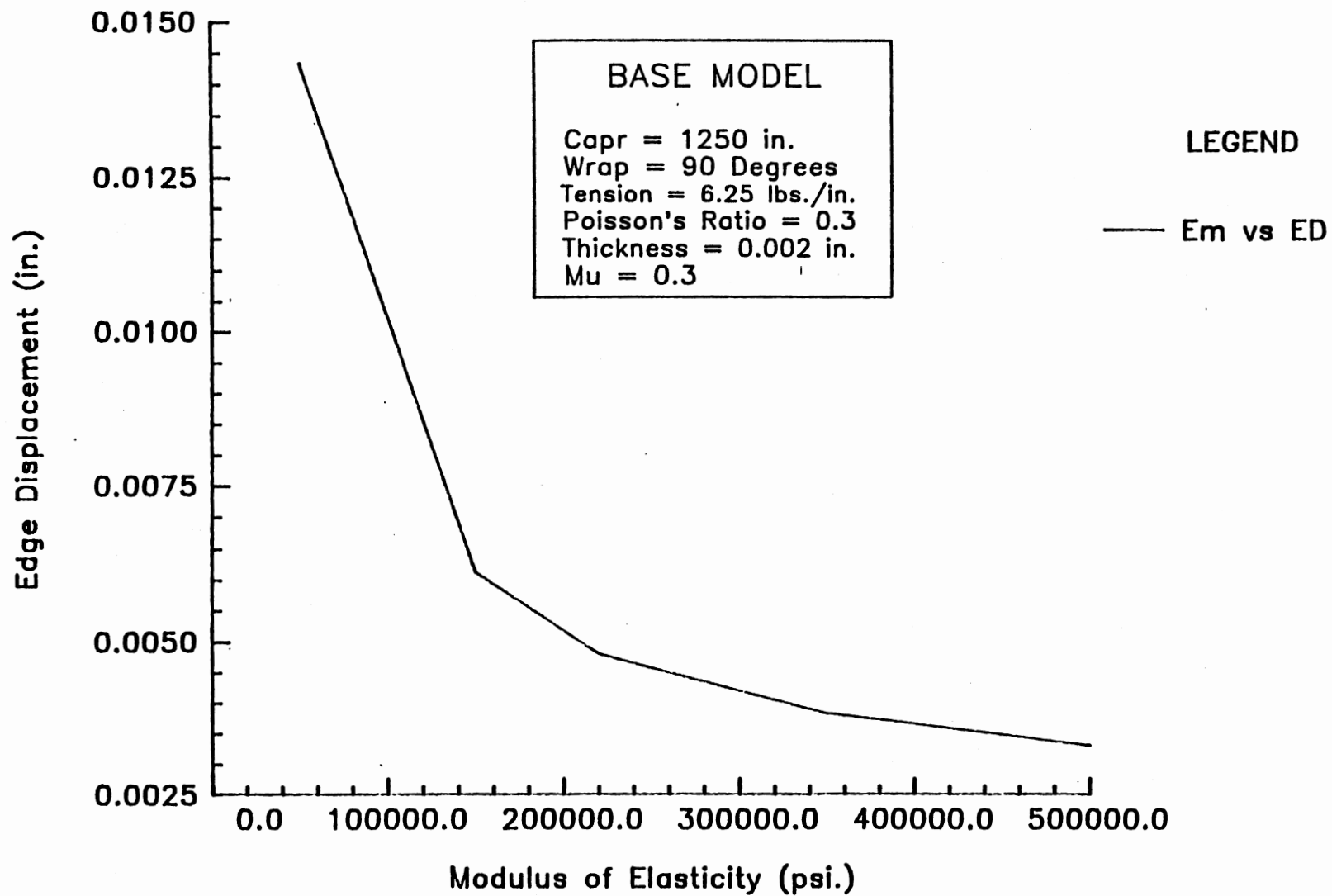


Figure 38. Edge Displacement on Concave Roller as a Function of the Modulus of Elasticity

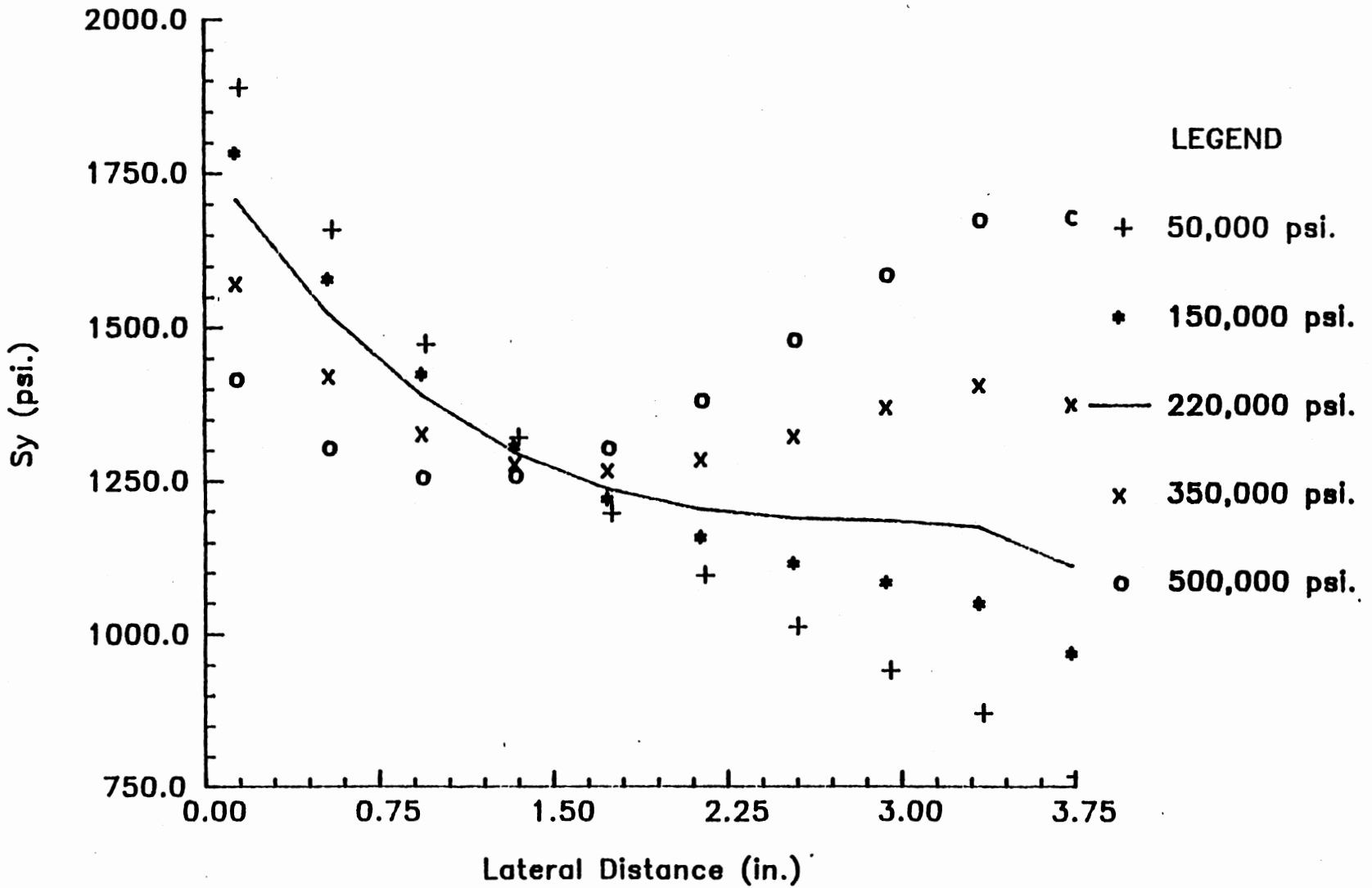


Figure 39. Lateral S_y Distribution at M.D. Distance 16.05 in. for Various Moduli of Elasticity

these trends, it is necessary to understand changes in the initial machine direction stress induced by the changing moduli. Recall that the strain distribution is constant for this parameter since the radius of curvature is a constant value of 1250 inches. Significantly increasing the modulus of elasticity results in large increases in the initial machine direction stress distribution via Equation (2.7). This distribution of the initial machine direction stress can again be seen by referring to Figure 23 for the curve representing the 1250-inch radius. The uniform trend of the curve in the interior portion of the web causes the initial decrease shown in Figure 39. The lack of significant lateral increase in the machine direction stress combines with the lateral increase in the radius of the concave roller to result in impending lateral slip being achieved sooner for each subsequent node in this interior region. The lower moduli also show higher stresses relative to the higher moduli in this interior region of the web. This result is due to the various stiffnesses represented by the different moduli. Although the higher moduli have higher initial machine direction stresses, they also have increased stiffness. This stiffness resists spreading thereby meeting the lateral slip criteria earlier with respect to the lower moduli.

However, these trends change for the exterior portion of the web. The higher initial machine direction stresses of the higher moduli provide considerably more spreading ability due to the increasing trends shown in Figure 23. The lower moduli result in much smaller changes in the initial machine direction stress for this exterior region. These smaller changes again coupled with the

increasing roller radius provide the continued decreasing trends of the small moduli as shown in Figure 39.

Spreading stresses at a lateral location of 3.33 inches are plotted as a function of the various moduli of elasticity in Figure 40. This plot shows a linear relationship between the spreading stress at this location and the various moduli. This plot corresponds with the previous analysis in that each larger modulus is capable of supporting higher frictional forces.

4.5 Poisson's Ratio

Figure 41 shows the effect of various values of Poisson's ratio on the spreading of the web. Refer to section 4.1 for Equation (4.5) and the discussion on Poisson's ratio. The plot indicates that lower Poisson values result in higher edge displacements of the web. This trend is understood by considering the amount of contraction, induced by the initial machine direction strains, that the spreading must overcome. Small Poisson values represent small lateral contractions and therefore less contraction to overcome. This results in increased spreading ability given the available friction forces. Likewise, larger Poisson values represent large contractions. Spreading displacements must overcome this contraction before positive displacements, relative to the undeformed web width, result.

Lateral stresses across the roll are shown in Figure 42. The results presented in this plot logically follow the trends shown in Figure 41. Refer to Figure 43 for lateral stresses down the length of the web for various Poisson values. Particularly note the lateral stresses of the contracted state of the web. These lateral stresses

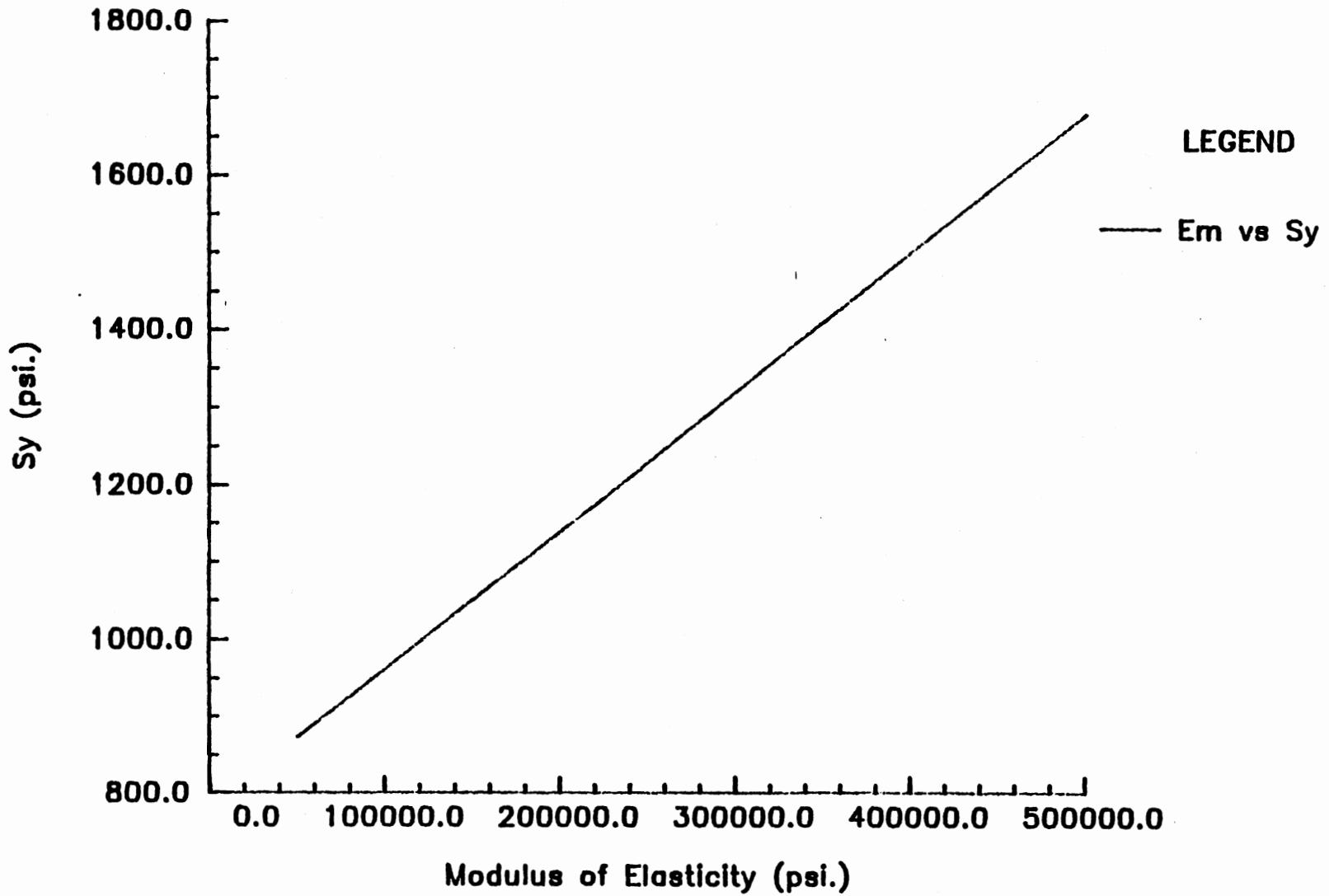


Figure 40. Sy at M.D. Distance 16.05 in. and Lateral Distance 3.33 in. for Various Moduli of Elasticity

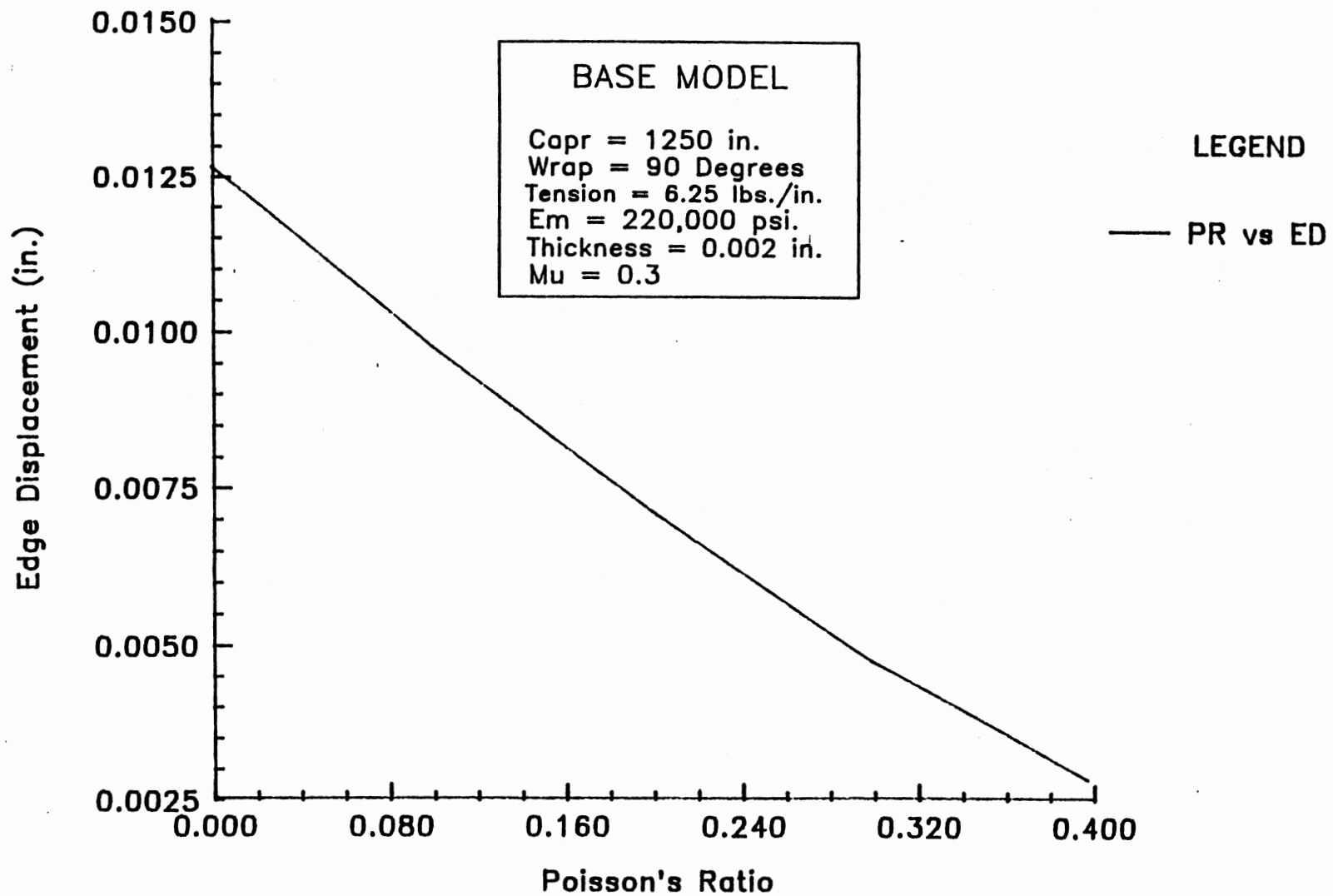


Figure 41. Edge Displacement on Concave Roller as a Function of Poisson's Ratio

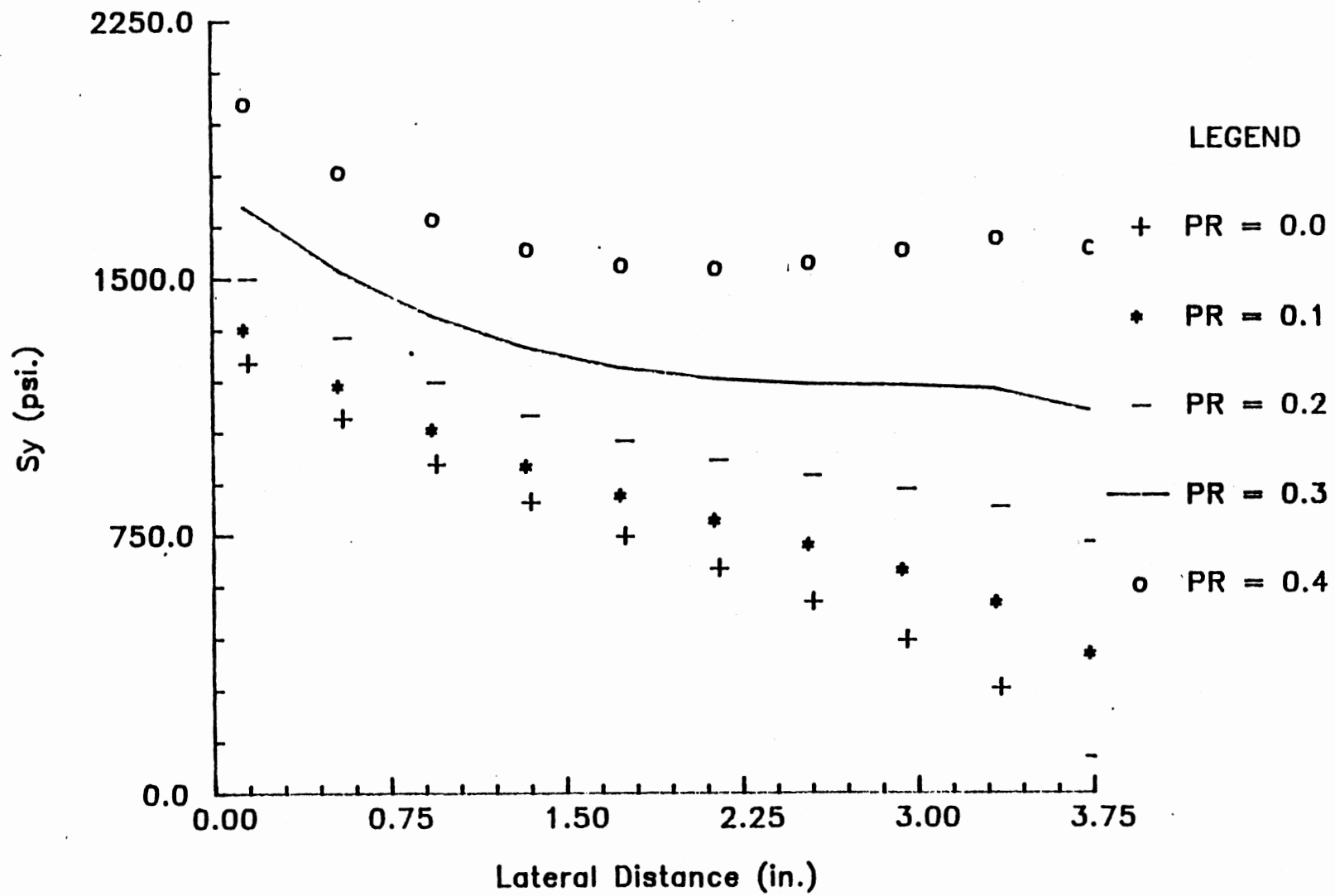


Figure 42. Lateral S_y Distribution at M.D. Distance 16.05 in. for Various Poisson's Ratio Values

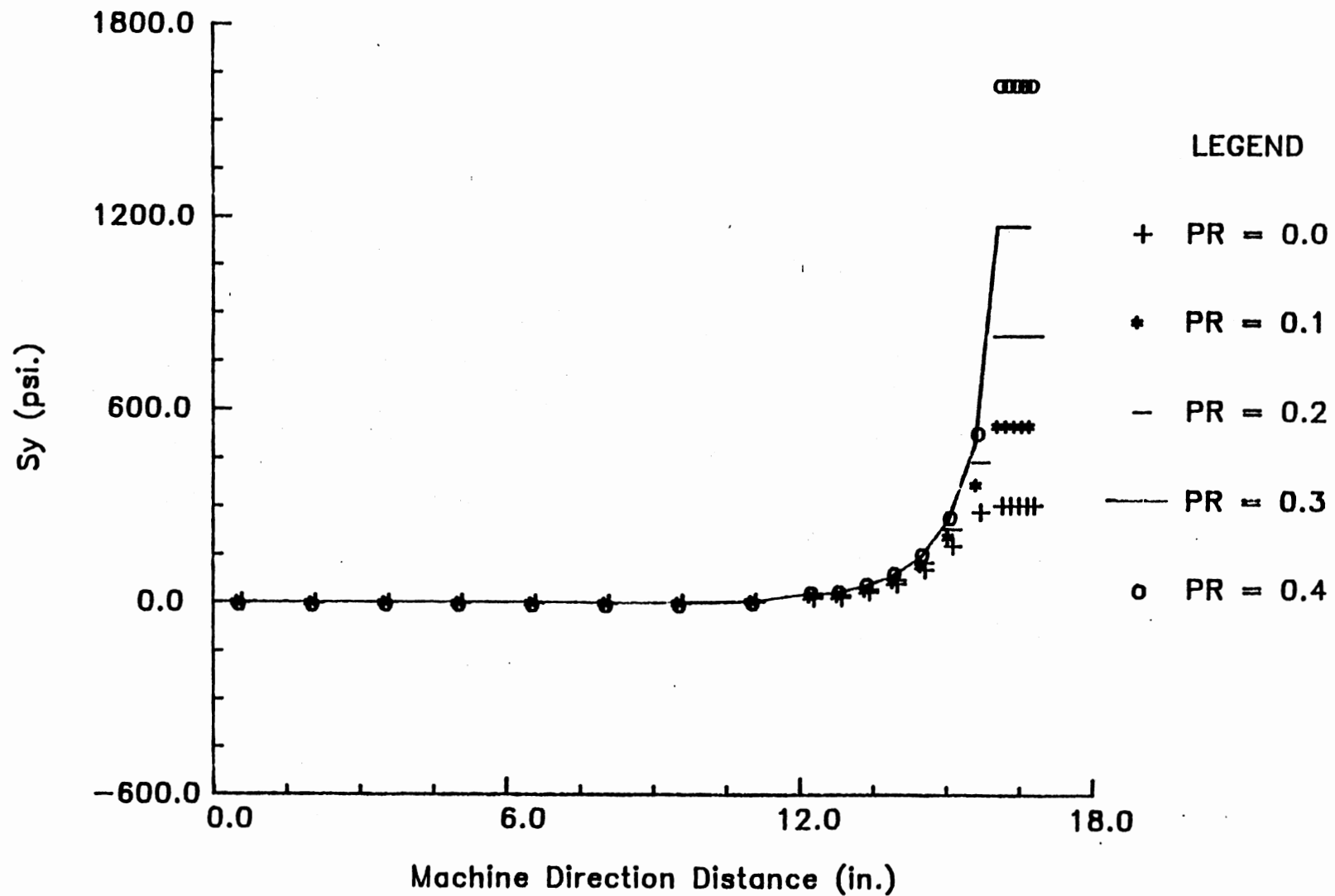


Figure 43. M.D. Sy Distribution at Lateral Distance 3.33 in. for Various Poisson's Ratio Values

are virtually zero, although they all represent different contractions of the web. Therefore, any spreading from this contracted state results in positive spreading stresses (i.e., no negative lateral stresses to overcome). Although the larger Poisson values show less positive displacements, they represent more net spreading, as shown in Figure 44. This larger net spreading of larger Poisson values and lower net spreading of lower Poisson values result in the corresponding stresses shown in Figure 42. The increasing net spreading values shown in Figure 44 are again a result of each outer node also experiencing the spreading associated with the nodes interior to it.

4.6 Thickness

The next parameter studied was web thickness. Figure 45 is a plot of the edge displacement as a function of web thickness. The curve shows that lower thicknesses increase the spreading ability of the concave roller. With the tension, web width, and modulus of elasticity the same for all values of the thickness, a smaller thickness would result in higher initial machine direction strain distribution via Equation (2.8) and thus a higher initial machine direction stress distribution via Equation (2.7). The larger initial machine direction stresses associated with the smaller thicknesses would then result in higher spreading abilities in the web. This is the trend shown in Figure 45.

Figure 46 shows the lateral stress distributions across the web for the various thicknesses. The same discussion presented for the other parameters again holds for this plot. The increasing curves of the larger thicknesses result from the laterally increasing initial

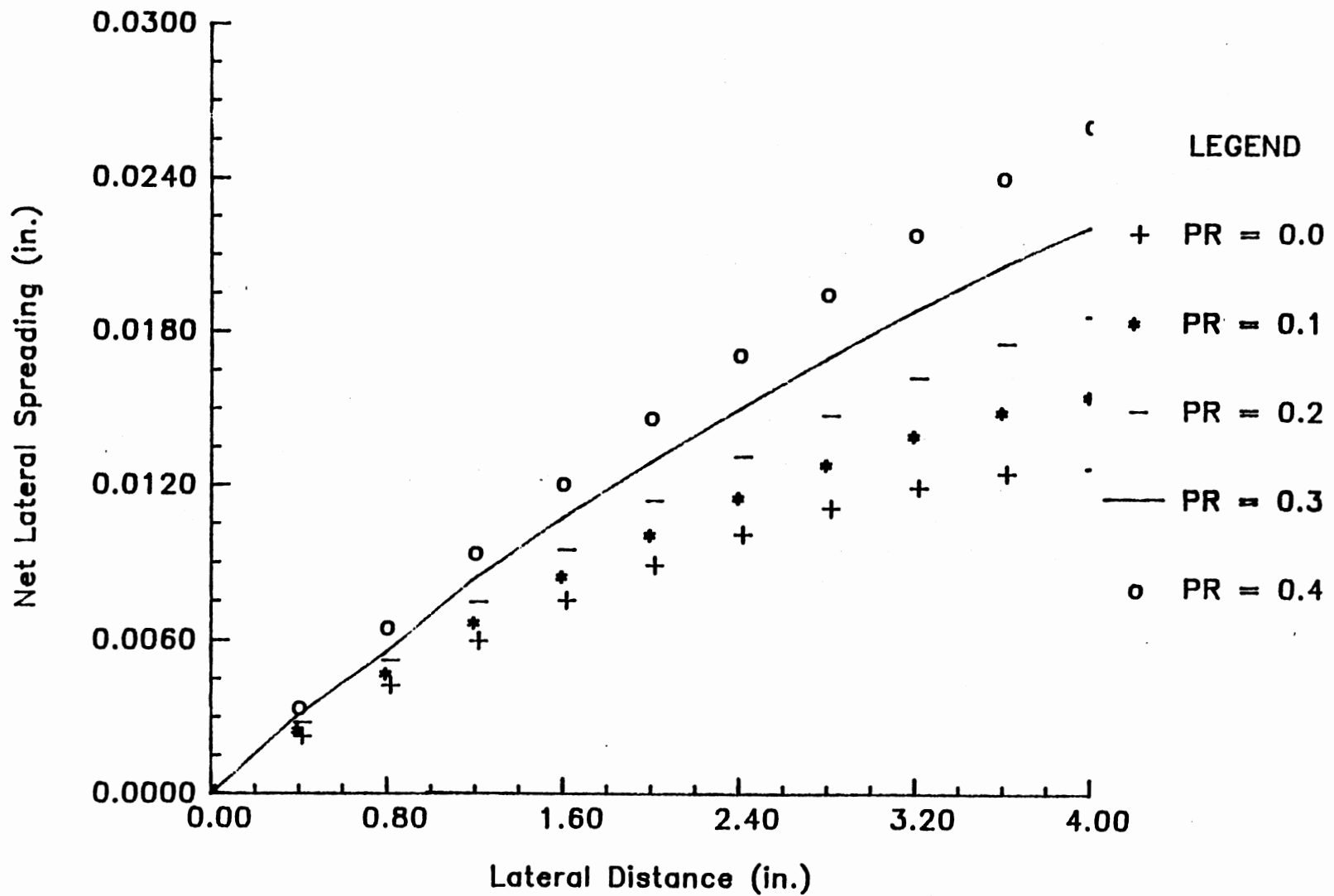


Figure 44. Net Lateral Spreading for Various Poisson's Ratio Values

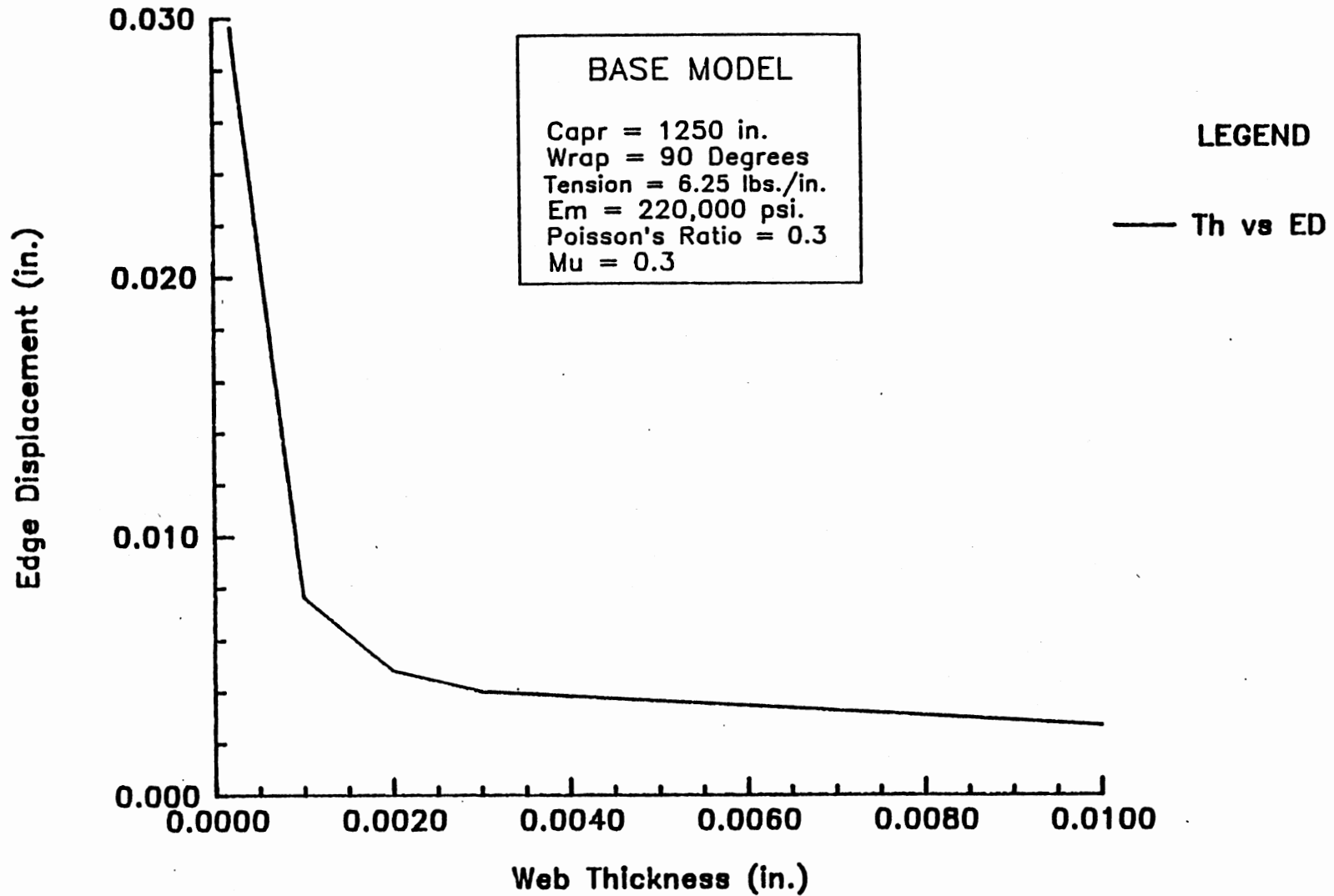


Figure 45. Edge Displacement on Concave Roller as a Function of Web Thickness

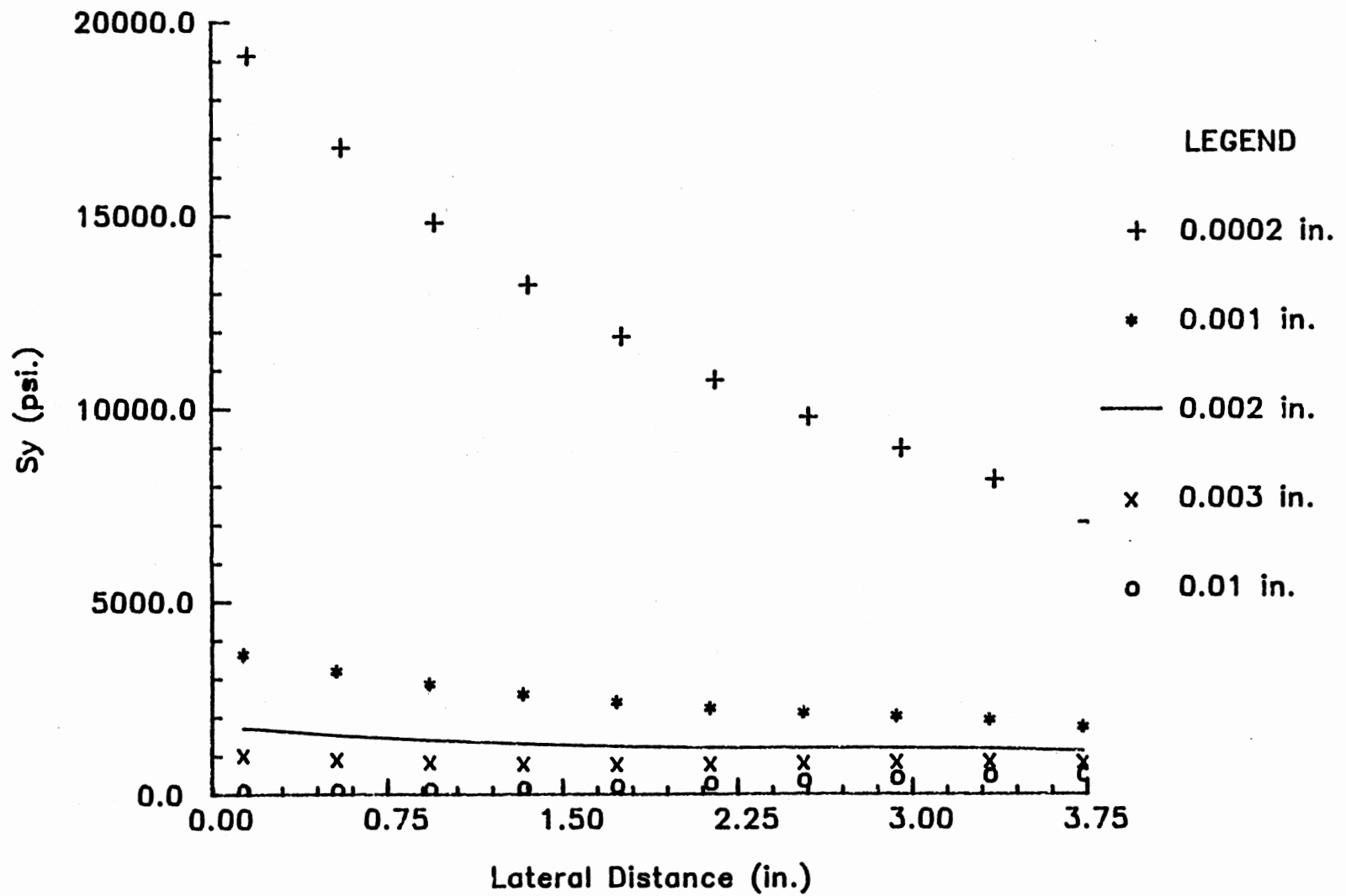


Figure 46. Lateral Sy Distribution at M.D. Distance 16.05 in. for Various Web Thicknesses

machine direction stress distribution. However, the curves for the smaller thicknesses decrease. This decrease is again due to the increasing radius of the concave roller, whereby impending slippage occurs sooner for each subsequent node.

Figure 47 shows a plot of the lateral stress at a lateral location of 3.33 inches. The curve shown has a strong correlation to the edge displacement curve shown in Figure 47. This curve is understood by considering the use of the thickness in the finite element method. The thickness is just used as a constant in the development of the elemental stiffness matrices. Therefore, changes in this parameter can simply be thought of as "scaling factors" for the stiffness matrix and do not affect elastic characteristics of the material. This results in the correlation between Figures 47 and 45, whereby a given stress results in a given displacement.

4.7 Coefficient of Friction

The last parameter in this study is the coefficient of friction. Figure 48 shows the edge displacement on the roll as a function of this parameter. The resulting curve is linear, indicating a direct correlation between the coefficient of friction and the edge displacement of the web. The coefficient of friction is an operating system parameter and not a material property parameter. A high correlation between changes in this parameter and the resulting spreading of the web would therefore be expected. Recall that the coefficient of friction is used to calculate the spreading force via Equation (3.6). Increases in this variable would provide higher frictional forces and thus result in larger spreading displacements as shown in Figure 48.

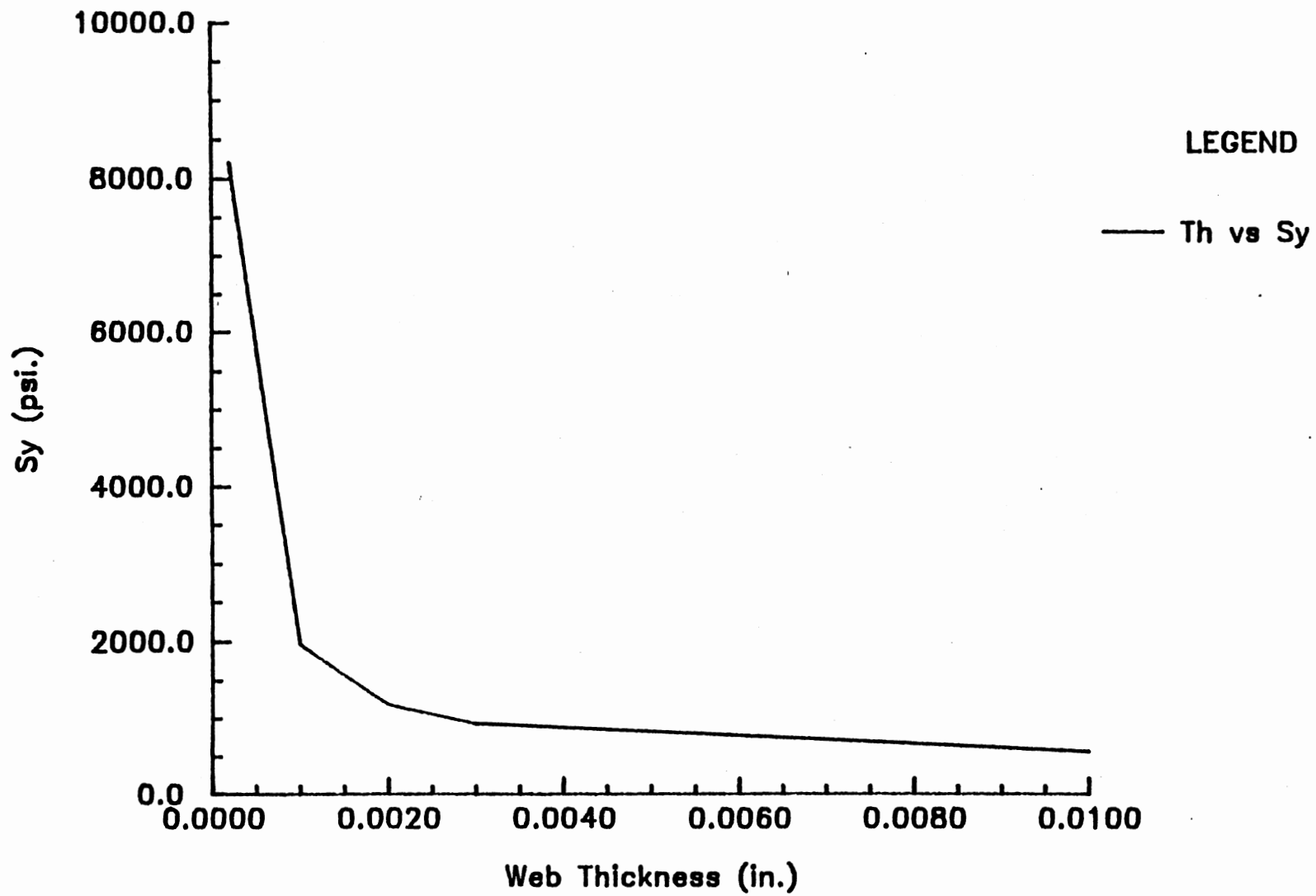


Figure 47. Sy at M.D. Distance 16.05 in. and Lateral Distance 3.33 in. as a Function of Web Thickness

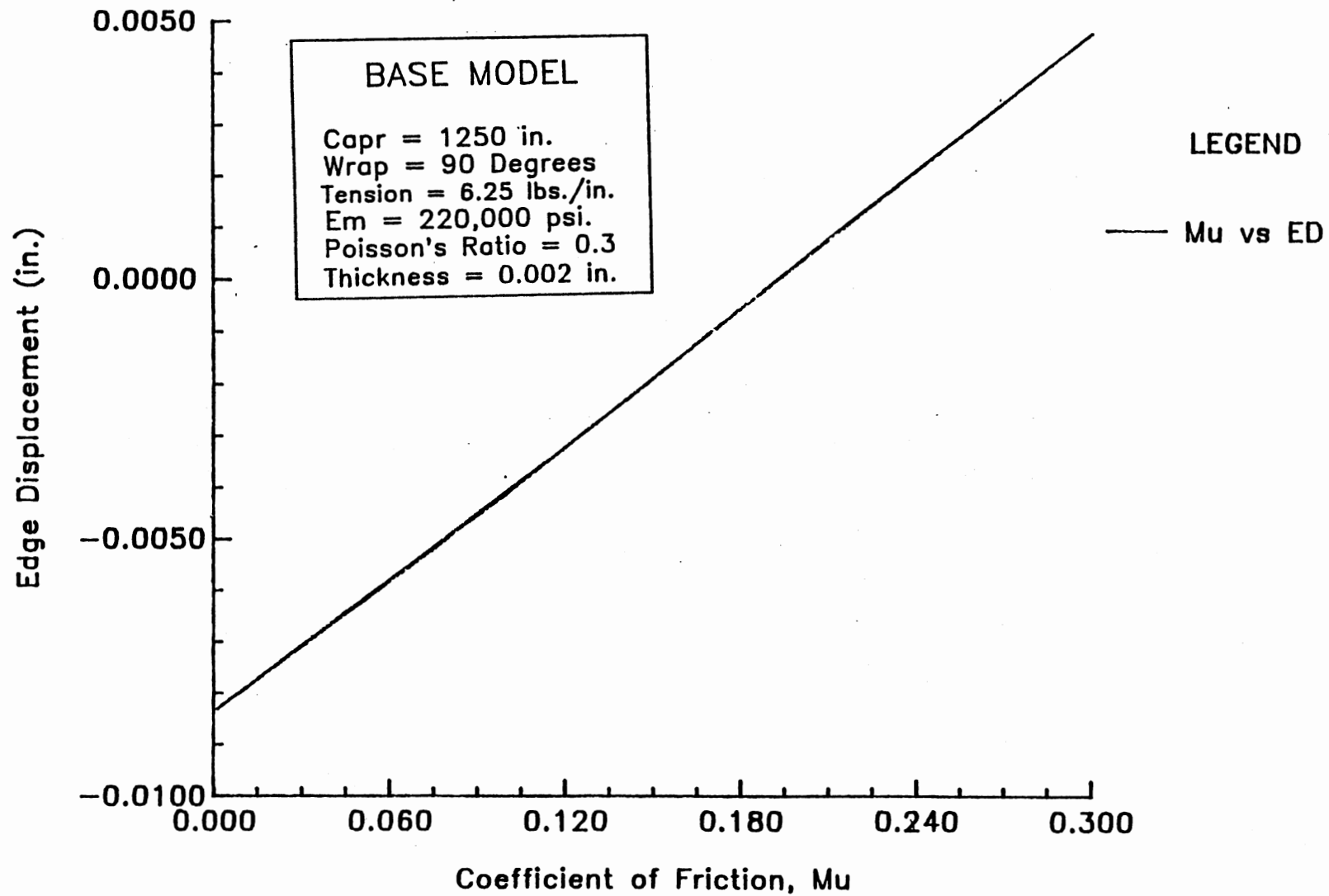


Figure 48. Edge Displacement on Concave Roller as a Function of the Coefficient of Friction

Figure 49 shows the S_y distribution laterally across the web for various coefficients. This plot again shows the higher coefficients of friction resulting in higher spreading tractions. The convergence at the edge of the web was not expected.

To address this convergence as well as the convergence of the wrap angle and tension parameters, it becomes necessary to consider the equilibrium requirements of the outer elements. Recall that the outside edge of the web cannot support any traction. A theoretical element would therefore appear as Figure 50, with the variables representing their usual meanings. Summing forces in the x and y directions result in equations (4.6) and (4.7), respectively.

$$\frac{\partial \sigma_x}{\partial x} - \frac{\partial \tau_{yx}}{\partial y} = 0 \quad (4.6)$$

$$\frac{\partial \sigma_y}{\partial y} - \frac{\partial \tau_{xy}}{\partial x} = 0 \quad (4.7)$$

Equation (4.8) is obtained by summing the moments about the center of the element.

$$\begin{aligned} & \left[\tau_{xy} + \frac{\partial \tau_{xy}}{\partial x} \left(\frac{dx}{2} \right) + \tau_{xy} - \frac{\partial \tau_{xy}}{\partial x} \left(\frac{dx}{2} \right) \right] \frac{dx}{2} dy dz \\ & - \left[\frac{\partial \tau_{yx}}{\partial y} \left(\frac{dy}{2} \right) - \frac{\partial \tau_{yx}}{\partial y} \left(\frac{dy}{2} \right) \right] dx \frac{dy}{2} dz = 0 \end{aligned} \quad (4.8)$$

Simplifying,

$$2 \tau_{xy} = 0 \quad (4.9)$$

or

$$\tau_{xy} = 0 \quad (4.10)$$

By incorporating (4.10) into the theoretical element, Figure 51 is obtained.

Summing the forces about Point C yields

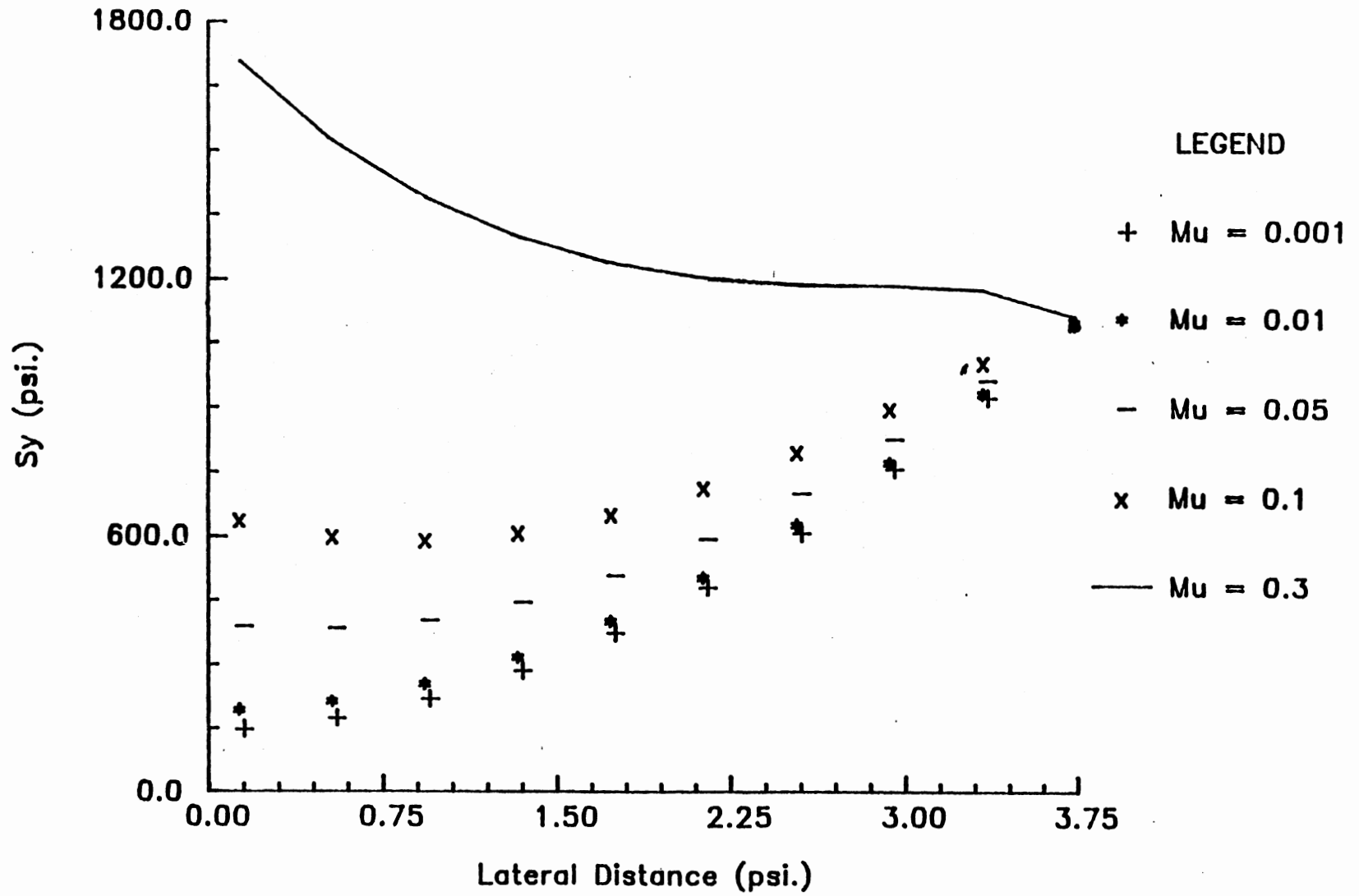


Figure 49. Lateral Sy Distribution at M.D. Distance 16.05 in. for Various Coefficients of Friction

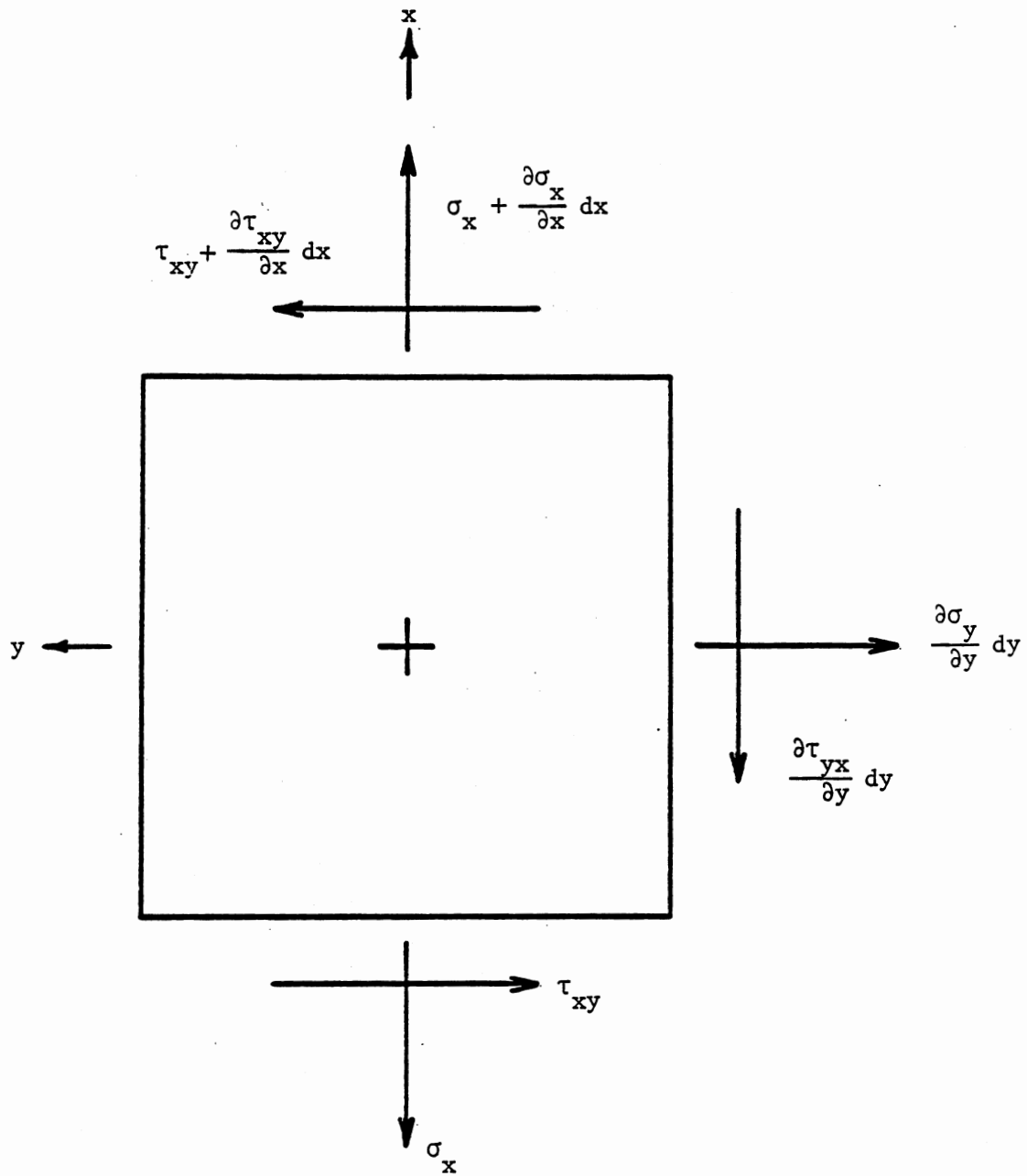


Figure 50. Theoretical Element
Incorporating Zero
Traction at Outside
Edge of Web

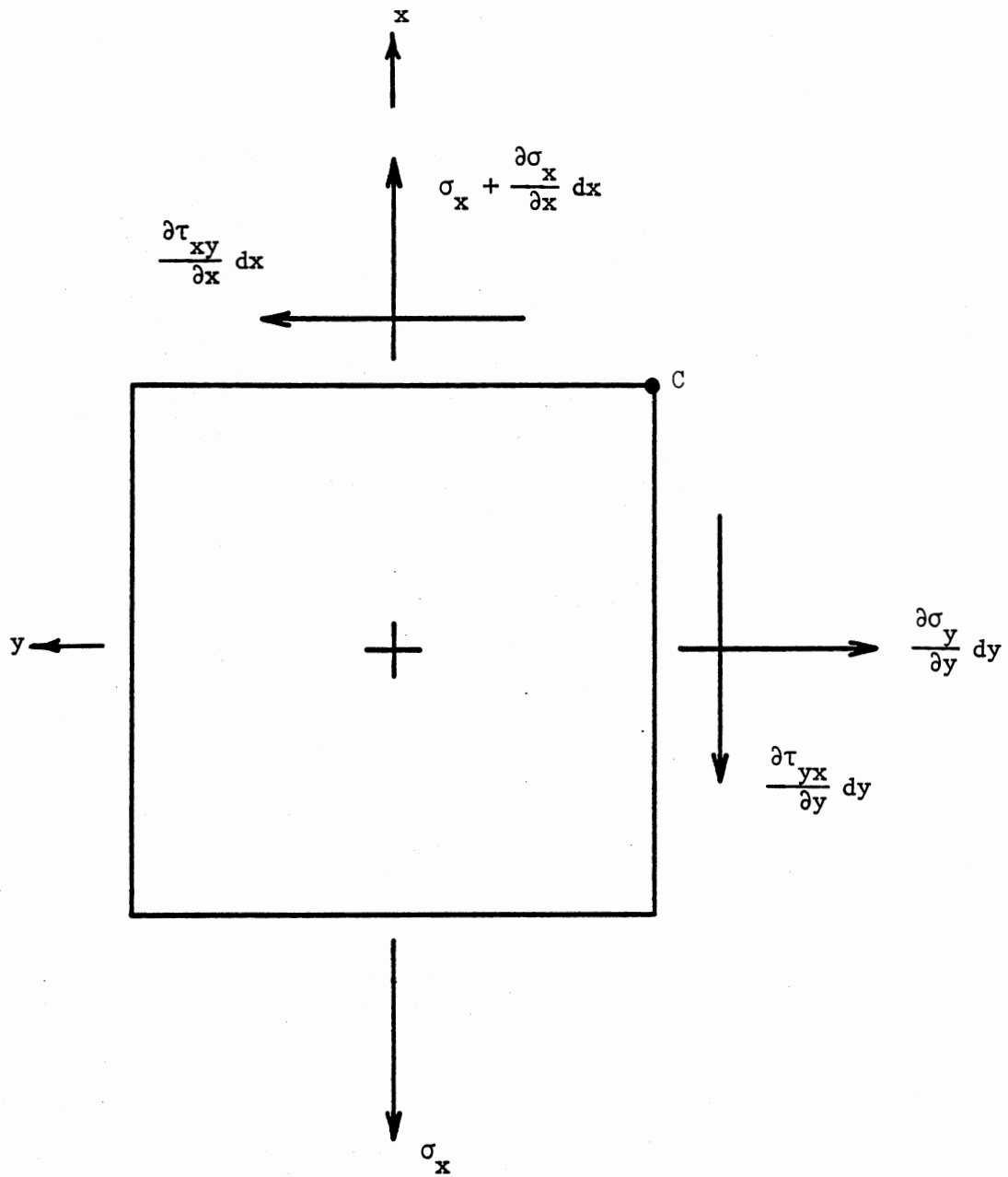


Figure 51. Theoretical Element
 Incorporating $\tau_{xy} = 0$

$$\left(\sigma_x - \sigma_x - \frac{\partial \sigma_x}{\partial x} dx\right) \frac{dy}{2} dydz + \frac{\partial \sigma_y}{\partial y} dy \left(\frac{dx}{2}\right) dx dz = 0 \quad (4.11)$$

or

$$\frac{\partial \sigma_x}{\partial x} dy = \frac{\partial \sigma_y}{\partial y} dx \quad (4.12)$$

This equation explains the convergence of the lateral stress for the edge elements of the wrap angle, tension, and coefficient of friction parameters. Recall that the machine direction stresses are enforced and therefore the rate of change per unit width is also enforced. In other words, the right side of Equation (4.12) is set for constant material properties and a given geometry (i.e., Radius of Curvature is constant.) All stresses therefore converge at the edge of the web because the lateral stress at this location is totally dependent on the enforced machine direction displacements.

Herein lies a shortcoming of the coefficient of friction analysis. The problem is associated with the assumed boundary conditions. Recall that the procedure used to calculate the initial machine direction strain profile ignores the possibility of slippage in the machine direction. If slippage is occurring in the machine direction, then the initial strain profile will be nearly uniform across the web width and thus less spreading will occur. If this slippage was accounted for with respect to the various coefficients of friction, the lateral stresses at the outside edge of the web would not converge. Thus the results shown in Figure 49 must only be regarded as qualitative at best without a thorough study of the effect of machine direction slippage upon the lateral stresses.

This shortcoming of the coefficient of friction parameter does not invalidate the other lateral stress trends. Although the lateral stress of the outer element is controlled by Equation (4.12), the

interior elements are still capable of supporting all of the plane stress components. The trends they indicate are therefore still acceptable.

It should also be mentioned that the fact σ_y is prescribed for the outer element in no way invalidates the spreading analysis. The spreading results have frequently been described in terms of applied stresses. In actuality, the spreading analysis is based upon forces and displacements. The stresses are merely a derivative of this interaction and are therefore just a convenient tool in the analysis of the results.

CHAPTER V

CONCLUSIONS

5.1 Overview

In this study, finite element programs developed by Leport [2] were modified to better simulate the response of a web induced by a concave roller. The same average plane coordinate system was used to address out-of-plane nodal displacements. An average strain criteria was developed for web spans. This criteria led to the redistribution of the strain present in the web for the geometry of the concave roller. Displacements were calculated and enforced across and around the concave roller to ensure equal spreading. The nodes on the roller were constrained such that all the nodes at a given lateral location spread equally. New parameters were also added to provide more flexibility to the model.

Once the above boundary conditions were incorporated, a baseline set of parameters was selected and one parameter was allowed to vary within specified ranges. The output of the finite element model was studied as a result of allowing that parameter to vary in terms of machine direction and cross machine direction stresses and displacements. The analyses showed that increasing the radius of curvature, angle of wrap, web tension, and coefficient of friction all induced increased spreading of the web. Conversely, increases in the Modulus

of Elasticity, Poisson's ratio, and thickness of the web resulted in a decrease in the spreading response.

In typical applications, spreading devices are added after web lines are constructed. The usefulness of this model is as a design tool to help design engineers select the concave roller profile and the coefficient of friction, which can be controlled by selecting various roll coverings and by fluting the roll if air entrainment is a problem. For the range of parameters studied, the model behaved as expected except with regard to the coefficient of friction parameter as low values of this parameter cannot be expected to enforce the machine direction strains due to the concave roll which was originally assumed. Thus, for the model to be valid, it is required that the web/roll traction be sufficient to prevent machine direction slippage.

5.2 Recommendation for Future Study

As in any computer simulation, experimental verification is necessary. However, sensors are still unavailable to accurately detect very small displacements. Likewise, no method of stress determination in a moving web is available. Improvements in these areas are necessary to verify this computer model. This approach should also be applied to different geometries and different spreaders to predict their behavior. Once the model has been experimentally verified, parametric analysis should be performed to determine the sensitivity of the lateral spreading stresses and displacements to the various parameters.

An increasing amount of research and literature address the impact of air entrainment between the web and roll on the coefficient

of friction. This research is very important to this model because the coefficient of friction is likely to be a function of other parameters such as the tension and the wrap angle. This model merely assumes all the exterior influences of this parameter have already been accounted for in the prescribed value.

Lastly, this model should be condensed and made more efficient so it can run on a personal computer. This task can possibly be aided by incorporating higher order elements into the model. These higher order elements should also provide a better modeling in the region immediately prior to the concave roller.

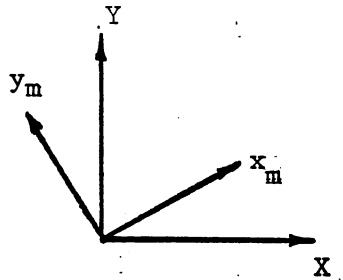
BIBLIOGRAPHY

1. Shelton, J. J. and Reid, K. N., "Lateral Dynamics of an Idealized Moving Web," Journal of Dynamic Systems, Measurements and Control, Vol. 93, No. 3 (September, 1971), pp. 187-192.
2. Leport, M. L. "The Mechanics of Webs Encountering Concave Rollers," M.S. Thesis, Oklahoma State University, 1987.
3. Swift, H. W., "Cambers for Belt Pulleys," Proceedings, Institute of Mechanical Engineers (London), Vol. 122 (June, 1932), pp. 627-683.
4. Pfeiffer, J. D., "Web Guidance Concepts and Applications," TAPPI, Vol. 60, No. 12 (December, 1977).
5. "Web Steering," Unpublished Web Handling Research Center Information Brochure. Oklahoma State University. No date.
6. Shelton, J. J., "Fundamentals of Lateral Web Behavior," Unpublished Web Handling Research Center Brochure. Oklahoma State University (February, 1988).
7. Daly, D. A., "Factors Controlling Traction Between Webs and Their Carrying Rolls," TAPPI, Vol. 48, No. 9 (September, 1965), pp. 88A-90A.
8. Shelton, J. J., "Dynamics of Web Tension Control with Velocity or Torque Control," Proceedings, 1986 American Control Conference, Seattle, Washington, Vol. 3, pp. 1423-1427.
9. Segerlind, L. J., Applied Finite Element Analysis. 2nd. Ed. New York: John Wiley and Sons, Inc. 1984.
10. Segerlind, L. J., Applied Finite Element Analysis. 2nd. Ed. New York: John Wiley and Sons, Inc. 1984, pp.g 340-350.
11. James, M. L., Smith, G. M., and Wolford, J. C., Applied Numerical Methods for Digital Computation. 3rd. Ed., New York: Harper and Row, Publishers, 1985.
12. Chapra, S. C. and Canale, R. P., Numerical Methods for Engineers with Personal Computer Applications. United States of America: McGraw-Hill, Inc., 1985.

APPENDIXES

APPENDIX A

MODIFICATIONS FOR SKEWED BOUNDARY CONDITIONS



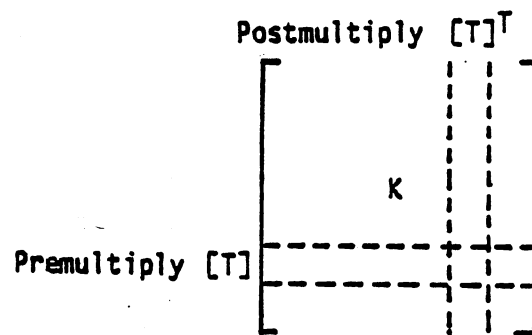
$$\begin{Bmatrix} x_m \\ y_m \end{Bmatrix} = [T] \begin{Bmatrix} X \\ Y \end{Bmatrix}$$

where

$$[T] = \begin{bmatrix} \cos\theta & \sin\theta \\ -\sin\theta & \cos\theta \end{bmatrix}$$

X and Y represent the global coordinate system x_m and y_m represent the average plane coordinate system. After the global stiffness matrix for the structure is established, modify only the rows and columns associated with the node to be transformed:

1. Premultiply the appropriate rows of [K] by [T].
2. Postmultiply the appropriate columns of [K] by $[T]^T$.



This is done for every node. The resulting [K] matrix will be entirely in the coordinate system of average planes. Since forces will be applied in the average plane system, the resulting displacements will also be in this system.

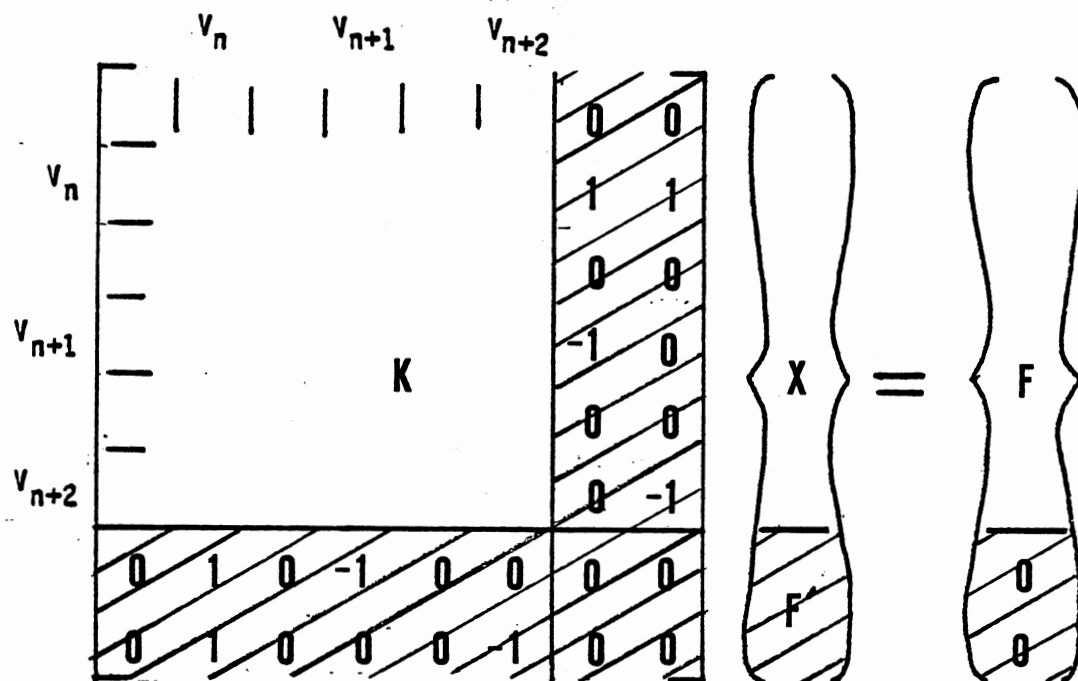
APPENDIX B

CONSTRAINT EQUATIONS FOR SYSTEM OF EQUATIONS

Additional constraint equations:

$$V_n - V_{n+1} = 0$$

$$V_n - V_{n+2} = 0$$



Shaded regions represent matrix additions. $[K]$ is appended with the additional equations. $\{F\}$ is appended with the displacements. When the new system of equations is solved, the F' portion of the $\{X\}$ matrix will represent the forces required to enforce the constraints.

APPENDIX C

COMPUTER CODE FOR PROGRAM MSHGMR

```

C *****
C
C                               PROGRAM MSHGNR.FOR
C
C THIS PROGRAM GENERATES THE FINITE ELEMENT DATA NEEDED FOR
C THE PROGRAM CONCAVE.FOR
C IT GENERATES THE MESH DATA, ENFORCED DISPLACEMENTS,
C AND THE APPLIED FORCES
C THE PROGRAM CREATES FOUR FILES: MESH.DAT CONSTR.DAT FORCE.DAT
C AND BCNSTR.DAT
C
C *****
C
C *****
C
C MACHINE DIRECTION SYMMETRY ABOUT THE CONCAVE ROLLER IS INCORPORATED.
C AN INCREASED ELEMENT DENSITY REGION EXISTS FOR 25% OF THE ENTRY SPAN
C   LENGTH PRECEEDING THE CONCAVE ROLLER.
C MACHINE DIRECTION DISPLACEMENTS ARE ENFORCED OVER THE ROLLER.
C W2 IS FOUND SUCH THAT THE AVERAGE STRAIN CRITERIA IS MET.
C CALCULATES DIFFERENTIAL FORCES TO REDISTRIBUTE STRAINS FOR CONCAVE
C   ROLLER.
C
C *****
C                               LAST UPDATE 5/16/88
C *****
C
C
C   DOUBLE PRECISION R,Y(400),CAPR
C   DIMENSION I(500),J(500),K(500)
C   DIMENSION X(400),XC(400),Z(400),UDISP1(20),UDISP2(20)
C   COMMON/DOMEGA/CAPR
C   COMMON/TLE/TITLE(20)
C   COMMON/OMEGA1/RZERO,WW,WL,STRA
C   COMMON/OMEGA2/W2,STRB
C
C *****
C DEFINITION OF THE INPUT VARIABLES
C *****

```

```

C
C MODEL PARAMETERS
C     WW - WIDTH OF THE WEB
C     ALBR - LENGTH OF WEB BEFORE THE ROLLER
C     RZERO - ROLLER BASE RADIUS
C     CAPR - CIRCULAR ARC PROFILE: RADIUS OF CURVATURE
C           LINEAR TAPER PROFILE: RADIUS AT OUTSIDE EDGE
C     NXB - NUMBER OF ELEMENT INTERVALS IN THE X-DIRECTION
C     NAR - NUMBER OF ELEMENT INTERVALS OVER THE ROLLER
C     NY - NUMBER OF ELEMENT INTERVALS IN THE Y-DIRECTION
C     TH - THICKNESS OF WEB
C     EM - MODULUS OF ELASTICITY OF WEB
C     PR - POISSON'S RATIO
C     AMU - COEFFICIENT OF FRICTION
C     W1 - ANGULAR VELOCITY OF FIRST ROLLER
C     FORCE - NODAL FORCE APPLIED AT END OF WEB
C     WRAP - ANGLE OF WRAP AROUND ROLLER
C
C NODAL COORDINATES
C     X(I) - X COORDINATES OF NODES IN NUMERICAL SEQUENCE
C     Y(I) - Y COORDINATES OF NODES IN NUMERICAL SEQUENCE
C     Z(I) - Z COORDINATES OF NODES IN NUMERICAL SEQUENCE
C
C ELEMENT CONNECTIVITIES
C     N - ELEMENT NUMBER
C     I(N) - NUMERICAL VALUE OF NODE I
C     J(N) - NUMERICAL VALUE OF NODE J
C     K(I) - NUMERICAL VALUE OF NODE K
C
C
C *****
C     INPUT SECTION OF THE PROGRAM
C *****
C
      READ(9,3) TITLE
3     FORMAT(20A3)
      READ(9,*) WW
      READ(9,*) ALBR
      READ(9,*) RZERO

```

```
READ (9, *) CAPR
READ (9, *) NXB
READ (9, *) NAR
READ (9, *) NY
READ (9, *) TH
READ (9, *) EM
READ (9, *) PR
READ (9, *) AMU
READ (9, *) W1
READ (9, *) FORCE
READ (9, *) WRAP
```

C

C ECHO INPUT DATA

C

```
WRITE (10,3) TITLE
WRITE (10,*) WW
WRITE (10,*) ALBR
WRITE (10,*) RZERO
WRITE (10,*) CAPR
WRITE (10,*) NXB
WRITE (10,*) NAR
WRITE (10,*) NY
WRITE (10,*) TH
WRITE (10,*) EM
WRITE (10,*) PR
WRITE (10,*) AMU
WRITE (10,*) W1
WRITE (10,*) FORCE
WRITE (10,*) WRAP
```

C

C

C CALCULATION OF NN AND NE

C

```
10   NXP1=NXB+1
      NYP1=NY+1
      NAR1=NAR+1
```

C

C NUMBER OF NODES NN

C

C BEFORE ROLLER

```
C
      NNB=NYP1*NXB
C
C           ON ROLLER
C
      NNO=NYP1*NAR1
C
C           TOTAL
C
      NN=NNB+NNO
C
C NUMBER OF ELEMENTS NE
C
C           BEFORE ROLLER
C
      NEB=(NY*2)*NXB
C
C           ON ROLLER
C
      NEO=(NY*2)*NAR
C
C           TOTAL
C
      NE=NEB+NEO
C
C WRITE MESH DATA TO FILE MESH.DAT
C
      WRITE(10,*) NNB
      WRITE(10,*) NNO
      WRITE(10,*) NEB
      WRITE(10,*) NEO
      WRITE(10,*) NN
      WRITE(10,*) NE
C
C *****
C           CALCULATION OF THE NODAL COORDINATES
C *****
C
```

```

C MESH BEFORE ROLLER
C
C X COORDINATES
C ELEMENT DENSITY IS INCREASED BY APPROX A
C FACTOR OF 3 IN THE SPAN 25% OF ALBR IN
C FRONT OF THE CONCAVE ROLLER
C

```

```

      IREMD=MOD(NXB,2)
      IF (IREMD.EQ.0) GO TO 95
      NXB1=(NXB+1)/2
      NXB2=NXB1-1
      GO TO 96
95     NXB1=NXB/2
      NXB2=NXB1
96     ALBR1=(0.75*ALBR)
      DXB1=ALBR1/NXB1
      ALBR2=(0.25*ALBR)
      DXB2=ALBR2/NXB2
      NEB1=(NY*2)*NXB1
      NEB2=(NY*2)*NXB2

```

```

C
      WRITE(10,*) NXB1
      WRITE(10,*) NXB2
      WRITE(10,*) ALBR1
      WRITE(10,*) ALBR2
      WRITE(10,*) NEB1
      WRITE(10,*) NEB2

```

```

C
      X(1)=0.0
      DO 97 II=2,NXB1+1
      X(II)=X(II-1)+DXB1
97     CONTINUE
      DO 98 JJ=NXB1+2,NXB+1
      X(JJ)=X(JJ-1)+DXB2
98     CONTINUE

```

```

C
C Y COORDINATES
C

```

```

      DY=WW/NY
      Y(1)=0.0

```

```

                DO 200 II=2,NYP1
200      Y (II)=Y (II-1)+DY
C
C Z COORDINATES
C WRITE NODAL COORDINATES TO FILE MESH.DAT
C
                DO 400 IX=1,NXP1
                DO 300 IY=1,NYP1
                R=-DSQRT (CAPR**2-Y (IY)**2)+CAPR+RZERO
                SLOPEX=(R-RZERO)/ALBR
                Z (IY)=SLOPEX*X (IX)
                WRITE (10,201) X (IX),Y (IY),Z (IY)
201      FORMAT (F9.5,2X,F9.5,2X,F15.10)
300      CONTINUE
400      CONTINUE
C
C MESH ON ROLLER
C
C X,Z COORDINATES
C WRITE NODAL COORDINATES TO FILE MESH.DAT
C
                WRAP=WRAP/2.0
                THINC=WRAP/NAR
                THETA=THINC
                DO 500 ISTEP=1,NAR
                THRAD=(THETA*3.14159265)/180.
                DO 475 IY=1,NYP1
                R=-DSQRT (CAPR**2-Y (IY)**2)+CAPR+RZERO
                XC (IY)=ALBR+R*SIN (THRAD)
                Z (IY)=(R*COS (THRAD))-RZERO
                WRITE (10,201) XC (IY),Y (IY),Z (IY)
475      CONTINUE
                THETA=THETA+THINC
500      CONTINUE
C
C
C *****
C          CALCULATION OF THE ELEMENT CONNECTIVITIES
C *****

```

C ODD NUMBERED ELEMENTS

C

```

        ICOUNT=0
        I(1)=2
        J(1)=1
        K(1)=NYP1+1
        NJ=1
        WRITE(10,*) NJ,I(1),J(1),K(1)
        DO 1200 N=3,NE,2
        ICOUNT=ICOUNT+1
        IREM=MOD(ICOUNT,NY)
        IF(IREM.EQ.0) GO TO 1100
        I(N)=I(N-2)+1
        J(N)=J(N-2)+1
        K(N)=K(N-2)+1
        GO TO 1200
1100    I(N)=I(N-2)+2
        J(N)=J(N-2)+2
        K(N)=K(N-2)+2
1200    CONTINUE

```

C

C EVEN NUMBERED ELEMENTS

C

```

        ICOUNT=0
        I(2)=2
        J(2)=NYP1+1
        K(2)=NYP1+2
        NK=2
        WRITE(10,*) NK,I(2),J(2),K(2)
        DO 1400 N=4,NE,2
        ICOUNT=ICOUNT+1
        IREM=MOD(ICOUNT,NY)
        IF(IREM.EQ.0) GO TO 1300
        I(N)=I(N-2)+1
        J(N)=J(N-2)+1
        K(N)=K(N-2)+1
        GO TO 1400
1300    I(N)=I(N-2)+2
        J(N)=J(N-2)+2
        K(N)=K(N-2)+2

```



```

1400    CONTINUE
C
C WRITE ELEMENT DATA TO FILE MESH.DAT
C
          DO 1500 N=3,NE
1500    WRITE (10,*) N,I(N),J(N),K(N)
C
C
C *****
C      CONSTRAINTS
C      ENFORCED DISPLACEMENTS
C *****
C
C INCREMENT SEARCH FOR W2 SUCH THAT STRA = STRB
C
          W2INC=(W1*0.001)
          ICOUNT=0
          W2LAST=W1
          TOTF=FORCE*NY
67      FORMAT (2X,F10.4)
          STRA=TOTF/(WW*TH*EM)
          UDISPA=STRA*ALBR
          IF (STRA .LE. 0.0) THEN
              IDCHEK = 2
              WRITE (14,*) IDCHEK
              WRITE (14,49)
              WRITE (12,49)
49      FORMAT (//2X,'STRAIN A IS ZERO OR NEGATIVE.'//2X,
$          'PLEASE REVISE INITIAL CONDITIONS.')
```

GOTO 2600

```

          END IF
          W2=W1
          CALL SMPINT
          TOL=STRA/1000.
          IF (ABS (STRB-STRA) .LE. TOL) GO TO 1900
1660    W2LAST=W2
          W2=W2-W2INC
          STRB2=STRB
1680    CALL SMPINT
```

```

IF (ABS (STRB-STRA) .LE.TOL) GO TO 1900
ICOUNT=ICOUNT+1
IF (ICOUNT.GE.50) THEN
  IDCHEK = 3
  WRITE (14,*) IDCHEK
  WRITE (14,51)
  WRITE (12,51)
51  FORMAT (//2X, 'AVERAGE STRAIN DID NOT CONVERGE WITHIN 50 ITERATI
$    IONS. ')
  GOTO 2600
END IF
IF ((STRB-STRA)*(STRB2-STRA) .GT.0.0) GO TO 1660
W2INC=W2INC/10
W2=W2LAST-W2INC
GO TO 1680

C
C  CALCULATION OF DIFFERENTIAL STRAIN FORCES
C
1900  WRITE (10,*) W2
      C1=(1-STRA)*RZERO*W1
      C2=CAPR+RZERO
      DO 2001 IA=1,NYP1
      STRB=1-C1/((C2-DSQRT(CAPR**2-Y(IA)**2))*W2)
      IF (STRB.LT.0.0) THEN
        IDCHEK = 4
        WRITE (14,*) IDCHEK
        WRITE (14,54) Y(IA),STRB
        WRITE (12,54) Y(IA),STRB
        WRITE (12,53)
53    FORMAT (//2X, 'NO FORCES CALCULATED. ')
54    FORMAT (//2X, 'NEGATIVE STRAIN'//5X,3HY =,F15.10,10X,
$      8HSTRAIN =,E15.6)
      GO TO 2600
      END IF
      IDCHEK = 1
      IF (IA.EQ.1) WRITE (14,*) IDCHEK

C
C  CALCULATION OF FORCES
      AREA=(WW/NY)*TH

```

```

IF (IA.EQ.1) AREA=0.5*AREA
IF (IA.EQ.NYP1) AREA=0.5*AREA
FORCE=(STRB-STRA)*EM*AREA
NFN=(NNB+IA)
IDOF=3*NFN-2
WRITE (12,56) NFN, IDOF, FORCE
C
2001 CONTINUE
NFN=0
IDOF=0
VALUE=0.0
WRITE (12,55) NFN, IDOF, VALUE
55 FORMAT (I4,2X,I4,2X,F3.1)
56 FORMAT (I4,2X,I4,2X,F14.10)
C
C CONSTRRAIN Z AND SYMMETRIC Y DOFS FOR APRON BEFORE ROLLER
C
DO 2004 IX=1,NNB+NYP1
VALUE=0.0
IREM=MOD((IX-1),NYP1)
IF (IREM.EQ.0) THEN
IDOF=3*IX-1
WRITE (14,55) IX, IDOF, VALUE
END IF
IDOF=3*IX
WRITE (14,55) IX, IDOF, VALUE
2004 CONTINUE
C
IX=0
IDOF=0
WRITE (14,55) IX, IDOF, VALUE
C
C CONSTRRAIN Z AND SYMMETRIC Y DOFS ON ROLLER
C
DO 2005 IY=NNB+NYP1+1,NN
VALUE=0.0
IREM=MOD((IY-1),NYP1)
IF (IREM.EQ.0) THEN
IDOF=3*IY-1
WRITE (14,55) IY, IDOF, VALUE

```

```

        END IF
        IDOF=3*IY
        WRITE (14,55) IY, IDOF, VALUE
2005    CONTINUE
C
        IX=0
        IDOF=0
        WRITE (14,55) IX, IDOF, VALUE
C
C    CALCULATE UNADJUSTED DISTANCES OVER ROLLER
C
        C1=(1-STRA)*RZERO*W1
        C2=CAPR+RZERO
        DO 2045 IR=1, NYP1
            STRB=1-C1/((C2-DSQRT(CAPR**2-Y(IR)**2))*W2)
            R2=-DSQRT(CAPR**2-Y(IR)**2)+C2
            ROLINC=((WRAP/360.)*2.0*R2*3.14159265*STRB)/NAR
            DO 2050 IP=1, NAR+1
                IRR=IR+NNB+(IP-1)*NYP1
                IDOF=3*IRR-2
                UDISPC=(IP-1)*ROLINC
                WRITE (14,56) IRR, IDOF, UDISPC
            2050    CONTINUE
        2045    CONTINUE
C
C    LOCK Y DISPLACEMENTS TOGETHER OVER ROLLER
C
        DO 2305 ID=NNB+2, NNB+NYP1
            IDOF=3*ID-1
            DO 2306 II=1, NAR
                ID1=ID+(NYP1*II)
                IDOF1=3*ID1-1
                WRITE (14,57) ID, IDOF, ID1, IDOF1
            2306    CONTINUE
        2305    CONTINUE
        57    FORMAT (I4, 2X, I4, 2X, I4, 2X, I4)
C
C    WRITE CONSTRAINTS FOR FIRST ROW ON APRON
C    -THESE ARE USED ONLY FOR DEVELOPMENT OF FINAL

```

```

C   BOUNDARY CONDITIONS (1ST PRELIMINARY RUN)
C
      DO 2175 IL=1,NYP1
          IDOF=3*IL-2
          WRITE (17,55) IL,IDOF,VALUE
2175  CONTINUE
          IDOF=0
          WRITE (17,55) IB,IDOF,VALUE
C
C   WRITE ENFORCED DISPL FOR FIRST ROW TO BCNSTR*
C   -THESE ARE USED FOR DEVELOPMENT OF FINAL
C   BOUNDARY CONDITIONS (FINAL RUN)
C
      UDISPA=-UDISPA
      DO 2100 IB=1,NYP1
          IDOF=3*IB-2
          WRITE (17,56) IB,IDOF,UDISPA
2100  CONTINUE
          IB=0
          IDOF=0
          VALUE=0.0
          WRITE (17,56) IB,IDOF,VALUE
C
C
2600  STOP
      END
C
C
C *****
C *****
      SUBROUTINE SMPINT
C *****
C *****
C
      DOUBLE PRECISION R,Y(400),CAPR
      COMMON/DOMEGA/CAPR
      COMMON/OMEGA1/RZERO,WW,W1,STRA
      COMMON/OMEGA2/W2,STRB
C
      C1=(1-STRA)*RZERO*W1

```

```
C2=CAPR+RZERO
PART1=0.0
PART2=0.0
STRB=0.0
N=10
C
C STEP SIZE - N MUST BE EVEN
STSIZE=WW/N
C
II=0
50 YVAL=II*STSIZE
VAL=1-C1/((C2-DSQRT(CAPR**2-YVAL**2))*W2)
IF (II.EQ.0) THEN
    VAL0=VAL
    GO TO 90
END IF
IF (II.EQ.N) GO TO 100
IREM=MOD(II,2)
IF (IREM.EQ.0) THEN
    PART2=PART2+VAL
    GO TO 90
END IF
PART1=PART1+VAL
90 II=II+1
GO TO 50
C
100 SUM=VAL0+4*PART1+2*PART2+VAL
STRB=(WW*SUM/(3*N))/WW
C
RETURN
END
C
```

APPENDIX D
COMPUTER PROGRAM FOR PROGRAM CONCAVE

C

C

PROGRAM CONCAVE.FOR

C

C THIS PROGRAM ANALYZES A WEB ON A CONCAVE ROLLER

C IT ITERATIVELY SPREADS THE WEB ON THE ROLLER TO THE

C POINT AT WHICH THE SPREADING FORCES EQUAL THE AVAILABLE

C FRICTION FORCES

C THE PROGRAM HANDLES ONLY LINEAR TRIANGULAR PLANE STRESS ELEMENTS

C

C *****

C

C *****

C

C MACHINE DIRECTION SYMMETRY ABOUT THE CONCAVE ROLLER IS INCORPORATED.

C AN INCREASED ELEMENT DENSITY REGION EXISTS FOR 25% OF THE ENTRY

C SPAN PRECEDING THE CONCAVE ROLLER.

C MACHINE DIRECTION DISPLACEMENTS ARE ENFORCED OVER THE ROLLER.

C THE NODES AT EQUAL LATERAL LOCATIONS ON THE ROLL ARE REQUIRED

C TO SPREAD EQUALLY.

C 1 PRELIMINARY RUN THROUGH THE ENTRY SPAN IS REQUIRED TO

C GENERATE THE NECESSARY BOUNDARY CONDITIONS FOR THE FINAL RUN.

C

C THE PROGRAM REQUIRES FOUR FILES: MESH.DAT CONSTR.DAT FORCE.DAT

C AND BCNSTR.DAT

C

C THE PRIMARY OUTPUT IS FOUND IN FILE OUT.DAT

C

C *****

C

C *****

C

LAST UPDATE 5/23/88

C

C

PARAMETER (IMAXNN=231, IMAXNY=10)

COMMON/GRAD/B(3,6),AR2

COMMON/ELMATX/ESM(9,9),X(3),Y(3),Z(3),D(3,3),GESM(9,9),

\$ GSM(3*IMAXNN,3*IMAXNN),GTSM(3*IMAXNN+120,3*IMAXNN+120),IELR

COMMON/MTL/EM,PR,TH,AMU


```

COMMON/TLE/TITLE (20)
COMMON/N/NP, NN, NE, NS (9), ICK (500), NS1, NS2, UU (9)
COMMON/ELM/NEL (500, 3), XC (IMAXNN), YC (IMAXNN), ZC (IMAXNN)
COMMON/DUMM/DUM1 (9, 9), DUM2 (9, 9), DUM3 (3, 3*IMAXNN),
$ DUM4 (3, 3*IMAXNN), DUM5 (3*IMAXNN, 3), DUM6 (3*IMAXNN, 3)
COMMON/TMATX/AL (3, 3), T (9, 9), ALT (3, 3), TT (9, 9)
COMMON/DOF/F (3*IMAXNN+120), U (3*IMAXNN+120), STRA (6), STRE (6), THM,
$ TM, S1, S2
COMMON/LOCAL/XYZ (9), STOR (9), XL (3), YL (3), ZL (3),
$ FL (3*IMAXNN)
COMMON/LAM/TEMP (3, 3), ALN (3, 3), ALNT (3, 3)
COMMON/PARAM/NY, NYP1, WW, NAR
COMMON/PARAM2/NNB, NNO, NEB, NEO
COMMON/PARAM3/ALBR, NXB
COMMON/PARAM4/RZERO, CAPR, W1, W2, FORCE, WRAP
COMMON/PARAM5/NXB1, NXB2, ALBR1, ALBR2, NEB1, NEB2
COMMON/ANGL/SLOPE, FRICTF (IMAXNN), FEXT (IMAXNN), ADIV (IMAXNN),
$ CONST (IMAXNN)
COMMON/MODIF/NEWID (120), TMPDSP (110)
DIMENSION W (3*IMAXNN+120, 3*IMAXNN+120)
INTEGER IPIVOT (3*IMAXNN+120)

C
C *****
C
C                               MAIN PROGRAM
C
C *****
C
C *****
C       INPUT SECTION OF THE PROGRAM
C *****
C
C CHECK DATA FILES
C
C       READ (14, *) IDCHEK
C       IF (IDCHEK.NE. 1 ) THEN
C           IF (IDCHEK.EQ.2) THEN
C               WRITE (15, 131)

```

```

        WRITE (18,131)
131     FORMAT (//2X, 'NEGATIVE STRAIN ON BOUNDARY ROLLER.'//2X,
$         'NO OUTPUT GENERATED. ')
        END IF
        IF (IDCHEK.EQ.3) THEN
            WRITE (15,132)
            WRITE (18,132)
132     FORMAT (//2X, 'AVERAGE STRAIN DID NOT CONVERGE WITHIN 50
$         ITERATIONS.'//2X, 'NO OUTPUT GENERATED. ')
        END IF
        IF (IDCHEK.EQ.4) THEN
            WRITE (15,133)
            WRITE (18,133)
133     FORMAT (//2X, 'NEGATIVE STRAIN ON CONCAVE ROLLER.'//2X,
$         'NO OUTPUT GENERATED. ')
        END IF
        GO TO 110
    END IF

C
C
    CALL INPUTS
C
    LOOPFL=0
    KMTRX=0
C
C *****
C     GENERATION OF THE SYSTEM OF EQUATIONS
C *****
C
C     INITIALIZATION OF THE STIFFNESS MATRIX
C
    3     KMTRX=KMTRX+1
C
    DO 555 I=1,NP
    DO 555 J=1,NP
555     GSM(I,J)=0.0
C
C     START OF THE LOOP FOR THE ELEMENT MATRICES
C
    ITER=0

```

```

        IELR=0
        KK=1

C
C GENERATION OF THE NODAL DEGREES OF FREEDOM
C RETRIEVAL OF THE NODAL COORDINATES
C
5      DO 10 I=1,3
        J=NEL(KK,I)
        NS(3*I-2)=J*3-2
        NS(3*I-1)=J*3-1
        NS(3*I)=J*3
        X(I)=XC(J)
        Y(I)=YC(J)
10     Z(I)=ZC(J)
C
        CALL LAMDA(KK)
        CALL TRNSMX

C
C GENERATION OF THE LOCAL COORDINATES
C
        JJ=1
        DO 30 I=1,9,3
            XYZ(I)=X(JJ)
            XYZ(I+1)=Y(JJ)
            XYZ(I+2)=Z(JJ)
            JJ=JJ+1
30     CONTINUE
C
        DO 40 I=1,9
            STOR(I)=0.0
            DO 40 J=1,9
40     STOR(I)=STOR(I)+T(I,J)*XYZ(J)
C
        JK=1
        DO 50 I=1,3
            XL(I)=STOR(JK)
            YL(I)=STOR(JK+1)
            ZL(I)=STOR(JK+2)
            JK=JK+3

```

```
50      CONTINUE
C
C *****
C          CALCULATION OF THE ELEMENT MATRICES
C          TRANSFORMATION TO GLOBAL COORDINATES
C          ASSEMBLY VIA DIRECT STIFFNESS PROCEDURE
C *****
C
C          CALL ELSTMX(KK)
C          CALL TRNSFM
C          CALL ASSEMB
C
C          KK=KK+1
C          IF (KMTRX.EQ.1) THEN
C              IF (KK.LE.NEB) GO TO 5
C          ELSE
C              IF (KK.LE.NE) GO TO 5
C          END IF
C
C *****
C          SKEWED COORDINATE TRANSFORMATION
C *****
C
C          KN=1
C
C          200      CALL SKEWED (KN)
C
C          KN=KN+1
C          IF (KMTRX.EQ.1) THEN
C              IF (KN.LE.NNB+NYP1) GO TO 200
C          ELSE
C              IF (KN.LE.NN) GO TO 200
C          END IF
C
C *****
C          MODIFICATION OF THE SYSTEM OF EQUATIONS
C          DATA IS CALLED BY MODIFY
C *****
C
C          205      LOOPFL=LOOPFL+1
```

```

C
      CALL MODIFY (LOOPFL)
C
C *****
C      SOLUTION OF THE MODIFIED SYSTEM OF EQUATIONS
C *****
C
      CALL FACTOR (GTSM, IPIVOT, IFLAG, LOOPFL)
      IF (IFLAG.EQ.0) THEN
        WRITE (15, *) 'SYSTEM CANNOT BE SOLVED--0 ON DIAGONAL'
        GO TO 110
      END IF
      CALL SUBST (GTSM, IPIVOT, F, U, LOOPFL)
C
      IF (LOOPFL.EQ.1) THEN
        DO 209 KJ2=1, NYP1
          TMPDSP (KJ2)=U (3* (KJ2+NNB)-2)
          IVAL=3* (KJ2+NNB)-2
          WRITE (20, 213) KJ2, IVAL, TMPDSP (KJ2)
209      CONTINUE
          GO TO 3
        END IF
C
C
C SAVE FORCES GENERATED FROM ENFORCED Y-LOCK DISPLACEMENTS
C FORCES ARE FOUND IN SECTION ADDED TO DISPLACEMENT VECTOR U
      DO 215 N=1, NAR*NY
        WRITE (21, 213) N, NEWID (N), U (NP+N)
213      FORMAT (3X, I5, 3X, I5, 3X, E15.6)
215      CONTINUE
C
C SAVE ENFORCED DISPLACEMENT CONSTRAINT FORCES
      WRITE (21, 221)
221      FORMAT (//, 5X, 'IDOF', 9X, 'FORCE')
      DO 225 N=1, NP
        WRITE (21, 223) N, F (N)
223      FORMAT (3X, I5, 3X, E15.6)
225      CONTINUE
C

```

```

C *****
C      OUTPUT OF THE CALCULATED NODAL DISPLACEMENTS
C      DATA IS WRITTEN TO FILE OUT.DAT
C *****
C
      IFLAG4=0
250  WRITE (15,31) TITLE,NN,NE
      IF (ITER.EQ.0) WRITE (18,31) TITLE,NN,NE
31   FORMAT (1H1,////,10X,20A3,/,13X,'NN =',I4/
      $      ,13X,5HNE = ,I4)
      IF (ITER.EQ.0) WRITE (18,29)
29   FORMAT (//,'VALUES SHOWN ARE AFTER 1 ITERATION'//)
      WRITE (15,32) EM,PR,TH,AMU
      IF (ITER.EQ.0) WRITE (18,32) EM,PR,TH,AMU
32   FORMAT (//10X,'PARAMETER VALUES' /
      $      /13X,4HEM =,E12.5/13X,4HPR =,
      $      E12.5/13X,4HTH =,E12.5,/13X,
      $      4HMU =,E12.5/)
      WRITE (15,33) CAPR,RZERO,W1,W2
      IF (ITER.EQ.0) WRITE (18,33) CAPR,RZERO,W1,W2
33   FORMAT (13X,6HCAPR =,E12.5,/13X,7HRZERO =,E12.5,/
      $      13X,4HW1 =,E12.5,/13X,11HW2 (CALC) =,E12.5,/)
      WRITE (15,34) FORCE,WRAP
      IF (ITER.EQ.0) WRITE (18,34) FORCE,WRAP
34   FORMAT (13X,13HNODAL FORCE =,E12.5,/13X,12HWRAP ANGLE =,
      $      E12.5)
      WRITE (15,35)
      IF (ITER.EQ.0) WRITE (18,35)
35   FORMAT (//10X,'MESH PARAMETER VALUES'//)
      WRITE (15,36) NNB,NNO
      IF (ITER.EQ.0) WRITE (18,36) NNB,NNO
36   FORMAT (13X,5HNNB =,I4,/13X,5HNNO =,I4/)
      WRITE (15,37) WW,NY,NAR
      IF (ITER.EQ.0) WRITE (18,37) WW,NY,NAR
37   FORMAT (13X,4HWW =,E12.5,/13X,4HNY =,I4,/13X,5HNAR =,I4/)
      WRITE (15,38) ALBR,ALBR1,ALBR2
      IF (ITER.EQ.0) WRITE (18,38) ALBR,ALBR1,ALBR2
38   FORMAT (13X,6HALBR =,E12.5,/15X,7HALBR1 =,E12.5,/15X,
      $      7HALBR2 =,E12.5/)
      WRITE (15,39) NXB,NXB1,NXB2

```

```

IF (ITER.EQ.0) WRITE (18,39) NXB,NXB1,NXB2
39  FORMAT (13X,5HNXB =,I4,/15X,6HNXB1 =,I4,/15X,6HNXB2 =,I4/)
WRITE (15,41) NEB,NEB1,NEB2,NEO
IF (ITER.EQ.0) WRITE (18,41) NEB,NEB1,NEB2,NEO
41  FORMAT (13X,5HNEB =,I4,/15X,6HNEB1 =,I4,/15X,6HNEB2 =,I4,
$      //13X,5HNEO =,I4)
WRITE (15,2)
IF (ITER.EQ.0) WRITE (18,2)
2   FORMAT (///10X,25HNODAL DISPLACEMENT VALUES/
$ //10X,4HNODE,6X,12HX DEFLECTION,6X,12HY DEFLECTION,
$ 6X,12HZ DEFLECTION)
C
DO 6 I=1,NN
WRITE (15,4) I,U(3*I-2),U(3*I-1),U(3*I)
IF (ITER.EQ.0) WRITE (18,4) I,U(3*I-2),U(3*I-1),U(3*I)
4   FORMAT (11X,I3,3X,E15.6,3X,E15.6,3X,E15.6)
6   CONTINUE
C
C *****
C     CALCULATION OF THE ELEMENT STRESS AND STRAIN COMPONENTS
C     AND THE PRINCIPAL STRESSES
C *****
C
C     IELR=1
C
C START OF THE ELEMENT LOOP
C
C     KK=1
C
C GENERATION OF THE NODAL DEGREES OF FREEDOM
C
12  DO 15 I=1,3
      J=NEL(KK,I)
      NS(3*I-2)=3*J-2
      NS(3*I-1)=3*J-1
      NS(3*I)=3*J
      X(I)=XC(J)
      Y(I)=YC(J)
15  Z(I)=ZC(J)

```

```
C
      CALL LAMDA(KK)
      CALL TRNSMX
C
C GENERATION OF THE LOCAL COORDINATES
C
      JJ=1
      DO 60 I=1,9,3
      XYZ(I)=X(JJ)
      XYZ(I+1)=Y(JJ)
      XYZ(I+2)=Z(JJ)
      JJ=JJ+1
60    CONTINUE
C
      DO 70 I=1,9
      STOR(I)=0.0
      DO 70 J=1,9
70    STOR(I)=STOR(I)+T(I,J)*XYZ(J)
C
      JK=1
      DO 80 I=1,3
      XL(I)=STOR(JK)
      YL(I)=STOR(JK+1)
      ZL(I)=STOR(JK+2)
      JK=JK+3
80    CONTINUE
C
C RETRIEVAL OF THE NODAL DISPLACEMENTS
C
      DO 16 I=1,9,3
      NS1=NS(I)
      NS2=NS(I+1)
      UU(I)=U(NS1)
16    UU(I+1)=U(NS2)
C
      CALL SANDS(KK)
C
C *****
C OUTPUT OF THE STRESS RESULTS TO FILE OUT.DAT
```



```

C *****
C
      WRITE (15,8) KK
      IF (ITER.EQ.0) THEN
        WRITE (18,8) KK
      END IF
8     FORMAT (/10X, 'ELEMENT ', I4)
      WRITE (15,20) STRA (1), STRE (1), S1, STRA (2), STRE (2), S2,
$     STRA (3), STRE (3), TM, THM
      IF (ITER.EQ.0) WRITE (18,20) STRA (1), STRE (1), S1, STRA (2),
$     STRE (2), S2, STRA (3), STRE (3), TM, THM
20    FORMAT (15X, 5HEXX =, E12.5, 5X, 5HSXX =, E12.5, 5X, 5HS1 =,
$     E12.5/15X, 5HEYY =, E12.5, 5X, 5HSYY =, E12.5, 5X, 5HS2 =,
$     E12.5/15X, 5HGXY =, E12.5, 5X, 5HTXY =, E12.5, 4X,
$     6HTMAX =, E12.5/59X, 5HANGLE, F8.2, 4H DEG)
C
      KK=KK+1
      IF (KK.LE.NE) GO TO 12
C
C *****
C     CALCULATION OF NORMAL FORCES
C *****
C
101   IROWS=3* (NNB+1) -2
      IROWF=3*NN
      DO 90 I=IROWS, IROWF
        FL (I)=0.0
        DO 90 J=1, NP
          FL (I)=FL (I)+GSM (I, J) *U (J)
90    CONTINUE
      IF (IFLAG4.EQ.1) THEN
        WRITE (15,361)
        DO 500 KN=NNB+1, NN
          IF (KN.LE.NNB+NYP1) ADIV (KN)=0.0
          IF (KN.GT.NN-NYP1) ADIV (KN)=0.0
          WRITE (15,363) KN, FEXT (KN), FRICTF (KN), ADIV (KN)
500   CONTINUE
      WRITE (15,362) ITER
      GO TO 100
      END IF

```

```

361     FORMAT(/' NODE',5X,'SPREADING FORCE',5X,'FRICTION FORCE',
          $ 5X,'RATIO'/)
362     FORMAT(/' IN ITERATION NUMBER ',I4)
363     FORMAT(I4,7X,E12.5,8X,E12.5,6X,F6.4)
C
C *****
C SPREADING ANALYSIS
C *****
C
  95     ITER=ITER+1
C
C *****
C CALCULATE SPREADING FORCES
C APPLY SPREADING FORCES TO NODES ON ROLLER
C *****
C
  290    DO 300 KN=NNB+NYP1+2,NN-NYP1
          IREM=MOD((KN-1),NYP1)
          IF (IREM.EQ.0) GO TO 300
          CALL FRICTN(KN)
          CALL APFORS(KN,ITER)
  300    CONTINUE
          DO 302 KN1=NNB+2,NNB+NYP1
          FRICTF(KN1)=FRICTF(KN1+NYP1)/2.0
          CALL APFORS(KN1,ITER)
  302    CONTINUE
          DO 304 KN2=NN-NYP1+2,NN
          FRICTF(KN2)=FRICTF(KN2-NYP1)/2.0
          CALL APFORS(KN2,ITER)
  304    CONTINUE
C
C *****
C SOLVE FOR NEW DISPLACEMENTS AND FORCES
C *****
C
          CALL SUBST(GTSM,IPIVOT,F,U,LOOPFL)
C
C CALCULATE NEW NORMAL FORCES
C

```

```

      IROWS=3*(NNB+1)-2
      IROWF=3*NN
      DO 325 I=IROWS,IROWF
      FL(I)=0.0
      DO 325 J=1,NP
      FL(I)=FL(I)+GSM(I,J)*U(J)
325   CONTINUE
C
C *****
C CHECK TO SEE IF SLIPPAGE OCCURRED
C *****
C
      IFLAG3=0
      DO 350 KN=NNB+NYP1+2,NN-NYP1
      CALL FRICTN(KN)
      CALL CHKFOR(KN,IFLAG2)
      IREM=MOD((KN-1),NYP1)
      IF (IREM.EQ.0) IFLAG2=1
      IF (IFLAG2.EQ.0) IFLAG3=1
350   CONTINUE
C
      IF (ITER.GT.100) GO TO 520
      IF (IFLAG3.EQ.1) GO TO 95
C
C
520   REWIND(15)
      IFLAG4=1
      GO TO 250
C
C
100   CONTINUE
C
110   STOP
      END
C
C *****
C
C *****
      SUBROUTINE INPUTS

```

```

C *****
C
      PARAMETER (IMAXNN=231, IMAXNY=10)
      COMMON/ELMATX/ESM(9,9),X(3),Y(3),Z(3),D(3,3),GESM(9,9),
$     GSM(3*IMAXNN,3*IMAXNN),GTSM(3*IMAXNN+120,3*IMAXNN+120)
      COMMON/MTL/EM,PR,TH,AMU
      COMMON/TLE/TITLE(20)
      COMMON/N/NP,NN,NE,NS(9),ICK(500),NS1,NS2,UU(9)
      COMMON/ELM/NEL(500,3),XC(IMAXNN),YC(IMAXNN),ZC(IMAXNN)
      COMMON/PARAM/NY,NYP1,WW,NAR
      COMMON/PARAM2/NNB,NNO,NEB,NEO
      COMMON/PARAM3/ALBR,NXB
      COMMON/PARAM4/RZERO,CAPR,W1,W2,FORCE,WRAP
      COMMON/PARAM5/NXB1,NXB2,ALBR1,ALBR2,NEB1,NEB2
C
C *****
C *****
C
C DEFINITION OF THE INPUT VARIABLES FOR THIS PROGRAM
C
C *****
C *****
C TITLE AND PARAMETERS
C
C     TITLE - A DESCRIPTIVE STATEMENT OF THE PROBLEM
C     WW - WIDTH OF THE WEB
C     ALBR - LENGTH OF WEB BEFORE ROLLER
C     RZERO - ROLLER BASE RADIUS
C     CAPR - RADIUS OF CURVATURE OF CONCAVE ROLLER
C     NXB - NUMBER OF ELEMENTS IN X-DIR BEFORE ROLLER
C     NAR - NUMBER OF ELEMENTS AROUND ROLLER (MACHINE DIR)
C     NY - NUMBER OF ELEMENTS LATERALLY ACROSS ROLLER
C     TH - THICKNESS OF WEB
C     EM - MODULUS OF ELASTICITY OF WEB
C     W1 - ANGULAR VELOCITY OF WEB
C     FORCE - NODAL FORCE APPLIED TO END OF WEB
C     WRAP - ANGLE OF WRAP AROUND ROLLER
C     NN - NUMBER OF NODES
C     NE - NUMBER OF ELEMENTS

```

```
C
C MATERIAL PROPERTIES AND THICKNESS
C
C     EM - MODULUS OF ELASTICITY
C     PR - POISSON'S RATIO
C     TH - THICKNESS OF THE REGION
C     AMU - COEFFICIENT OF FRICTION BETWEEN THE WEB AND ROLL
C
C NODAL COORDINATES
C
C     XC(I) - X COORDINATES OF THE NODES IN NUMERICAL SEQUENCE
C     YC(I) - Y COORDINATES OF THE NODES IN NUMERICAL SEQUENCE
C     ZC(I) - Z COORDINATES OF THE NODES IN NUMERICAL SEQUENCE
C
C ELEMENT DATA
C
C     N - ELEMENT NUMBER
C     NEL(N,I) - NUMERICAL VALUE OF NODE I
C     NEL(N,J) - NUMERICAL VALUE OF NODE J
C     NEL(N,K) - NUMERICAL VALUE OF NODE K
C
C *****
C     INPUT SECTION
C *****
C
C INPUT OF THE TITLE CARD AND PARAMETERS
C
C     READ(10,3) TITLE
3     FORMAT(20A3)
C     READ(10,*) WW
C     READ(10,*) ALBR
C     READ(10,*) RZERO
C     READ(10,*) CAPR
C     READ(10,*) NXB
C     READ(10,*) NAR
C     READ(10,*) NY
C     READ(10,*) TH
C     READ(10,*) EM
C     READ(10,*) PR
C     READ(10,*) AMU
```

```
      READ(10,*) W1
      READ(10,*) FORCE
      READ(10,*) WRAP
      READ(10,*) NNB
      READ(10,*) NNO
      READ(10,*) NEB
      READ(10,*) NEO
      READ(10,*) NN
      READ(10,*) NE
      READ(10,*) NXB1
      READ(10,*) NXB2
      READ(10,*) ALBR1
      READ(10,*) ALBR2
      READ(10,*) NEB1
      READ(10,*) NEB2
C
      NP=3*NN
      NYP1=NY+1
C
C COMPARISON CHECK OF NN AND NE WITH THE VALUES USED
C IN THE DIMENSION STATEMENTS
C
      ISTOP=0
C
C CHECK NUMBER OF NODES
C
      IF(NN.LE.400) GO TO 15
      WRITE(15,10)
10    FORMAT(10X,'NUMBER OF NODES EXCEEDS 400'/
$ 10X,26HCHECK DIMENSION STATEMENTS/
$ 10X,20HEXECUTION TERMINATED)
      ISTOP=1
C
C CHECK NUMBER OF ELEMENTS
C
15    IF(NE.LE.500) GO TO 25
      WRITE(15,20)
20    FORMAT(10X,'NUMBER OF ELEMENTS EXCEEDS 500'/
$ 10X,26HCHECK DIMENSION STATEMENTS/
```

```

$ 10X,20HEXECUTION TERMINATED)
  ISTOP=1
25  IF (ISTOP.EQ.1) STOP
C
C INPUT OF THE NODAL COORDINATES FROM FILE MESH.DAT
C
      READ (10,*) (XC(I),YC(I),ZC(I),I=1,NN)
C
C INPUT AND ECHO PRINT OF ELEMENT DATA
C CHECK TO SEE IF THE ELEMENTS ARE IN SEQUENCE
C
      NID=0
      DO 45 KK=1,NE
        READ (10,*) N, (NEL(N,I),I=1,3)
        IF ((N-1).NE.NID) WRITE (15,42) N
42    FORMAT (10X,7HELEMENT,I4,16H NOT IN SEQUENCE)
        NID=N
45    CONTINUE
C
C READ MESH PARAMETERS FROM FILE MESH.DAT
C
      READ (10,*) W2
C
C
C *****
C      ANALYSIS OF THE NODE NUMBERS
C *****
C
C INITIALIZATION OF A CHECK VECTOR
C
      DO 50 I=1,NN
50    ICK(I)=0
C
C CHECK TO SEE IF ANY NODE NUMBER EXCEEDS NN
C
      DO 54 I=1,NE
      DO 52 J=1,3
      K=NEL(I,J)
      ICK(K)=1

```

```

52     IF (K.GT.NN) WRITE (15,53)
53     FORMAT (/ ,10X,4HNODE,I4,11H OF ELEMENT,I4,
    $     13H EXCEEDS NN = ,I4)
54     CONTINUE
C
C CHECK TO SEE IF ALL NODE NUMBERS THROUGH NN ARE INCLUDED
C
    DO 55 I=1,NN
55     IF (ICK(I).EQ.0) WRITE (15,56) I
56     FORMAT (/10X,4HNODE,I4,15H DOES NOT EXIST)
C
    RETURN
    END
C
C
C *****
    SUBROUTINE ELSTMX (KK)
C *****
C
    PARAMETER (IMAXNN=231,IMAXNY=10)
    COMMON/MIL/EM,PR,TH,AMU
    COMMON/GRAD/B(3,6),AR2
    COMMON/ELMATX/ESM(9,9),X(3),Y(3),Z(3),D(3,3),GESM(9,9),
    $ GSM(3*IMAXNN,3*IMAXNN),GTSM(3*IMAXNN+120,3*IMAXNN+120),IELR
    COMMON/N/NP,NN,NE,NS(9),ICK(500),NS1,NS2,UU(9)
    COMMON/DUMM/DUM1(9,9),DUM2(9,9),DUM3(3,3*IMAXNN),
    $ DUM4(3,3*IMAXNN),DUM5(3*IMAXNN,3),DUM6(3*IMAXNN,3)
    COMMON/ELM/NEL(500,3),XC(IMAXNN),YC(IMAXNN),ZC(IMAXNN)
    COMMON/LOCAL/XYZ(9),STOR(9),XL(3),YL(3),ZL(3),
    $ FL(3*IMAXNN)
    DIMENSION C(6,3)
C
C GENERATION OF THE B MATRIX
C
    DO 20 I=1,3
    DO 20 J=1,6
20    B(I,J)=0.0
    B(1,1)=YL(2)-YL(3)
    B(1,3)=YL(3)-YL(1)
    B(1,5)=YL(1)-YL(2)

```



```

      B(2,2)=XL(3)-XL(2)
      B(2,4)=XL(1)-XL(3)
      B(2,6)=XL(2)-XL(1)
110   B(3,1)=B(2,2)
      B(3,2)=B(1,1)
      B(3,3)=B(2,4)
      B(3,4)=B(1,3)
      B(3,5)=B(2,6)
      B(3,6)=B(1,5)
      C1=(Y(1)*Z(2)+Y(2)*Z(3)+Y(3)*Z(1)-Y(1)*Z(3)-
$     Y(2)*Z(1)-Y(3)*Z(2))**2
      C2=(Z(1)*X(2)+Z(2)*X(3)+Z(3)*X(1)-Z(1)*X(3)-
$     Z(2)*X(1)-Z(3)*X(2))**2
      C3=(X(2)*Y(3)+X(3)*Y(1)+X(1)*Y(2)-X(2)*Y(1)-
$     X(3)*Y(2)-X(1)*Y(3))**2
      AR2=SQRT(C1+C2+C3)
C
C GENERATION OF THE MATERIALS PROPERTY MATRIX MATRIX D
C
100   R=EM/(1.-PR**2)
      D(1,1)=R
      D(2,2)=D(1,1)
      D(3,3)=R*(1.0-PR)/2.
      D(1,2)=PR*R
      D(2,1)=D(1,2)
      D(1,3)=0.0
      D(3,1)=0.0
      D(2,3)=0.0
      D(3,2)=0.0
C
      IF(IELR.EQ.1) RETURN
C
C MATRIX MULTIPLICATION TO OBTAIN C = BT * D
C
      DO 22 I=1,6
      DO 22 J=1,3
      C(I,J)=0.0
      DO 22 K=1,3
22    C(I,J)=C(I,J)+B(K,I)*D(K,J)

```

```
C
C MATRIX MULTIPLICATION TO OBTAIN ESM
C
      DO 27 I=1,6
      DO 27 J=1,6
      SUM=0.0
      DO 28 K=1,3
28     SUM=SUM+C(I,K)*B(K,J)
      ESM(I,J)=SUM*TH/(2.*AR2)
27     CONTINUE
C
      DO 55 I=1,9
      DO 50 J=1,9
50     DUM1(I,J)=0.0
55     CONTINUE
C
C EXPAND ELEMENT STIFFNESS MATRIX TO INCLUDE
C THE OUT-OF-PLANE DEGREES OF FREEDOM
C
      DO 65 I=1,2
      DO 60 J=1,6
      JJ=J
      IF((J.EQ.3).OR.(J.EQ.4)) JJ=J+1
      IF((J.EQ.5).OR.(J.EQ.6)) JJ=J+2
60     DUM1(I,JJ)=ESM(I,J)
65     CONTINUE
C
      DO 75 I=4,5
      DO 70 J=1,6
      JJ=J
      IM1=I-1
      IF((J.EQ.3).OR.(J.EQ.4)) JJ=J+1
      IF((J.EQ.5).OR.(J.EQ.6)) JJ=J+2
70     DUM1(I,JJ)=ESM(IM1,J)
75     CONTINUE
C
      DO 85 I=7,8
      DO 80 J=1,6
      JJ=J
      IM2=I-2
```

```

      IF ((J.EQ.3).OR.(J.EQ.4)) JJ=J+1
      IF ((J.EQ.5).OR.(J.EQ.6)) JJ=J+2
80     DUM1 (I, JJ)=ESM(IM2, J)
85     CONTINUE
C
      DO 95 I=1, 9
      DO 90 J=1, 9
90     ESM(I, J)=DUM1 (I, J)
95     CONTINUE
C
      RETURN
      END
C
C
C *****
      SUBROUTINE LAMDA (KK)
C *****
C
      PARAMETER (IMAXNN=231, IMAXNY=10)
      COMMON/ELMATX/ESM(9, 9), X(3), Y(3), Z(3), D(3, 3), GESM(9, 9),
$     GSM(3*IMAXNN, 3*IMAXNN), GTSM(3*IMAXNN+120, 3*IMAXNN+120), IELR
      COMMON/TMATX/AL(3, 3), T(9, 9), ALT(3, 3), TT(9, 9)
      COMMON/LAM/TEMP(3, 3), ALN(3, 3), ALNT(3, 3)
C
      A=((Y(2)-Y(1))*(Z(3)-Z(1)))-((Y(3)-Y(1))*(Z(2)-Z(1)))
      B=-((X(2)-X(1))*(Z(3)-Z(1)))+(X(3)-X(1))*(Z(2)-Z(1))
      C=((X(2)-X(1))*(Y(3)-Y(1)))-((X(3)-X(1))*(Y(2)-Y(1)))
C
      IF ((A.EQ.0.) .AND. (B.EQ.0.)) THEN
          CXX=1.0
          CXY=0.0
          CXZ=0.0
          CYX=0.0
          CYY=1.0
          CYZ=0.0
          CZX=0.0
          CZY=0.0
          CZZ=1.0
          IF (KK.EQ.0) GO TO 100

```

```
                GO TO 5
            END IF

C
C DIRECTION COSINES OF THE NORMAL Z
C
        CONST=SQRT(A**2+B**2+C**2)
        CZX=A/CONST
        CZY=B/CONST
        CZZ=C/CONST

C
C DIRECTION COSINES OF X
C
C DETERMINE SIDE OF ELEMENT PARALLEL WITH GLOBAL X AXIS
C
        IF((Y(2)-Y(1)).EQ.0.) THEN
            XL=SQRT((X(2)-X(1))**2+(Y(2)-Y(1))**2+(Z(2)-Z(1))**2)
            CXX=(X(2)-X(1))/XL
            CXY=(Y(2)-Y(1))/XL
            CXZ=(Z(2)-Z(1))/XL
            GO TO 50
        END IF

C
        IF((Y(3)-Y(1)).EQ.0.) THEN
            XL=SQRT((X(3)-X(1))**2+(Y(3)-Y(1))**2+(Z(3)-Z(1))**2)
            CXX=(X(3)-X(1))/XL
            CXY=(Y(3)-Y(1))/XL
            CXZ=(Z(3)-Z(1))/XL
            GO TO 50
        END IF

C
        IF((Y(3)-Y(2)).EQ.0.) THEN
            XL=SQRT((X(3)-X(2))**2+(Y(3)-Y(2))**2+(Z(3)-Z(2))**2)
            CXX=(X(3)-X(2))/XL
            CXY=(Y(3)-Y(2))/XL
            CXZ=(Z(3)-Z(2))/XL
            GO TO 50
        END IF

C
C DIRECTION COSINES OF Y
C
```

```

50    CYX=(CZY*CXZ)-(CZZ*CXY)
      CYY=- (CZX*CXZ)+(CZZ*CXX)
      IF (ABS (CYY-1.0) .LE.0.00005) CYY=1.00
      CYZ=(CZX*CXY)-(CZY*CXX)

C
C GENERATION OF THE LOCAL NODAL LAMDA MATRIX
C
100   IF (KK.EQ.0) THEN
      TEMP (1,1)=ACOS (CXX)
      TEMP (1,2)=ACOS (CXY)
      TEMP (1,3)=ACOS (CXZ)
      TEMP (2,1)=ACOS (CYX)
      TEMP (2,2)=ACOS (CYY)
      TEMP (2,3)=ACOS (CYZ)
      TEMP (3,1)=ACOS (CZX)
      TEMP (3,2)=ACOS (CZY)
      TEMP (3,3)=ACOS (CZZ)
      RETURN
    END IF

C
C GENERATION OF THE LAMDA MATRIX
C
5     AL (1,1)=CXX
      AL (1,2)=CXY
      AL (1,3)=CXZ
      AL (2,1)=CYX
      AL (2,2)=CYY
      AL (2,3)=CZY
      AL (3,1)=CZX
      AL (3,2)=CZY
      AL (3,3)=CZZ

C
C GENERATION OF THE TRANSPOSE OF LAMDA
C
      DO 10 I=1,3
      DO 10 J=1,3
10    ALT (J,I)=AL (I,J)

C
      RETURN

```

```

      END
C
C
C *****
      SUBROUTINE TRNSMX
C *****
C
      PARAMETER (IMAXNN=231, IMAXNY=10)
      COMMON/ELMATX/ESM(9,9), X(3), Y(3), Z(3), D(3,3), GESM(9,9),
$     GSM(3*IMAXNN, 3*IMAXNN), GTSM(3*IMAXNN+120, 3*IMAXNN+120), IELR
      COMMON/TMATX/AL(3,3), T(9,9), ALT(3,3), TT(9,9)
C
C GENERATION OF THE TRANSFORMATION MATRIX T
C
      DO 10 I=1,9
      DO 10 J=1,9
10     T(I,J)=0.0
      DO 15 I=1,3
      DO 15 J=1,3
15     T(I,J)=AL(I,J)
C
      DO 20 I=4,6
      DO 20 J=4,6
      IA=I-3
      JA=J-3
20     T(I,J)=AL(IA,JA)
C
      DO 30 I=7,9
      DO 30 J=7,9
      IB=I-6
      JB=J-6
30     T(I,J)=AL(IB,JB)
C
C GENERATION OF THE TRANSPOSE OF T
C
      DO 40 I=1,9
      DO 40 J=1,9
40     TT(J,I)=T(I,J)
C
      RETURN

```

```

      END

C
C
C *****
      SUBROUTINE TRNSFM
C *****
C
      PARAMETER (IMAXNN=231, IMAXNY=10)
      COMMON/ELMATX/ESM(9,9),X(3),Y(3),Z(3),D(3,3),GESM(9,9),
$ GSM(3*IMAXNN,3*IMAXNN),GTSM(3*IMAXNN+120,3*IMAXNN+120),IELR
      COMMON/TMATX/AL(3,3),T(9,9),ALT(3,3),TT(9,9)
      COMMON/DUMM/DUM1(9,9),DUM2(9,9),DUM3(3,3*IMAXNN),
$ DUM4(3,3*IMAXNN),DUM5(3*IMAXNN,3),DUM6(3*IMAXNN,3)
C
C MATRIX MULTIPLICATION TO OBTAIN DUM2 = TT * ESM
C
      DO 10 I=1,9
      DO 10 J=1,9
      DUM2(I,J)=0.0
      DO 10 K=1,9
10    DUM2(I,J)=DUM2(I,J)+TT(I,K)*ESM(K,J)
C
C MATRIX MULTIPLICATION TO OBTAIN GLOBAL ELEMENT STIFFNESS MATRIX
C
      DO 20 I=1,9
      DO 20 J=1,9
      GESM(I,J)=0.0
      DO 20 K=1,9
20    GESM(I,J)=GESM(I,J)+DUM2(I,K)*T(K,J)
C
      RETURN
      END

C
C
C *****
      SUBROUTINE ASSEMB
C *****
C
      PARAMETER (IMAXNN=231, IMAXNY=10)

```

```

COMMON/ELMATX/ESM(9,9),X(3),Y(3),Z(3),D(3,3),GESM(9,9),
$ GSM(3*IMAXNN,3*IMAXNN),GTSM(3*IMAXNN+120,3*IMAXNN+120),IELR
COMMON/N/NP,NN,NE,NS(9),ICK(500),NS1,NS2,UU(9)

C
C DIRECT STIFFNESS PROCEDURE
C
      DO 20 I=1,9
      IC=NS(I)
      DO 10 J=1,9
      JC=NS(J)
10     GSM(IC,JC)=GSM(IC,JC)+GESM(I,J)
20     CONTINUE

C
      RETURN
      END

C
C
C *****
      SUBROUTINE SKEWED (KN)
C *****
C
      PARAMETER (IMAXNN=231,IMAXNY=10)
      COMMON/ELMATX/ESM(9,9),X(3),Y(3),Z(3),D(3,3),GESM(9,9),
$ GSM(3*IMAXNN,3*IMAXNN),GTSM(3*IMAXNN+120,3*IMAXNN+120),IELR
      COMMON/TMATX/AL(3,3),T(9,9),ALT(3,3),TT(9,9)
      COMMON/DUMM/DUM1(9,9),DUM2(9,9),DUM3(3,3*IMAXNN),
$ DUM4(3,3*IMAXNN),DUM5(3*IMAXNN,3),DUM6(3*IMAXNN,3)
      COMMON/ELM/NEL(500,3),XC(IMAXNN),YC(IMAXNN),ZC(IMAXNN)
      COMMON/N/NP,NN,NE,NS(9),ICK(500),NS1,NS2,UU(9)
      COMMON/LAM/TEMP(3,3),ALN(3,3),ALNT(3,3)
      COMMON/PARAM/NY,NYP1,WW,NAR
      DIMENSION N(12),NB(6),TEMP1(3,3),TEMP2(3,3)

C
C CHECK TO SEE IF NODE KN IS ON A BOUNDARY
C AND WHICH BOUNDARY IT IS ON
C
C ONE OF THE CORNERS
C
      IF (KN.EQ.1) THEN

```



```
      N1=KN+1
      N2=KN
      N3=KN+NYP1
      GO TO 200
END IF
C
      IF (KN.EQ.NYP1) THEN
        N1=KN
        N2=KN-1
        N3=KN+NYP1
        GO TO 200
      END IF
C
      IF (KN.EQ. (NN-NY)) THEN
        N1=KN-NYP1
        N2=KN
        N3=KN+1
        GO TO 200
      END IF
C
      IF (KN.EQ.NN) THEN
        N1=KN-NYP1
        N2=KN-1
        N3=KN
        GO TO 200
      END IF
C
C FRONT EDGE
C
      IF ((KN.GT.1) .AND. (KN.LT.NYP1)) THEN
        NB(1)=KN
        NB(2)=KN+NYP1
        NB(3)=KN+1
        NB(4)=NB(1)
        NB(5)=KN-1
        NB(6)=NB(2)
        GO TO 400
      END IF
C
C RIGHT-HAND EDGE
```

C

```
IF (YC (KN) .EQ.0.) THEN
  NB (1) =KN
  NB (2) =KN+NYP1
  NB (3) =KN+1
  NB (4) =KN-NYP1
  NB (5) =KN
  NB (6) =KN+1
  GO TO 400
END IF
```

C

C LEFT-HAND EDGE

C

```
IF (YC (KN) .EQ.WW) THEN
  NB (1) =KN
  NB (2) =KN-1
  NB (3) =KN+NYP1
  NB (4) =KN-NYP1
  NB (5) =KN-1
  NB (6) =KN
  GO TO 400
END IF
```

C

C REAR EDGE

C

```
IF ((KN.GT. (NN-NY)) .AND. (KN.LT.NN)) THEN
  NB (1) =KN-NYP1
  NB (2) =KN-1
  NB (3) =KN
  NB (4) =KN-NYP1
  NB (5) =KN
  NB (6) =KN+1
  GO TO 400
END IF
```

C

GO TO 245

C

C RECALL NODAL COORDINATES

C

```
200   X(1)=XC(N1)
      Y(1)=YC(N1)
      Z(1)=ZC(N1)
      X(2)=XC(N2)
      Y(2)=YC(N2)
      Z(2)=ZC(N2)
      X(3)=XC(N3)
      Y(3)=YC(N3)
      Z(3)=ZC(N3)

C
      KK=0
      CALL LAMDA(KK)

C
C GENERATION OF LOCAL NODAL LAMDA MATRIX
C FOR NODES ON ONE OF THE CORNERS
C
      DO 20 I=1,3
      DO 20 J=1,3
      AA=TEMP(I,J)
      ALN(I,J)=COS(AA)
      IF(ABS(ALN(I,J)).LE.0.00001) ALN(I,J)=0.0
      ALNT(J,I)=ALN(I,J)
20    CONTINUE

C
      GO TO 300

C
C NODES NOT ON A BOUNDARY
C
245   N(1)=KN
      N(2)=KN-1
      N(3)=KN+NYP1
      N(4)=KN
      N(5)=N(3)
      N(6)=KN+1
      N(7)=KN-NYP1
      N(8)=N(1)
      N(9)=KN+1
      N(10)=N(7)
      N(11)=N(2)
      N(12)=N(1)
```

C

```

      KK=0
      IFLAG=0
      DO 210 I=1,3
      DO 210 J=1,3
210    TEMP2(I,J)=0.0

```

C

```

C CALCULATION OF AVERAGE NODAL LAMDA MATRIX
C FOR NODES ONT ON A BOUNDARY

```

C

```

      JK=1
      DO 45 PLNE=1,4
      DO 40 I=1,3
      X(I)=XC(N(JK))
      Y(I)=YC(N(JK))
      Z(I)=ZC(N(JK))
      JK=JK+1
40    CONTINUE
      CALL LAMDA(KK)
      DO 50 I=1,3
      DO 50 J=1,3
50    TEMP2(I,J)=TEMP2(I,J)+TEMP(I,J)*0.25
45    CONTINUE
      GO TO 250

```

C

```

C CALCULATION OF AVERAGE NODAL LAMDA MATRIX
C FOR NODES ON ONE OF THE EDGES

```

C

C

```

400    KK=0
      DO 401 I=1,3
      DO 401 J=1,3
401    TEMP1(I,J)=0.0

```

C

```

      JJ=1
      DO 420 PLNE=1,2
      DO 410 I=1,3
      X(I)=XC(NB(JJ))
      Y(I)=YC(NB(JJ))

```

```

      Z(I)=ZC(NB(JJ))
      JJ=JJ+1
410   CONTINUE
      CALL LAMDA(KK)
      DO 405 I=1,3
      DO 405 J=1,3
405   TEMP1(I,J)=TEMP1(I,J)+TEMP(I,J)*0.5
420   CONTINUE
      IFLAG=1

C
C GENERATION OF THE AVERAGE NODAL LAMDA MATRIX AND ITS TRANSPOSE
C
250   DO 60 I=1,3
      DO 60 J=1,3
      IF(IFLAG.EQ.0) AB=TEMP2(I,J)
      IF(IFLAG.EQ.1) AB=TEMP1(I,J)
      ALN(I,J)=COS(AB)
      IF(ABS(ALN(I,J)).LE.0.00001) ALN(I,J)=0.0
      ALNT(J,I)=ALN(I,J)
60    CONTINUE

C
C *****
C     PRE-MULTIPLY ROWS BY LAMDA
C *****
C
300   DO 80 I=1,3
      IF(I.EQ.1) IROW=3*KN-2
      IF(I.EQ.2) IROW=3*KN-1
      IF(I.EQ.3) IROW=3*KN
      DO 80 J=1,NP
80    DUM3(I,J)=GSM(IROW,J)

C
C MATRIX MULTIPLICATION TO OBTAIN DUM4 = ALN * DUM3
C
      DO 90 I=1,3
      DO 90 J=1,NP
      DUM4(I,J)=0.0
      DO 90 K=1,3
90    DUM4(I,J)=DUM4(I,J)+ALN(I,K)*DUM3(K,J)

C

```

```

C CHANGE BACK TO GSM = DUM4
C
      DO 100 I=1,3
      IF(I.EQ.1) I2ROW=3*KN-2
      IF(I.EQ.2) I2ROW=3*KN-1
      IF(I.EQ.3) I2ROW=3*KN
      DO 100 J=1,NP
100   GSM(I2ROW,J)=DUM4(I,J)
C
C *****
C       POST-MULTIPLY COLUMNS BY TRANSPOSE OF LAMDA
C *****
C
      DO 110 J=1,3
      IF(J.EQ.1) ICOL=3*KN-2
      IF(J.EQ.2) ICOL=3*KN-1
      IF(J.EQ.3) ICOL=3*KN
      DO 110 I=1,NP
110   DUM5(I,J)=GSM(I,ICOL)
C
C MATRIX MULTIPLICATION TO OBTAIN DUM6 = DUM5 * ALNT
C
      DO 120 I=1,NP
      DO 120 J=1,3
      DUM6(I,J)=0.0
      DO 120 K=1,3
120   DUM6(I,J)=DUM6(I,J)+DUM5(I,K)*ALNT(K,J)
C
C CHANGE BACK TO GTSM = DUM6
C
      DO 130 J=1,3
      IF(J.EQ.1) I2COL=3*KN-2
      IF(J.EQ.2) I2COL=3*KN-1
      IF(J.EQ.3) I2COL=3*KN
      DO 130 I=1,NP
130   GSM(I,I2COL)=DUM6(I,J)
C
      DO 150 I=1,NP
      DO 150 J=1,NP

```

```

150     GTSM(I, J)=GSM(I, J)
C
      RETURN
      END
C
C
C *****
      SUBROUTINE MODIFY (LOOPFL)
C *****
C
C
      PARAMETER (IMAXNN=231, IMAXNY=10)
      COMMON/ELMATX/ESM(9, 9), X(3), Y(3), Z(3), D(3, 3), GESM(9, 9),
$     GSM(3*IMAXNN, 3*IMAXNN), GTSM(3*IMAXNN+120, 3*IMAXNN+120), IELR
      COMMON/DOF/F(3*IMAXNN+120), U(3*IMAXNN+120), STRA(6), STRE(6),
$     THM, TM, S1, S2
      COMMON/N/NP, NN, NE, NS(9), ICK(500), NS1, NS2, UU(9)
      COMMON/PARAM/NY, NYP1, WW, NAR
      COMMON/PARAM2/NNB, NNO, NEB, NEO
      COMMON/MODIF/NEWID(120), TMPDSP(110)
C
C *****
      INPUT OF THE NODAL FORCE VALUES FROM FILE FORCE.DAT
C *****
C
      NV - NODE NUMBER
      IDOF - DEGREE OF FREEDOM OF THE FORCE
      VF - VALUE OF THE FORCE
C
      INPUT IS TERMINATED BY INPUTTING A ZERO VALUE FOR NV
C
      IF (LOOPFL.EQ.1) THEN
          LIMVAL=3*(NNB+NYP1)
      ELSE
          LIMVAL=NP+NAR*NY
      END IF
C
C READ IN VALUES AND PLACE IN FORCE VECTOR F
C

```

```

C ALSO EXTEND FORCE VECTOR WITH ZERO DISPLACEMENTS VALUES TO
C COMPENSATE FOR ADDITIONAL CONSTRAINTS
C
      DO 2 I=1,LIMVAL
2      F(I)=0.0
C
      IF (LOOPFL.EQ.1) THEN
5      READ(12,*) NV,IDOF,VF
      IF(NV.GT.0) THEN
          F(IDOF)=VF
          GO TO 5
      END IF
      END IF
C
C
C *****
C      INPUT OF THE PRESCRIBED NODAL VALUES AND CONSTRAINTS
C      FROM FILE CONSTR.DAT
C *****
C
C      NV - NODE NUMBER
C      IDOF - DEGREE OF FREEDOM OF THE KNOWN DISPLACEMENT
C      VD - VALUE OF THE DISPLACEMENT
C
C      INPUT IS TERMINATED BY INPUTTING A ZERO VALUE FOR NV
C
C EXTEND DISPLACEMENT VECTOR WITH ZERO FORCE VALUES TO COMPENSATE
C FOR ADDITIONAL CONSTRAINTS
C
      IF (LOOPFL.GE.2) THEN
          DO 37 I=NP+1,LIMVAL
              U(I)=0.0
37      CONTINUE
      END IF
C
C READ IN Z AND SYMMETRIC Y DOFS FOR ENTRY APRON
C - THIS IS USED FOR ALL RUNS
C
41     READ(14,*) NV,IDOF,VD
      IF (NV.GT.0) THEN

```



```
        CALL SUBMOD (NV, IDOF, VD, LIMVAL)
        GO TO 41
    END IF
C
        WRITE (20,12) LOOPFL
12     FORMAT (2X, I4)
C
C
C READ IN VALUES FOR 1ST PRELIMINARY RUN
C
C READ IN X CONSTRAINTS FOR 1ST ROW ON APRON
    IF (LOOPFL.EQ.1) THEN
44     READ (17,*) NV, IDOF, VD
        WRITE (20,13) NV, IDOF, VD
        IF (NV.GT.0) THEN
            CALL SUBMOD (NV, IDOF, VD, LIMVAL)
            GO TO 44
        END IF
13     FORMAT (2X, I4, 2X, I4, F14.10)
C
        REWIND (14)
        READ (14,*) JUNK
        RETURN
    END IF
C
C VALUES FOR FINAL RUN
C
C READ IN UA DISPL FOR 1ST ROW
    IF (LOOPFL.GE.2) THEN
46     READ (17,*) NV, IDOF, VD
        WRITE (20,13) NV, IDOF, VD
        IF (NV.GT.0) THEN
            CALL SUBMOD (NV, IDOF, VD, LIMVAL)
            GO TO 46
        END IF
C
C READ IN Z AND SYMMETRIC Y CONSTRAINTS OVER ROLLER
47     READ (14,*) NV, IDOF, VD
        IF (NV.GT.0) THEN
```

```

        CALL SUBMOD (NV, IDOF, VD, LIMVAL)
        GO TO 47
    END IF

C
C READ IN M.D. DISPLACEMENTS OVER ROLLER
C - ADD DIFFERENTIAL STRAIN DISPL ADJUSTMENTS
    DO 48 IK=1, NYP1
        DO 49 IL=1, NAR+1
            READ (14, *) NV, IDOF, VD
            VD=VD+TMPSD (IK)
            CALL SUBMOD (NV, IDOF, VD, LIMVAL)
49        CONTINUE
48        CONTINUE
    END IF

C

C
C LOCK Y-DISPLACEMENTS TOGETHER OVER ROLLER
C
C INITIALIZE ALL MATRIX EXTENSION ENTRIES TO ZERO
C
100    DO 120 JJ=NP+1, NP+NAR*NY
        DO 125 KK=1, NP+NAR*NY
            GTSM (JJ, KK)=0.0
125    CONTINUE
120    CONTINUE

C
        DO 130 LL=1, NP
            DO 135 MM=NP+1, NP+NAR*NY
                GTSM (LL, MM)=0.0
135    CONTINUE
130    CONTINUE

C
C READ IN VALUES FROM CONSTR.DAT
C ID - CONTROLLING NODE ON FIRST ROW OF ROLLER
C IDOF - CORRESPONDING DEGREE OF FREEDOM
C ID1 - NODE TO BE LOCKED IN
C IDOF1 - DEGREE OF FREEDOM OF NODE ID1
C
        DO 200 N=1, NAR*NY

```

```

      READ (14,*) ID, IDOF, ID1, IDOF1
      NEWID (N) = IDOF1
      GTSM (NP+N, IDOF) = 1.0
      GTSM (IDOF, NP+N) = 1.0
      GTSM (NP+N, IDOF1) = -1.0
      GTSM (IDOF1, NP+N) = -1.0
200  CONTINUE
      RETURN
      END
C
C
C *****
      SUBROUTINE SUBMOD (NV, IDOF, VD, LIMVAL)
C *****
C
C
      PARAMETER (IMAXNN=231, IMAXNY=10)
      COMMON/ELMATX/ESM (9, 9), X (3), Y (3), Z (3), D (3, 3), GESM (9, 9),
$     GSM (3*IMAXNN, 3*IMAXNN), GTSM (3*IMAXNN+120, 3*IMAXNN+120), IELR
      COMMON/DOF/F (3*IMAXNN+120), U (3*IMAXNN+120), STRA (6), STRE (6),
$     THM, TM, S1, S2
      COMMON/N/NP, NN, NE, NS (9), ICK (500), NS1, NS2, UU (9)
      COMMON/PARAM/NY, NYP1, WW, NAR
      COMMON/PARAM2/NNB, NNO, NEB, NEO
      COMMON/MODIF/NEWID (120), TMPDSP (110)
C
      U (IDOF) = VD
C
C     MODIFICATION OF GLOBAL STIFFNESS MATRIX 'GTSM'
C     AND GLOBAL FORCE VECTOR
C
C SET COEFFICIENTS OF ROW IDOF EQUAL TO ZERO
C
      DO 50 J=1, LIMVAL
      IF (J.EQ.IDOF) GO TO 50
      GTSM (IDOF, J) = 0.0
50  CONTINUE
C
C REPLACE IDOF COMPONENT IN FORCE VECTOR

```

```

C
      F(IDOF)=GTSM(IDOF, IDOF)*VD
      IF (GTSM(IDOF, IDOF).EQ.0.0) GTSM(IDOF, IDOF)=1.0
C
      DO 60 I=1, LIMVAL
      IF (I.EQ.IDOF) GO TO 60
      F(I)=F(I)-GTSM(I, IDOF)*VD
      GTSM(I, IDOF)=0.0
60    CONTINUE
C
      RETURN
      END
C
C
C
C *****
      SUBROUTINE SANDS (KK)
C *****
C
      PARAMETER (IMAXNN=231, IMAXNY=10)
      COMMON/GRAD/B(3, 6), AR2
      COMMON/ELMATX/ESM(9, 9), X(3), Y(3), Z(3), D(3, 3), GESM(9, 9),
$     GSM(3*IMAXNN, 3*IMAXNN), GTSM(3*IMAXNN+120, 3*IMAXNN+120), IELR
      COMMON/DOF/F(3*IMAXNN+120), U(3*IMAXNN+120), STRA(6), STRE(6),
$     THM, TM, S1, S2
      COMMON/N/NP, NN, NE, NS(9), ICK(500), NS1, NS2, UU(9)
      COMMON/ELM/NEL(500, 3), XC(IMAXNN), YC(IMAXNN), ZC(IMAXNN)
      COMMON/LOCAL/XYZ(9), STOR(9), XL(3), YL(3), ZL(3),
$     FL(3*IMAXNN)
C
C CALCULATION OF THE STRAIN VECTOR STRAIN = B * U
C
      CALL ELSTMX(KK)
      DO 30 I=1, 3
      STRA(I)=0.0
      DO 30 K=1, 6
      KA=K
      IF((K.EQ.3).OR.(K.EQ.4)) KA=K+1
      IF((K.EQ.5).OR.(K.EQ.6)) KA=K+2
30    STRA(I)=STRA(I)+B(I, K)*UU(KA)/AR2

```

```

C
C CALCULATION OF THE STRESS VECTOR  STRESS = D * STRAIN
C
      DO 40 I=1,3
      STRE(I)=0.0
      DO 40 K=1,3
40    STRE(I)=STRE(I)+D(I,K)*STRA(K)
C
C CALCULATION OF THE PRINCIPAL STRESSES
C
      AA=(STRE(1)+STRE(2))/2.
      AB=SQRT(((STRE(1)-STRE(2))/2.)**2+STRE(3)**2)
      S1=AA+AB
      S2=AA-AB
      TM=AB
      IF (ABS(STRE(1)-STRE(2)).LT.0.001) GO TO 50
      AC=ATAN2(2.*STRE(3),STRE(1)-STRE(2))
      THM=((180./3.14159265)*AC)/2.
      GO TO 100
50    THM=90.0
C
100   RETURN
      END
C
C
C *****
      SUBROUTINE FACTOR(W,IPIVOT,IFLAG,LOOPFL)
C *****
C
      PARAMETER(IMAXNN=231,IMAXNY=10)
      COMMON/N/NP,NN,NE,NS(9),ICK(500),NS1,NS2,UU(9)
      COMMON/PARAM/NY,NYP1,WW,NAR
      COMMON/PARAM2/NNB,NNO,NEB,NEO
      INTEGER IPIVOT(3*IMAXNN+120)
      REAL D(3*IMAXNN+120),W(3*IMAXNN+120,3*IMAXNN+120)
C
C INPUTS
C W - ARRAY CONTAINING THE MATRIX TO BE FACTORED
C N - ORDER OF THE MATRIX

```

```

C
      IF (LOOPFL.EQ.1) THEN
        LIMVAL=3*(NNB+NYP1)
      ELSE
        LIMVAL=NP+NAR*NY
      END IF
C
      N=LIMVAL
      IFLAG=1
C
C INITIALIZE IPIVOT,D
C
      DO 9 I=1,N
        IPIVOT(I)=I
        ROWMAX=0.
        DO 5 J=1,N
5          ROWMAX=AMAX1(ROWMAX,ABS(W(I,J)))
          IF (ROWMAX.EQ.0.) THEN
            IFLAG=0
            ROWMAX=1.
          END IF
9          D(I)=ROWMAX
          IF (N.LE.1) GO TO 30
C
C FACTORIZATION
C
      DO 20 K=1,N-1
C
C DETERMINE PIVOT ROW, THE ROW ISTAR
C
        COLMAX=ABS(W(K,K))/D(K)
        ISTAR=K
        DO 13 I=K+1,N
          AWIKOD=ABS(W(I,K))/D(I)
          IF (AWIKOD.GT.COLMAX) THEN
            COLMAX=AWIKOD
            ISTAR=I
          END IF
13        CONTINUE
        IF (COLMAX.EQ.0.) THEN

```

```

        IFLAG=0
        ELSE
        IF (ISTAR.GT.K) THEN
C
C MAKE K THE PIVOT ROW BY INTERCHANGING IT WITH
C THE CHOSEN ROW ISTAR
C
        IFLAG=-IFLAG
        I=IPIVOT(ISTAR)
        IPIVOT(ISTAR)=IPIVOT(K)
        IPIVOT(K)=I
        TEMP=D(ISTAR)
        D(ISTAR)=D(K)
        D(K)=TEMP
        DO 15 J=1,N
        TEMP=W(ISTAR,J)
        W(ISTAR,J)=W(K,J)
15      W(K,J)=TEMP
        END IF
C
C ELIMINATE X(K) FROM ROWS K=1,....,N
C
16      DO 19 I=K+1,N
        W(I,K)=W(I,K)/W(K,K)
        RATIO=W(I,K)
        DO 19 J=K+1,N
        W(I,J)=W(I,J)-RATIO*W(K,J)
19      CONTINUE
        END IF
20      CONTINUE
        IF (W(N,N).EQ.0.) IFLAG=0
C
30      RETURN
        END
C
C
C *****
        SUBROUTINE SUBST(W,IPIVOT,B,X,LOOPFL)
C *****

```

```

C
PARAMETER (IMAXNN=231, IMAXNY=10)
COMMON/N/NP, NN, NE, NS (9), ICK (500), NS1, NS2, UU (9)
COMMON/PARAM/NY, NYP1, WW, NAR
COMMON/PARAM2/NNB, NNO, NEB, NEO
INTEGER IPIVOT (3*IMAXNN+120)
REAL B (3*IMAXNN+120), X (3*IMAXNN+120),
$   W (3*IMAXNN+120, 3*IMAXNN+120)
C
IF (LOOPFL.EQ.1) THEN
  LIMVAL=3* (NNB+NYP1)
ELSE
  LIMVAL=NP+NAR*NY
END IF
C
N=LIMVAL
IF (N.LE.1) THEN
  X (1)=B (1) /W (1, 1)
  RETURN
END IF
C
IP=IPIVOT (1)
X (1)=B (IP)
DO 15 I=2, N
  SUM=0.
  DO 14 J=1, I-1
14   SUM=W (I, J) *X (J) +SUM
  IP=IPIVOT (I)
15   X (I)=B (IP) -SUM
C
X (N)=X (N) /W (N, N)
DO 20 I=N-1, 1, -1
  SUM=0.
  DO 19 J=I+1, N
19   SUM=W (I, J) *X (J) +SUM
20   X (I)=(X (I) -SUM) /W (I, I)
C
RETURN
END

```



```

C
C
C *****
      SUBROUTINE FRICTN (KN)
C *****
C
      PARAMETER (IMAXNN=231, IMAXNY=10)
      COMMON/MTL/EM, PR, TH, AMU
      COMMON/LOCAL/XYZ (9), STOR (9), XL (3), YL (3), ZL (3),
$     FL (3*IMAXNN)
      COMMON/ANGL/SLOPE, FRICTF (IMAXNN), FEXT (IMAXNN), ADIV (IMAXNN),
$     CONST (IMAXNN)
C
C CALCULATE FRICTION FORCE
C
      FRICTF (KN) = FL (3*KN) * AMU
C
      RETURN
      END
C
C
C *****
      SUBROUTINE APFORS (KN, ITER)
C *****
C
      PARAMETER (IMAXNN=231, IMAXNY=10)
      COMMON/MTL/EM, PR, TH, AMU
      COMMON/DOF/F (3*IMAXNN+120), U (3*IMAXNN+120), STRA (6), STRE (6),
$     THM, TM, S1, S2
      COMMON/ANGL/SLOPE, FRICTF (IMAXNN), FEXT (IMAXNN), ADIV (IMAXNN),
$     CONST (IMAXNN)
C
C APPLY SPREADING FORCE TO NODE KN IN Y-DIRECTION
C
      AITER=FLOAT (ITER)
      IDOF=3*KN-1
      IF (ITER.EQ.1) FEXT (KN)=0.0
      FEXT (KN) = FEXT (KN) + (1./AITER) * (FRICTF (KN) - FEXT (KN))
      F (IDOF) = FEXT (KN)
C

```

```
      RETURN
      END

C
C *****
      SUBROUTINE CHKFOR (KN, IFLAG2)
C *****
C
      PARAMETER (IMAXNN=231, IMAXNY=10)
      COMMON/LOCAL/XYZ (9), STOR (9), XL (3), YL (3), ZL (3),
$      FL (3*IMAXNN)
      COMMON/ANGL/SLOPE, FRICTF (IMAXNN), FEXT (IMAXNN), ADIV (IMAXNN),
$      CONST (IMAXNN)
C
      IFLAG2=1
C
C CHECK TO SEE IF THE RATIO OF SPREADING FORCE TO FRICTION FORCE
C IS WITHIN THE SPECIFIED LIMITS
C
      ADIV (KN) = FEXT (KN) / FRICTF (KN)
      IF ( (ADIV (KN) .LT. 0.9800) .OR. (ADIV (KN) .GT. 1.02) ) IFLAG2=0
C
      RETURN
      END
```

VITA²

Greg Alan Kliewer

Candidate for the Degree of

Master of Science

Thesis: DEVELOPMENT OF A MODEL OF WEBS ENCOUNTERING CONCAVE ROLLERS

Major Field: Mechanical Engineering

Biographical:

Personal Data: Born on November 24, 1961, in Oklahoma City, Oklahoma, the son of Donald L. and Edna M. Kliewer.

Education: Graduated from Putnam City High School, Oklahoma City, Oklahoma, in May, 1980; attended Oklahoma State University and received the Bachelor of Science Degree in Civil Engineering in May, 1985; completed the requirements for the Master of Science degree at Oklahoma State University, December, 1988.

Professional Experience: Engineering Trainee, City of Broken Arrow, Tulsa, May, 1984 to August 1984; Project Engineer, McLaughlin Water Engineers, Ltd., Tulsa, Oklahoma, May, 1985 to May, 1986; Graduate Research Assistant, Oklahoma State University, Stillwater, Oklahoma, May, 1987 to July, 1988. Member of National Society of Professional Engineers, American Society of Civil Engineers, and Chi Epsilon.